INVESTIGATIONS IN SEMI-CLASSICAL GRAVITY AND COSMOLOGY

A THESIS

submitted by

D. JAFFINO STARGEN

for the award of the degree

DOCTOR OF PHILOSOPHY

DEPARTMENT OF PHYSICS

INDIAN INSTITUTE OF TECHNOLOGY MADRAS

NOVEMBER 2017

Dedicated to

my Amma and Appa

for their love and dreams

Thesis certificate

This is to certify that the thesis titled **Investigations in semi-classical gravity and cosmology**, submitted by **D. Jaffino Stargen**, to the Indian Institute of Technology Madras, for the award of the degree of **Doctor of Philosophy**, is a bona fide record of the research work done by him under our supervision. The contents of this thesis, in full or in parts, have not been submitted to any other Institute or University for the award of the degree.

Prof. L. Sriramkumar
Guide
Professor
Department of Physics
Indian Institute of Technology Madras
Chennai 600036

Dr. Dawood Kothawala
Co-guide
Assistant Professor
Department of Physics
Indian Institute of Technology Madras
Chennai 600036

Place: Chennai
Date: November 20, 2017

Acknowledgements

My Ph.D. life, like others, started with a great amount of excitement and fantasy. When I started working on my first problem, a great deal of self-doubt crept in due to the contradiction between my beliefs about my abilities and the reality. Needless to say, due to this I have spent a reasonable amount of time in mild discomfort, with occasional amusements. Now I look back and ask myself –- what have I learned primarily in these years? This may be a trivial revelation, but I would say that "Now I know what I do not know" — knowledge about my own ignorance. With this important lesson (in my view) I am at the end of my Ph.D. life. So I take this as an opportunity to show my gratitude to people who were of support during hard times, and who included me in their moments of happiness.

First and foremost, I would like to thank my thesis supervisors Prof. L. Sriramkumar and Dr. Dawood Kothawala for their constant support and guidance; without them this thesis would not have been possible.

I would like to thank my doctoral committee members, Prof. Ghanashyam Date, Dr. Shanti Bhattacharya, Dr. Prasanta Kumar Tripathy and Dr. Manoj Gopalakrishnan, for their valuable suggestions. I am grateful to Profs. Arul Lakshminarayan, Lakshmi Bala and Suresh Govindarajan for being welcoming and encouraging of physics discussions. I thank my collaborators Dr. V. Sreenath, who is also my senior, and Dr. Nirmalya Kajuri for coming forward with their constructive suggestions and advice when it mattered most to me.

I would like to thank my colleagues: Rathul, Debika and Ragavendra, for being helpful and making our office a better place to work in. Specifically, I thank Ragavendra for night-long discussions, usually on physics and politics. I am grateful to my senior Dr. Ramkarthik for providing me with his suggestions and advice when I was in need. I would like to thank my friends and well wishers: Ankur, Krishnakumar, Ajoy, Gokul, Anoop, Raghu, Rajiv, Abhik, Prasanth Krishnan, Ajit, Swetamber, Taniya and many others who were there for me when it mattered most. Special thanks to Subair for his ability to relate a given situation with a Tamil movie comedy. Thanks Subair for cheering me up when I felt low. I also thank my senior Dr. Ramesh, Swaminathan, Kaushik and Arjun for including me in their political discussions.

This list would not be complete without thanking my family members. I am thankful to my Amma and Appa for their love and for giving me the freedom to pursue my interests. I would not have been at this stage of my life without them. I also thank my brother

Darjan Jenif, who is more like a close friend to me, for his love and affection. I would also like to thank my school friend Vinith for his support and love. Thanks for being with me for so long.

Sincere thanks to my father-in-law and mother-in-law who stood with me during difficult times. Special thanks to my wife Rashmi, who didn't get staggered during hard times, for being constantly supportive even during crisis situations.

Last but not the least, I thank everyone who has directly or indirectly helped me in my progress.

Abstract

KEYWORDS: Semi-classical and quantum gravity, Cosmology

Semi-classical gravity corresponds to the domain wherein the quantum nature of matter fields are taken into account, while gravity is treated classically. In other words, semi-classical gravity essentially deals with the dynamics of quantum fields in curved spacetimes. A variety of interesting phenomena, such as the Casimir effect and Hawking radiation from black holes, arise in this domain. Careful analyses of these phenomena are expected to provide us with clues towards eventually arriving at a complete quantum theory of gravity. Cosmology provides an important setting wherein the quantum nature of matter fields and strong gravitational fields come together in a natural fashion. The physics of the early universe provides a fertile ground to examine various aspects of semi-classical gravity.

Quantum gravity, as the name evidently suggests, refers to a theory that describes the quantum nature of the gravitational field. In such a domain, both the matter and gravitational fields are to be treated as quantum fields. Simple arguments based on quantum mechanics and relativistic theories of gravity suggest that there exists a lower limit on measurements of distance, below which the classical notions of space and time lose their meaning. This lower bound is known as the Planck length. It should be emphasized that this limitation is inherent to the theory, and is not associated with the accuracy of any measuring device. It is generally expected that Planck length may leave imprints in the semi-classical domain.

This thesis work is aimed at studying different issues related to semi-classical gravity and cosmology. The four problems that have been investigated in these contexts, which constitute this thesis, have been briefly described below.

• **Minimal length and the small scale structure of spacetime:** By minimal length, we refer to the lower bound in distances between any two points in spacetime below which one cannot probe. As we mentioned above, this limitation is a generic implication of attempts towards the unification of fundamental principles of quantum field theory and general theory of relativity. It is expected that the continuum nature of spacetime, which is an assumption of the general theory of relativity, breaks down at small scales where the quantum effects of gravitation are dominant. This suggests that, at small scales, spacetime can have a non-trivial structure. In this work, we carry out a semi-classical analysis to understand the geometrical implications due to the presence of a minimal length in the

background spacetime manifold. The main implication is that imposing a minimal length modifies the geometry of the background spacetime, and it can no more be described in terms of local tensorial quantities, but instead in terms of bitensors. A bitensor is a non-local tensorial quantity which depends on two spacetime points. We calculate the Ricci biscalar, the simplest of the curvature invariants, associated with the modified geometry. Interestingly, we find that the Ricci biscalar at a particular spacetime point can be solely expressed in terms of geometry induced on the equigeodesic surfaces which are centered about that point. We also show that the Ricci biscalar has an interesting non-trivial behavior in the limit when the two spacetime points coincide. This behavior strongly suggests that the existence of a minimal length can leave residues independent of the exact details of the quantum theory of gravitation.

• **Response of a rotating detector in polymer quantum field theory:** Assuming that high energy effects may alter the standard dispersion relations governing quantized fields, the influence of such modifications on various phenomena has been studied extensively in the literature. In different contexts, it has generally been found that, while super-luminal dispersion relations hardly affect the standard results, sub-luminal relations can lead to (even substantial) modifications to the conventional results. A polymer quantized scalar field is characterized by a series of modified dispersion relations along with suitable changes to the standard measure of the density of modes. Amongst the modified dispersion relations, one finds that the lowest in the series can behave sub-luminally over a small domain in wavenumbers. In this work, we study the response of a uniformly rotating Unruh-DeWitt detector that is coupled to a polymer quantized scalar field. While certain sub-luminal dispersion relations can alter the response of the rotating detector considerably, in the case of polymer quantization, due to the specific nature of the dispersion relations, the modification to the transition probability rate of the detector does not prove to be substantial. We discuss the wider implications of the result.

• **Moving mirrors and the fluctuation-dissipation theorem:** It is well known that small particles which are immersed in a thermal bath exhibit Brownian motion. In this work, we investigate the random motion of a mirror in $(1 + 1)$-spacetime dimensions that is immersed in a thermal bath of massless scalar particles which are interacting with the mirror through a boundary condition. Imposing the Dirichlet or the Neumann boundary conditions on the moving mirror, we evaluate the mean radiation reaction force on the mirror and the correlation function describing the fluctuations in the force about the mean value. From the correlation function thus obtained, we explicitly establish the fluctuation-dissipation theorem governing the moving mirror. Using the fluctuation-dissipation theorem, we compute the mean-squared displacement of the mirror at finite and zero temperature. We clarify a few points concerning the various limiting behavior of the mean-squared displacement of the mirror. While we recover the standard result at finite temperature, we find that the mirror diffuses logarithmically at zero temperature, confirming similar conclusions that have been arrived at earlier in this context. We also comment on a subtlety concerning the comparison between zero temperature limit of the finite temperature result and the exact zero temperature result.

• **Quantum-to-classical transition and imprints of wavefunction collapse in bouncing universes:** The perturbations in the early universe are generated as a result of the interplay between quantum field theory and gravitation. Since these primordial perturbations lead to the anisotropies in the cosmic microwave background and eventually to the inhomogeneities in the Large Scale Structure (LSS), they provide a unique opportunity to probe issues which are fundamental to our understanding of quantum physics and gravitation. One such fundamental issue that remains to be satisfactorily addressed is the transition of the primordial perturbations from their quantum origins to the LSS which can be characterized completely in terms of classical quantities. Bouncing universes provide an alternative to the more conventional inflationary paradigm as they can help overcome the horizon problem in a fashion very similar to inflation. While the problem of the quantum-to-classical transition of the primordial perturbations has been investigated extensively in the context of inflation, we find that there has been a rather limited effort towards studying the issue in bouncing universes. In this work, we analyze certain aspects of this problem with the example of tensor perturbations produced in bouncing universes. We investigate the issue mainly from two perspectives. Firstly, we approach the problem by examining the extent of squeezing of a quantum state associated with the tensor perturbations with the help of the Wigner function. Secondly, we analyze this issue from the perspective of the quantum measurement problem. In particular, we study the effects of wave function collapse, using a phenomenological model known as continuous spontaneous localization, on the tensor power spectra. We conclude with a discussion of the results obtained.

Contents

List of Figures

Chapter 1

Background and overview

1.1 Gravity and the quantum

Theoretical physics attempts to explain phenomena that occur in nature with the aid of a minimal set of fundamental principles. It is found that most of the phenomena occurring over a wide range of energy scales can be explained in terms of four fundamental forces, *viz.* the strong, weak, electromagnetic, and gravitational interactions. Out of the four fundamental interactions, the strong and weak interactions have finite ranges, while the other two have an infinite range. The ranges of the strong and weak interactions are of the order of $10^{-15}\,\mathrm{m}$ and $10^{-18}\,\mathrm{m}$, respectively. Hence in the low energy domain (*i.e.* at large distances) the strong and weak interactions are feeble in strength, and cannot be detected. The range of the strong interaction determines the structure of nucleus. The arrangement of electrons around the nucleus to form an atom is determined by the electromagnetic interaction. But the weak interaction is destructive in nature, *i.e.* it cannot produce stable states of matter, while strong and electromagnetic interactions can. The primary role of the weak interactions seems to be to regulate the lifetime of unstable particles (in these contexts, see, for instance, the standard textbooks [1]).

Quantum theory provides a general framework to describe the fundamental interactions in nature. It is considered as a well established theory, apart from its interpretation issues, since it has passed a plethora of experimental tests. Electromagnetic interaction was the first interaction which was described in the framework of quantum theory. Referred to as quantum electrodynamics, the theory provides predictions with unprecedented accuracy. Later, the quantum theory of strong interactions, known as quantum chromodynamics, was developed, which partly resembles quantum electrodynamics in construction. The quantum theory of weak interaction is described by the electroweak theory which shows that the apparently distinct interactions, weak and electromagnetic, are different manifestations of a unified interaction known as the electroweak interaction (see, for example, the popular textbooks [2]).

Gravity is the only interaction which is yet to be formulated in the framework offered by quantum theory. At the largest scales and at the greatest strengths, gravity is described classically by Einstein's general theory of relativity, which is a geometrical theory (see, for instance, the following classic textbooks [3]). The theory has successfully passed many experimental tests, including the recent direct detection of gravitational waves by the Laser Interferometer Gravitational Wave Observatories [4]. Einstein's general theory of relativity drastically changed the understanding of gravitation in Newtonian physics. In general theory of relativity, gravity is not associated with a force, but it is a manifestation of the curvature of spacetime. Also, the strength of the gravitational interaction is directly related to the curvature of spacetime. General relativity proposes the spacetime to be a four dimensional Lorentzian manifold described by a metric tensor.

According to the general theory of relativity, under general conditions, the existence of singularities in spacetime seem unavoidable [3]. The presence of such spacetime singularities implies that there can exist a domain, where the strength of gravity is very strong, in which the classical geometrical description of gravity is no longer valid. In such a domain, it is believed that the quantum effects of gravity are dominant and cannot be ignored. This suggests that a quantum description of gravitation is essential.

The domain in which a complete quantum theory is required to describe the effects of gravitation is known as the Planck scale. The Planck length $L_{_{\rm Pl}}$, Planck time $T_{_{\rm Pl}}$ and Planck mass $M_{_{\rm Pl}}$ are derived from the three fundamental constants — the gravitational constant G, speed of light c, and Planck's constant $\hbar$ — and they are are given by (see, for instance, Ref. [5])

$$L_{_{\rm Pl}} = \sqrt{\frac{\hbar\, G}{c^3}} = 1.6 \times 10^{-35}\ {\rm m}, \tag{1.1a}$$

$$T_{_{\rm Pl}} = \sqrt{\frac{\hbar\, G}{c^5}} = 5.4 \times 10^{-44}\ {\rm s}, \tag{1.1b}$$

$$M_{_{\rm Pl}} = \sqrt{\frac{\hbar\, c}{G}} = 2.2 \times 10^{-8}\ {\rm kg}. \tag{1.1c}$$

As we shall discuss later, the quantum effects of gravitation become important when the Compton wavelength $\lambda_{_{\rm C}}$ of a system of mass, say, M, is of the order of its Schwarzschild radius r_{S}, *i.e.*

$$\lambda_{\mathrm{C}} = \frac{\hbar}{M\,c} \approx r_{\mathrm{S}} = \frac{2\,G\,M}{c^2}, \tag{1.2}$$

which leads to the Planck mass $M_{\mathrm{Pl}} = \sqrt{\hbar\,c/G}$. While there exist a few competing approaches towards arriving at a theory of quantum gravity — such as string theory, loop quantum gravity, causal set theory and non-commutative geometry — it would be fair to say that we still seem far converging on a complete and viable theory (in these contexts, see, for instance, the following books [6] and reviews [7]).

Though a complete formulation of quantum gravity still remains elusive, to make progress, a more pragmatic attempt would be to study the effects of classical gravity on quantum matter fields. In fact, the motivation to carry out such an attempt comes from the early days of quantum mechanics. Much before the complete formulation of quantum electrodynamics, many calculations were carried out wherein the classical electromagnetic field is assumed to interact with quantized matter. It is important to note that some of the results obtained from such a semi-classical treatment were in complete agreement with the full theory of quantum electrodynamics (see, for example, Ref. [8]). Hence, one can hope that there exists a domain, much away from the Planck scale, in which gravity can be treated as a classical background field, and the matter field can be considered to be quantum in nature. Since the classical gravitational field is effectively described by general relativity, the semi-classical theory of gravity leads to the study of dynamics of quantum fields in curved background spacetimes.

1.2 The domain of semi-classical gravity

As we described above, semi-classical gravity corresponds to the domain wherein the quantum nature of matter fields are taken into account, while gravity is treated classically (see the books [9] and the reviews [10]). Many interesting phenomena occur in this domain. Classic examples of such phenomena include the Casimir effect due to the presence of boundaries or non-trivial topologies and particle production due to time-dependent gravitational fields, notably, Hawking radiation from black holes [11]. While pair creation in, say, a cosmological setting has great similarities with the Schwinger effect in electromagnetic backgrounds (see, for instance, Ref. [12]), Hawking radiation from black holes is a novel phenomenon that is peculiar to gravitation. As we shall highlight below, the thermal nature of Hawking radiation essentially arises due to the presence of a horizon. Another interesting aspect that is encountered in the semi-classical domain is the fact that the concept of a particle proves to be, in general, coordinate dependent [13]. A physical manifestation of this aspect leads to the popular Unruh effect, a variant of which we will investigate in this thesis (for the original discussions, see Refs. [14, 15]; for recent reviews, see, for example, Refs. [16, 17]). It has been expected that a detailed analysis of these phenomena can provide us with some clues to the quantum nature of gravity. Apart from black holes, the early universe provides an interesting scenario to examine the quantum nature of matter in strong gravitational fields.

According to the general theory of relativity, a black hole is a spacetime region in which the gravitational effects are so strong that not even light can escape. Such regions prove to be causally disconnected from the rest of the universe and are enclosed in an one way boundary, called the horizon. Anything which crosses the horizon and falls into the black hole, including light, is lost for ever [3]. Analyzing the dynamics of quantized matter fields in the vicinity of black holes leads to the profound conclusion that they are not completely black, as in classical general relativity, but are objects with fascinating properties. Due to quantum fluctuations, black holes emit thermal radiation of all species of particles at a universal temperature, known as the Hawking temperature, given by [11]

$$T_{_{\rm H}} = \frac{\hbar\,\kappa}{2\,\pi\,k_{_{\rm B}}\,c}, \tag{1.3}$$

where κ is the surface gravity associated with the black hole and $k_{_{\rm B}}$ is the Boltzmann constant. In the case of the spherically symmetric, Schwarzschild black hole, the surface gravity can be determined to be

$$\kappa = \frac{c^4}{4\,G\,M}, \tag{1.4}$$

where M is the mass of the black hole. This implies that the corresponding Hawking temperature is $T_{\rm H} = \hbar\,c^3/(8\,\pi\,k_{_{\rm B}}\,G\,M)$. In other words, the smaller the mass of the black hole, the larger is its Hawking temperature. Due to this reason, black holes can literally end in explosions as they continue to lose their mass [11]

A phenomenon which has certain similarities to the Hawking radiation from black holes is also encountered in flat spacetime. It is found that a uniformly accelerated observer perceives the Minkowski vacuum as a thermal bath at the temperature (for the original discussions, see Refs. [13, 14]; for a relatively recent review, see Ref. [16])

$$T_{_{\rm U}} = \frac{\hbar\,a}{2\,\pi\,k_{_{\rm B}}\,c}, \tag{1.5}$$

where a is the proper acceleration of the observer. This phenomenon is known as the Unruh effect and, as in the case of Hawking radiation, it can be shown that the effect essentially arises due to the horizon that is generated in the frame of the uniformly accelerated observer [14]. It is useful to note that the Hawking temperature corresponds to setting $a = \kappa = c^4/(4\, G\, M)$ in the above expression for Unruh temperature, where κ is the surface gravity of a stationary black hole.

Recall that, the general theory of relativity is invariant under general non-linear coordinate transformations. However, this invariance is not always reflected when one studies the behavior of quantum fields in curved spacetime. As we mentioned, in a curved spacetime, the concept of a particle proves to be, in general, coordinate dependent. The Unruh effect is a manifestation of this phenomenon [13, 14]. It is well known that the Minkowski vacuum is invariant under Lorentz transformations. In other words, the structure of the quantum vacuum has the same form in all inertial frames of reference, *i.e.* under linear coordinate transformations. However, this aspect ceases to be true under general non-linear coordinate transformations. A uniformly accelerated frame in flat spacetime — often referred to as the Rindler coordinates — is a non-inertial frame of reference which is an integral curve of a timelike Killing vector field. The presence of the timelike Killing field in the uniformly accelerated frame permits one to carry out quantization of a field in the same fashion as it is usually done in an inertial frame. One finds that the quantization in the accelerated frame proves to be inequivalent to the quantization in an inertial frame [13]. Specifically, the expectation value of Rindler number operator in the Minkowski vacuum is found to be a thermal spectrum at the Unruh temperature $T_{\rm U}$ defined above. Such effects due to inequivalent quantization need to accounted for when studying the behavior of quantum fields in a generic curved spacetime.

1.3 The concept of minimal length

As we discussed before, since we lack a complete theory of quantum gravity, it is not yet clear as to how the quantum effects of gravity modifies the structure of spacetime at the Planck scale. But, a generic implication that one can arrive at by combining the basic principles of quantum mechanics and general relativity is the existence of a minimal length (in this context, see, for instance, the following reviews [18]). Minimal length is a fundamental limit to the distance between two spacetime points, below which one cannot probe. The existence of a minimal length can be demonstrated with the aid of a simple thought experiment. In fact, one can also argue that the minimal length should be of the order of the Planck length $L_{\rm Pl}$.

Consider a mass M, contained in a volume V, which is shrunk to an extent that is allowed by the theory. In the context of general relativity, according to the so-called hoop conjecture, if the mass M is compacted into a region whose spatial dimension in every direction, say, ℓ, is smaller than the Schwarzschild radius (*i.e.* $\ell < r_{\rm S} = 2\,G\,M/c^2$), then the shrunken mass will end up becoming a black hole [18, 19]. Note that, though the hoop conjecture has not been proven as yet, it has been shown analytically and numerically that it holds to a large extent [19].

In the context of quantum theory, shrinking the linear dimension of a system to a size ℓ leads to an uncertainty in its momentum given by $\Delta p \approx \hbar/\ell$. Such an uncertainty in momentum leads to a corresponding uncertainty in energy of the order of $\Delta E \approx \Delta p\, c \approx \hbar\, c/\ell$. If ℓ is made very small, then the uncertainty in the energy reaches a value such that the system produces pairs of particles and anti-particles in the region around the mass M. This phenomenon ruins the localization and the volume cannot be shrunk further. Such a limit occurs when

$$M\,c^2 \approx \Delta E \approx \frac{\hbar\, c}{\ell} \tag{1.6}$$

or, equivalently, when

$$\ell \approx \frac{\hbar}{M\,c} \equiv \lambda_{\rm c}, \tag{1.7}$$

where $\lambda_{\rm c}$ is the Compton wavelength associated with the mass M. When the volume is shrunk to a size such that the Schwarzschild radius and Compton wavelength are of the same order, we obtain that [5]

$$\lambda_{\rm c} = \frac{\hbar}{M\,c} \approx \frac{G\,M}{c^2}, \tag{1.8}$$

which leads to the Planck mass $M_{\rm Pl} = \sqrt{\hbar\, c/G}$. The associated Compton wavelength proves to be the minimal length, *i.e.*

$$\lambda_{\rm c} \approx \frac{\hbar}{M_{\rm Pl}\, c} = \sqrt{\frac{\hbar\, G}{c^3}}, \tag{1.9}$$

which is, evidently, of the order of the Planck length $L_{\rm Pl} = \sqrt{\hbar\, G/c^3}$.

It would be interesting to understand the semi-classical effects of the minimal length. As we shall describe later, in this thesis, we perform such analysis by imposing a minimal length by hand in a given background spacetime, and investigate its imprints in the semi-classical domain.

1.4 The idea of detectors

Another semi-classical effect that this thesis aims to investigate is related to the concept of a particle and the efforts to utilize the idea of detectors to examine the particle content of a quantum field. In particular, we shall be interested in examining the effects of high energy physics on the response of certain types of non-inertial detectors in flat spacetime.

We had mentioned earlier that concepts such as vacuum and particles do not prove to be general coordinate invariant. Even in flat spacetime, while these concepts are invariant under Lorentz transformations, they do not turn out to be invariant under a general non-linear coordinate transformation. A classic example that reflects this aspect is the fact that the quantization in a uniformly accelerating frame in Minkowski spacetime is inequivalent to the more conventional quantization carried out in an inertial frame[13]. The idea of detectors were originally introduced to provide an operational definition to the concept of a particle [14, 15]. Since particles interact with detectors thereby exciting them, one can possibly use this intuitive notion of detectors to define a particle [20]. With such a motivation in mind, the response of a variety of detectors that are coupled to quantum fields have been studied in flat as well as curved spacetimes. For instance, it is found that a uniformly accelerated detector in the Minkowski spacetimes indeed responds with a thermal spectrum [14, 15, 21], exactly as expected from the more conventional canonical quantization procedure [13].

While, in certain situations, such as the uniformly accelerated case in Minkowski spacetime, the response of detectors seems to match the results arrived at from the canonical quantization procedure, one can show that the response of detectors do not necessarily reflect the particle content of a quantum field (in this context, see, for instance, Refs. [17, 22]). A standard counter example to the results in the uniformly accelerated frame in flat spacetime would be to instead examine these phenomena in a rotating frame. In such a case, one can show that, whereas the quantization in the rotating frame indeed proves to be equivalent to the quantization in an inertial frame, it is found that rotating detector responds non-trivially [22]. Despite this limitation, the concept of a detector has its utility and, as we mentioned, the response of different types of detectors have been studied extensively in the literature.

Over the last couple of decades, there has been a considerable interest in examining if Planck scale effects can leave their imprints on low energy phenomena (see, for instance, the reviews [23]). Specifically, this issue has been investigated extensively in the contexts of Hawking radiation from collapsing black holes and the primordial power spectra generated in inflationary cosmology (in this context, see the reviews [24, 25]). In these situations, due to the exponential stretching of the modes that occur, it has been realized that scales of typical interest at late times would have frequencies which are of the order of the Planck scale at early times, when the initial conditions are imposed on the quantum field. However, in the absence of a working quantum theory of gravity, these high energy effects are typically studied with the help of models constructed by hand. These models typically contain the Planck scale and incorporate one or more features broadly expected from quantum gravity. Various analyses seem to suggest that the signatures of Planck scale physics can depend on the details of model that takes into account one or more of the purportedly quantum gravitational features. The general consensus seems to be that models which lead to significant changes to the conventional results (such as due to the so-called sub-luminal dispersion relations [23, 24, 25]) are quite likely to be ruled out.

We had mentioned earlier that the Unruh effect has a close relationship to Hawking radiation from black holes. Due to this reason, the effects of Planck scale physics on the Unruh effect has also been examined in the literature (see, for example, Ref. [26]). Recently, there has been an interest in the so-called polymer quantization approach, which can be broadly said to have its roots in loop quantum gravity [6]. Using the approach, one can arrive at a modified propagator describing quantum fields in flat spacetime (see Ref. [27]; in this context, also see Refs. [28]). The modified propagator contains the new high energy scale (often assumed to be the Planck scale). The response of detectors are essentially described by the Fourier transform of the propagator describing the quantum field that the detector is coupled to. The Fourier transform is evaluated along the trajectory of the detector which is in motion. Therefore, a modified propagator can be utilized to study the signatures of high energy effects on the response of detectors. In this thesis, we shall study detectors that are coupled to a polymer quantized field. Specifically, we shall investigate the response of rotating detectors in flat spacetime with the aim of understanding possible low energy imprints of physics at the highest energies.

1.5 Brownian motion and moving mirrors

We have been repeatedly emphasizing the fact that the domain of semi-classical gravity is an interesting regime offering a wide scope to analyze a variety of phenomena. One such interesting phenomenon is the fact that a mirror which is moving non-uniformly can radiate, *i.e.* emit particles corresponding to the quantum field the mirror is coupled to [29, 30, 31]. The presence of mirrors leads to non-trivial boundary conditions on quantum fields, which depends on the nature of the interaction of the field with the mirror. We had already discussed the fact that static boundaries alter the vacuum structure of quantum fields even in flat spacetime, leading to the so-called Casimir effect. For this reason, the phenomenon of radiation from moving mirrors is often referred to as the dynamical

Casimir effect [32].

In this thesis, we shall use the idea of a moving mirror to examine Brownian motion both at finite temperature and in the quantum vacuum. As is well known, Brownian motion refers to the random motion of particles that are immersed in a thermal bath [33]. In the conventional treatment of Brownian motion, it is assumed that a particle immersed in the bath is subject to a force that has a dissipative as well as a fluctuating component. While the dissipative component typically depends on the velocity of the particle, the fluctuating component is characterized by its correlation function. Moreover, it is known that certain properties of the dissipative component are related to the fluctuating component by the so-called fluctuation-dissipation theorem [34]. Using the theorem, it is possible to establish that the Brownian particle diffuses through the bath in a characteristic fashion. We find that the example of a mirror that is interacting with a quantum field provides an analytically tractable situation wherein all the quantities involved (*viz.* the dissipative and fluctuating forces as well as the mean-squared displacement of the mirror) can be explicitly evaluated. As we shall see, since a mirror moving with a non-uniform acceleration emits radiation, it leads to a backreaction on the mirror. This backreaction is responsible for the dissipative and the fluctuating forces on the mirror. Also, we shall show that one can explicitly establish the fluctuation-dissipation theorem for the example. Further, the tractability of the problem in this case also permits one to examine the crucial question of whether the mirror diffuses even at zero temperature [35].

1.6 Inflation and alternatives

As we mentioned earlier, cosmology provides an ideal setting for examining issues in semi-classical gravity. A problem that remains to be satisfactorily addressed in cosmology is the quantum-to-classical transition of the primordial perturbations.

According to the standard big bang model, our universe started in a hot and dense early phase, when the energy density of radiation dominated the energy density of matter (see, for instance, the textbooks [36]). The universe cooled down as it expanded and, since the energy density of radiation falls faster than that of matter, there arises an epoch — called the epoch of equality — when the energy densities in radiation and matter are equal. Thereafter, the energy density in matter begins to dominate. Soon after the epoch of equality, there occurs a regime wherein the radiation ceased to interact with matter and started streaming freely. It is this radiation which we observe today as the Cosmic Microwave Background (CMB). The hot big bang model has proved to be very successful in explaining a variety of phenomena such as the Hubble's law and the observed abundance of light elements in the universe.

The CMB proves to be extremely isotropic, with deviations from isotropy being of the order of one part in 10^5. Since it is a vestige of the radiation dominated epoch, the extent of isotropy of the CMB reflects the fact that the universe was highly homogeneous during the early stages. However, the extent of isotropy proves to be a puzzle in the conventional hot big bang model. The reason being that, within the model, regions of the sky which are widely separated (by, say, more than a degree) could not have causally interacted with each other by the epoch of decoupling. Nevertheless, one finds that the CMB from even opposite directions in the sky have virtually the same temperature. This difficulty within the hot big bang model is known as the horizon problem.

One often invokes an epoch of inflation — a period of accelerated expansion during the early stages of the radiation dominated epoch — to overcome the horizon problem. The most attractive aspect of the inflationary scenario is the fact that, apart from helping in overcoming some of the difficulties associated with the hot big bang model, it also provides a natural mechanism for the generation of inhomogeneities (see, for instance, the reviews [37]). Inflation is often assumed to be driven by scalar fields. It is the quantum fluctuations associated with the scalar fields that are supposed to be responsible for the origin of perturbations in the early universe. These perturbations leave their imprints as anisotropies in the CMB which, in turn, are amplified by gravitational instability during the matter dominated epoch into the structures we see around us today as galaxies and clusters of galaxies.

Inflation has been a rather compelling, efficient and successful paradigm. The efficiency of the inflationary paradigm has led to a situation wherein there exists many models of inflation that are consistent with the CMB and other cosmological data. In such a situation, there has been efforts to construct viable alternatives to inflation. One such alternative are the classical bouncing scenarios (see, for instance, the reviews [38]). In these scenarios, the universe is assumed to undergo an initial phase of contraction until the scale factor reaches a minimum value, before it begins to expand. Such scenarios can help us overcome the horizon problem and also lead to the generation of perturbations in a manner very similar to inflation. However, in contrast to the inflationary scenario wherein it is rather easy to propose a model which is consistent with the observations, viable and well motivated bouncing models are often hard to construct. Moreover, they are also plagued by certain issues such as the need for fine tuned conditions (see, for instance, Ref. [39]). For instance, inhomogeneities and anisotropies can rapidly grow during the contracting phase leading to a situation wherein perturbation theory (which is required to study the evolution of perturbations) ceases to be valid as one approaches the bounce. Despite these difficulties, there has been a constant and substantial effort towards the construction of bouncing models that are consistent with the observations.

As we mentioned, in cosmology, one of the issues that remains to be satisfactorily addressed is the problem of the quantum-to-classical transition of the primordial perturbations. While there has been some effort in this direction in the context of inflation (see, for instance, Refs. [12, 40, 41]), we find that the issue has not been investigated at all in the bouncing scenarios. In this thesis, we shall investigate the issue in bouncing scenarios in two ways. We shall first study the problem by examining the extent of squeezing of the quantum state corresponding to the tensor perturbations with the help of the Wigner function. We shall also study the effects of wave function collapse on the tensor power spectra, using a phenomenological model known as continuous spontaneous localization.

1.7 Organization of the thesis

The rest of the thesis, which consists of five more chapters, is organized as follows. In Chap. 2, we shall investigate the semi-classical effects of the existence of a minimal length. We shall impose a minimal length by hand in the background spacetime, and analyze the hints it can provide about the final theory of quantum gravity. In Chap. 3, we shall study the response of a rotating detector that is coupled to a field which is quantized using the approach of polymer quantization. In Chap. 4, we shall analyze the Brownian motion of a mirror that is coupled to a quantum scalar field in $(1+1)$-spacetime dimensions. Assuming the field to be at a finite temperature, we shall explicitly establish the fluctuation-dissipation theorem for the problem at hand. Also, apart from evaluating the mean square displacement of the mirror at a finite temperature, we shall examine the nature of diffusion of the mirror in the quantum vacuum. In Chap. 5, we shall investigate the quantum-to-classical transition of the tensor perturbations in a class of bouncing universes. We shall begin by examining the nature of the transition using the Wigner function in a specific bouncing model and then go on to study the effects of wavefunction collapse on the spectrum of tensor perturbations. We shall conclude the thesis in Chap. 6 with a summary and outlook.

We shall clarify the notations and conventions that we shall adopt separately in each of the chapters.

Chapter 2

Minimal length and the small scale structure of spacetime

2.1 Introduction

Quantum effects are expected to drastically affect the structure of space and time at the smallest of scales. However, our current theories of gravity and quantum mechanics are (fortunately) very stingy with the options they leave us as far as the small scale of structure of spacetime is concerned. For example, attempts to model such a structure by violating or deforming Lorentz invariance are either very strongly constrained by experiments, or run into deeper conceptual issues when one goes beyond the simple one-particle models. It is much more plausible that instead of Lorentz invariance, it is the assumption of locality that might have to be given up at small scales [42]. However, abandoning locality then also necessitates that we give up the classical description of spacetime in terms of local tensorial objects, in particular the metric tensor $g_{ab}(p)$. Finding the right geometric variables that can describe spacetime geometry down to smallest scales is of utmost significance not only for quantum gravity, but also for the proper physical interpretation of the field equations of gravity at the classical level. In particular, the deep connection between Einstein equations, thermodynamics, and information theory that has been studied in depth for over a decade very strongly suggests that we should question the conventional description of gravitational dynamics based on Einstein-Hilbert action. In any case, to properly understand the implications of results that have been accumulated from the study of quantum fields in curved spacetime, it is extremely important that one must first identify the correct geometric variables to describe spacetime geometry at the classical level itself.

Fortunately, the hint for doing so also comes from these very same results. In particular, one of the most significant results to have come out of semi-classical studies is the existence of a minimal spacetime length, say, ℓ_0, below which spacetime intervals loose any operational significance [18, 43]. Such a *zero-point length* appears in various forms in several candidate models of quantum gravity, and is often considered as the universal regulator for divergences in quantum field theory and general theory of relativity. In a recent work [44], one of us proposed that a more appropriate description of spacetime geometry in presence of a minimal length scale must be based on non-local bi-tensors instead of the metric tensor. The geodesic distance between two spacetime events, in particular, was proposed as a more fundamental object than the metric tensor. The relevant bi-tensor in this context is the so called Synge world function $\Omega(p, p_0)$ defined by [45]

$$\Omega(p, p_0) = \frac{1}{2}\left[\lambda(p) - \lambda(p_0)\right] \int\limits_{\lambda(p_0)}^{\lambda(p)} \mathrm{d}\lambda \,\left[g_{ab}\, q^a\, q^b\right](x(\lambda)) \,=\, \frac{1}{2}\,\sigma^2(p, p_0), \tag{2.1}$$

where $\sigma^2(p, p_0)$ is the square of the geodesic interval, with the corresponding geodesic distance given by

$$d(p, p_0) = \sqrt{\epsilon\,\sigma^2(p, p_0)}. \tag{2.2}$$

Here, q^a is tangent to the geodesics, and $\epsilon = q^a\, q_a = \pm 1$. (In this chapter, we shall use $\Omega(p, p_0), \sigma(p, p_0)^2$ and $d(p, p_0)$ interchangeably to keep the expressions and notation convenient. We will also often use $\lambda = d(p, p_0)$ in covariant Taylor series to keep track of terms of various orders without messing up the notation.)

Assuming that the small scale structure of spacetime is characterized (at least at a semi-classical level) by the existence of a minimal length, it was shown that one can construct a second rank bi-tensor, $q_{ab}(p, p_0; \ell_0)$, such that it yields geodesic distances with a lower bound ℓ_0. The construction of q_{ab} was based on two inputs [44]:

- **P1:** The requirement that geodesic distances have a Lorentz invariant lower bound *and* this arises from modification of geodesic distances as $\sigma^2 \to \sigma^2 + \ell_0^2$.

- **P2:** The requirement that the modified d'Alembartian $\widetilde{{}_{p_0}\Box_p}$ yields the following modification for the two point functions $G(p, p_0)$ of fields in *flat spacetime*:

$$G\left[\sigma^2\right] \to \widetilde{G}\left[\sigma^2\right] = G\left[\sigma^2 + \ell_0^2\right]. \tag{2.3}$$

  This essentially regulates the UV divergences in quantum field theory, and is based on several earlier works on the subject.

These two requirements then completely fix the form of q_{ab}. Being manifestly covariant, the extension to arbitrary curved spacetimes suggests itself naturally.

In subsequent work [46], it was shown that the Ricci bi-scalar $\widetilde{\mathbf{Ric}}(p, p_0)$ corresponding to this so called *qmetric* q_{ab} has a very specific non-analytic structure which results in a non-trivial result for the coincidence limit $\left[\widetilde{\mathbf{Ric}}\right]$ when $\ell_0 \to 0$. The specific result proved there was

$$\lim_{\ell_0 \to 0} \lim_{\sigma^2 \to 0^{\pm}} \widetilde{\mathbf{Ric}}(p, p_0) \propto R_{ab}\, q^a\, q^b \tag{2.4}$$

with q^a being arbitrary normalized vectors at each spacetime event. A similar analysis for the surface term $K\sqrt{|h|}$ of the Einstein-Hilbert action was also presented subsequently, and the very same term as above was shown to appear there as well (in this context, see the second reference in Refs. [46]).

The above results have many deep implications, in particular for understanding better the notion of entropy associated with each spacetime event p_0 and it's causal boundaries, and for the *emergent gravity paradigm* [46]. They not only provide a very strong hint towards the importance of the quantity $R_{ab}\, q^a\, q^b$ in the description of gravitational dynamics, but also give a precise quantitative manner in which the transmutation of the gravitational Lagrangian $R \to R_{ab}\, q^a\, q^b$ can arise as a relic of a minimal length.

On the other hand, the earlier analysis [46] does not give much insight on the robustness of the conclusions drawn from the final result, and much less insight on some of the miraculous cancellations responsible for it. In particular, the following issues concerning the main inputs **P1** and **P2** were left unclear:

1. The analysis *assumed* (see **P1**) that a lower bound on geodesic distances is realized via the modification $\sigma^2 \to \sigma^2 + \ell_0^2$. While the motivation for such a modification comes from several older results, it remained unclear as to how much of the final result depends on it. This question is of fundamental significance, since the precise manner in which a minimal length is introduced in spacetime can come only from a complete framework of quantum gravity. In absence of such a framework, it is important not to make any assumptions on how distances can get modified. In particular, the modifications introduced by quantum gravity can be non-perturbative, and hence need not possess a series expansion in ℓ_0 near $\sigma^2 = 0$.

   In this work, we shall establish our result without making any such assumption. Technically, we shall keep the function $\mathcal{S}_{\ell_0} : 2\,\Omega \mapsto 2\,\widetilde{\Omega}$, which represents modification of distances, completely arbitrary and satisfying only $\left[|\mathcal{S}_{\ell_0}|/\mathcal{S}_{\ell_0}'^2\right](0) < \infty$

in addition to it's defining properties (which will be given below). In particular, the function $\mathcal{S}_{\ell_0}$ need not admit a perturbative expansion in ℓ_0, unlike the form $\mathcal{S}_{\ell_0}(x) = x + \ell_0^2$ which was used earlier [44]. The construction of q_{ab} for arbitrary $\mathcal{S}_{\ell_0}(x)$ was already sketched (see App. A of Ref. [46]), except for a crucial difference, which brings us to our second point concerning the input **P2**.

2. The requirement **P2** that two point functions get modified as $G\left[\sigma^2\right] \to \widetilde{G}\left[\sigma^2\right] = G\left[\sigma^2 + \ell_0^2\right]$ makes sense only when $G(p, p_0)$ depends on p and p_0 only through σ^2 $\forall (p, p_0)$. This can not happen in arbitrary curved spacetimes, which very much reduces the possibilities available to fix the qmetric. This is, of course, good, since it reduces the room available for *adhoc* choices. The most general space(time)s in which $G(p, p_0)$ is only a function of σ^2 $\forall (p, p_0)$ are the maximally symmetric spaces, of which flat space(time) is but the simplest possibility with zero curvature. Fixing the qmetric based on flat spacetime, although it captures the correct leading singularity of the two point functions in the coincidence limit, wipes away all information about curvature. More precisely, the leading singular structure of two point functions associated with the d'Alembartian ${}_{p_0}\Box_p$ in $(3{+}1)$-dimensional arbitrary curved spacetime is given by the Hadamard form [47]

$$G(p, p_0) := \frac{1}{(2\,\pi)^2} \left\{ \frac{\sqrt{\Delta}}{(\sigma^2/2)} + \frac{R}{12} \ln\left(\sigma^2/2\right) + \text{higher order terms} \right\}. \tag{2.5}$$

As is evident, the information about curvature, at the leading order, therefore appears in the two point functions through the so called van Vleck determinant (VVD) $\Delta(p, p_0)$. In flat spacetime, $\Delta(p, p_0) = 1$ exactly, whereas, in arbitrary curved spacetimes,

$$\lim_{p \to p_0} \Delta(p, p_0) = 1. \tag{2.6}$$

One might therefore think that the dependence of qmetric on $\Delta(p, p_0)$ can not possibly affect the coincidence limit of the Ricci biscalar $\widetilde{\mathbf{Ric}}(p, p_0)$ (or any other curvature invariant) associated with q_{ab}. This expectation is, however, wrong. Curvature involves second derivatives of the metric, and the coincidence limit of the second (or higher) derivatives of $\Delta(p, p_0)$ is not zero in general. (The exact form of the coefficients in covariant Taylor expansion of VVD are well known, and are quoted later in this chapter.) This makes it crucial to identify the dependence of qmetric on VVD. As we shall show, doing so leads to some remarkable results, all following from certain identities satisfied by the VVD.

3. The modified $\widetilde{\mathbf{Ric}}(p, p_0)$ derived earlier (cf. Ref. [46]) is in fact singular in the coincidence limit $\sigma^2 \to 0$. This divergence is cubic in q^a's, and can be regularized using known methods in point splitting regularization, as has been suggested before [46]. However, this still leaves a certain amount of discomfort at the mathematical level. It does not make much sense to appeal to point splitting regularization since our starting point, based on existence of a minimal length, does not invoke point splitting at any level, but is instead based on use of a non local second rank bi-tensor. It is therefore important to have a deeper look at this divergence and it's origin, particularly so because it depends on $\nabla_i R_{ab}$ and hence vanishes for all maximally symmetric spaces! The argument given in point 2 above advocating the use of maximally symmetric spaces therefore is not expected to help here, since the divergence is anyway zero for these spaces. One requires a much more mathematically rigorous analysis to probe the structure of this divergent term. As we shall show, identifying the correct dependence of q_{ab} on the VVD in fact cancels this divergence in a rather surprising manner. In fact, the reason for this cancellation is buried deep within the expansion of extrinsic curvature of *equi-geodesic surfaces* Σ_{G,p_0} (see below) in an arbitrary spacetime to the fourth order in covariant Taylor series, and a close relationship between VVD and extrinsic curvature of Σ_{G,p_0}.

We shall address all the above issues in this work, and while doing so, reveal the mathematical robustness of the final result, and hence it's inevitability (given the two basic inputs) in any theory which admits a Lorentz invariance short distance cut-off. Our key inputs would be much less restrictive and/or specialized than the ones used earlier (see Refs. [44, 46]), which makes the results presented here significantly stronger. These can be stated as:

- **Q1:** The requirement that geodesic distances have a Lorentz invariant lower bound.
- **Q2:** The requirement that the modified d'Alembartian $\widetilde{{}_{p_0}\Box_p}$ yields the following modification for the two point functions $G(p, p_0)$ of fields in *all maximally symmetric spacetimes*: $G\left[\sigma^2\right] \to \widetilde{G}\left[\sigma^2\right] = G\left[\mathcal{S}_{\ell_0}\left[\sigma^2\right]\right]$.

As is evident, these inputs are much more minimalistic compared with **P1, P2**, and hence can be expected to provide much more general insights into the small scale structure of spacetime.

The remainder of this chapter is structured as follows. In Sec. 2.2, we shall discuss the geodesic structure of arbitrary curved space(time)s, with focus on intrinsic and extrinsic geometry of equi-geodesic surfaces Σ_{G,p_0} [48], which comprise of points p which are at some constant geodesic distance σ^2 from p_0, and connected to p_0 by non-null geodesics. We shall also discuss the geometric significance of VVD in studying the small scale structure of spacetime, and highlight some elementary identities relating derivatives of VVD to the extrinsic curvature of Σ_{G,p_0}, which are used later in Sec. 2.4. In Sec. 2.3, we shall present the derivation of the second rank bi-tensor, the qmetric $q_{ab}(p, p_0; \ell_0)$, based on the two inputs **Q1, Q2** stated above. In particular, we shall identify the dependence of the qmetric on the VVD using our condition **Q2**. In Sec. 2.4, the Ricci bi-scalar $\widetilde{\mathbf{Ric}}(p, p_0)$ for the qmetric is obtained in a closed form based on certain tools (developed earlier in Ref. [48]), and it's coincidence limit $\sigma^2 \to 0$ is evaluated to obtain a local scalar $\left[\widetilde{\mathbf{Ric}}\right](p_0)$ at p_0. It is then shown $\left[\widetilde{\mathbf{Ric}}\right](p_0) \neq \mathbf{Ric}(p_0)$, which is one of the key results of this work. In Sec. 2.5.2, we shall complete our analysis of the Einstein-Hilbert action by evaluating the Gibbons-Hawking-York surface term in the action on equi-geodesic surfaces, for the qmetric. In Sec. 2.6, we shall finally conclude with a general discussion and implications of the results obtained in this work.

The key results of this chapter are contained in Eqs. (2.33), (2.39) and (2.46). As far as this chapter is concerned, we shall work in D-spacetime dimensions, and use the sign convention $(-, +, +, \ldots)$ for Lorentzian spaces. Latin alphabets denote spacetime indices. Also, for notational convenience, we shall use ℓ_0^2 throughout to denote short distance cutoff on geodesic distances; for timelike/spacelike cases, the replacement $\ell_0^2 \to \epsilon \ell_0^2$ must be made in the final results after which $\ell_0^2 > 0$. For convenience, we give below a quick list of some of the most recurring symbols/notation used in this chapter:

- $D_k \overset{\text{def}}{:\Longrightarrow} D - k$,
- $\mathcal{E}_{ab} = R_{ambn} q^m q^n$,
- $\mathcal{E} = g^{ab} \mathcal{E}_{ab} = R_{ab} q^a q^b$,
- $\left[\widetilde{\mathbf{Ric}}\right](p_0)$ is the coincidence limit of $\widetilde{\mathbf{Ric}}(p, p_0)$.

2.2 The geodesic structure of spacetime

2.2.1 Equi-geodesic surfaces

Mathematically, a key role in our analysis would be played by the congruence of geodesics emanating from a fixed spacetime event p_0 and the surface comprised of

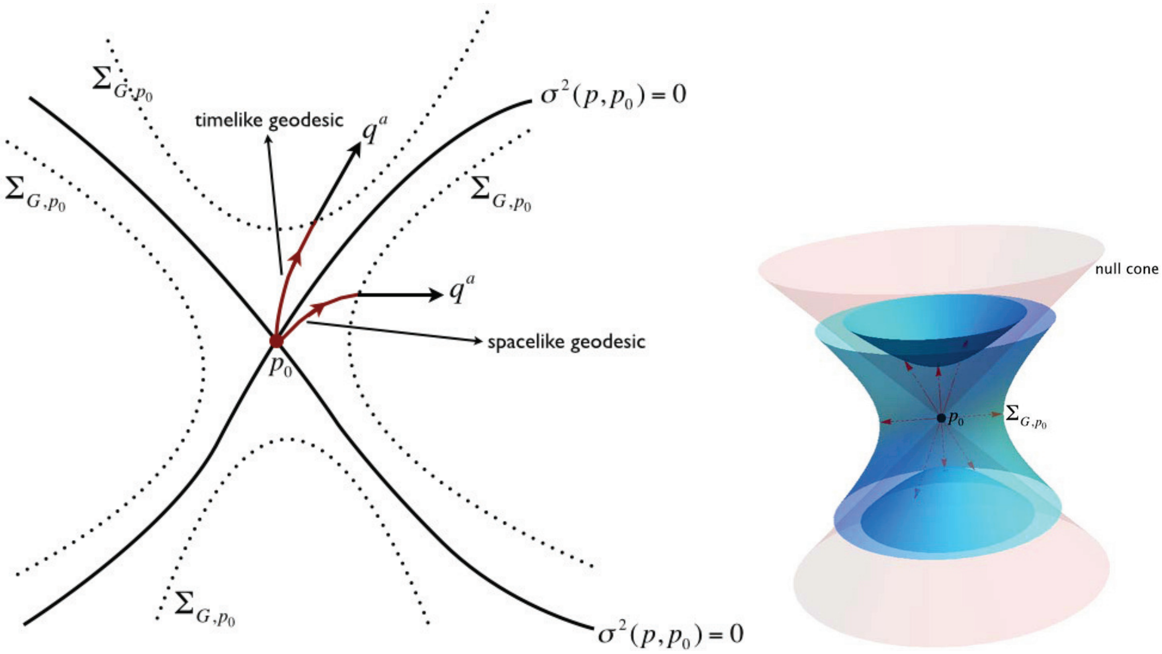

Figure 2.1: The geodesic structure of spacetime. Left: Equi-geodesic surfaces Σ_{G,p_0} attached to an event p_0 in an arbitrary curved spacetime. Right: Σ_{G,p_0} in Minkowski spacetime.

events p lying at constant geodesic interval from p_0, which we call as the *equi-geodesic* surface of event p_0 and denote it by Σ_{G,p_0} (in this context, see Fig. 2.1). The relevant geometrical properties of such surfaces in arbitrary curved spacetimes have been discussed earlier (see Ref. [48]), and we simply quote the results which we will need here.

We start with the affinely parametrized tangent vector q^a to the geodesic connecting p_0 to p

$$q_a = \frac{\nabla_a \sigma^2}{2\sqrt{\epsilon\,\sigma^2}} \tag{2.7}$$

and note that it is also the normal to Σ_{G,p_0}. The extrinsic curvature tensor of Σ_{G,p_0}, is therefore given by

$$K_{ab} = \nabla_a q_b = \frac{\nabla_a \nabla_b\,(\sigma^2/2) - \epsilon\, q_a\, q_b}{\sqrt{\epsilon\,\sigma^2}}. \tag{2.8}$$

This particular foliation, which characterizes the local geodesic structure of any spacetime, has many interesting properties, and all of these derive from the well known covariant Taylor series expansion of the bi-tensor $\nabla_a \nabla_b\,(\sigma^2/2)$ at p near p_0 [49]:

$$\nabla_a \nabla_b \left(\frac{1}{2}\sigma^2\right) = g_{ab} - \frac{\lambda^2}{3}\,\mathcal{E}_{ab} + \frac{\lambda^3}{12}\,\nabla_{\boldsymbol{q}}\mathcal{E}_{ab} - \frac{\lambda^4}{60}\left(\nabla^2_{\boldsymbol{q}}\mathcal{E}_{ab} + \frac{4}{3}\,\mathcal{E}_{ia}\,\mathcal{E}^{i}_{\ b}\right) + O(\lambda^5), \tag{2.9}$$

where $\nabla_{\boldsymbol{q}} \equiv q^i \nabla_i$.

Therefore, we see that the extrinsic geometry of such a equi-geodesic 'foliation' is very special, and completely characterized by the *tidal tensor* $\mathcal{E}_{ab} = R_{ambn}\, q^m\, q^n$. In fact, the intrinsic and extrinsic curvatures can be characterized by systematic Taylor expansions around p_0, given by [48]

$$
\begin{aligned}
K_{ab} &= \frac{1}{\lambda}\, h_{ab} - \frac{\lambda}{3}\, \mathcal{E}_{ab} + \frac{\lambda^2}{12}\, \nabla_{\boldsymbol{q}} \mathcal{E}_{ab} - \frac{\lambda^3}{60}\, F_{ab} + \mathcal{O}(\lambda^4), && \text{(2.10a)}\\
K &= \frac{D_1}{\lambda} - \frac{\lambda}{3}\, \mathcal{E} + \frac{\lambda^2}{12}\, \nabla_{\boldsymbol{q}}\, \mathcal{E} - \frac{\lambda^3}{60}\, F + \mathcal{O}(\lambda^4), && \text{(2.10b)}\\
\mathcal{R}_{\Sigma_{G,p_0}} &= \frac{\epsilon\, D_1\, D_2}{\lambda^2} + R - \frac{2\,\epsilon\,(D+1)}{3}\, \mathcal{E} + \lambda\, \frac{\epsilon\, D_2}{6}\, \nabla_{\boldsymbol{q}} \mathcal{E} \\
&\quad - \epsilon\, \lambda^2 \left[\frac{(9-2\,D)}{45}\, \mathcal{E}_{ab}^2 - \frac{\mathcal{E}^2}{9} + \frac{D_2}{30}\, \nabla_{\boldsymbol{q}}^2 \mathcal{E} \right] + \mathcal{O}(\lambda^3), && \text{(2.10c)}
\end{aligned}
$$

where

$$
\begin{aligned}
F_{ab} &= \nabla_{\boldsymbol{q}}^2 \mathcal{E}_{ab} + \frac{4}{3}\, \mathcal{E}_{ak}\, \mathcal{E}^k{}_b, && \text{(2.11a)}\\
F &= g^{ab}\, F_{ab}. && \text{(2.11b)}
\end{aligned}
$$

For later use, we also quote here the combination (easily derived from above):

$$
\begin{aligned}
K_{ab}^2 - \eta\, K^2 &= (1 - \eta\, D_1) \left[\frac{D_1}{\lambda^2} - \frac{2}{3}\, \mathcal{E} + \frac{\lambda}{6}\, \nabla_{\boldsymbol{q}} \mathcal{E} - \frac{\lambda^2}{30} \left(\nabla_{\boldsymbol{q}}^2 \mathcal{E} - \frac{4}{3} \mathcal{E}_{ab}^2 \right) \right] \\
&\quad + \frac{\lambda^2}{9}\, \left(\mathcal{E}_{ab}^2 - \eta\, \mathcal{E}^2 \right) + \mathcal{O}(\lambda^3) && \text{(2.12)}
\end{aligned}
$$

for any arbitrary η. As we shall see, the structure of the above expression, which requires keeping up to fourth order terms in K_{ab} and K [that is, terms of $\mathcal{O}(\lambda^3)$], hold the key to elimination of coincidence limit divergences in $\widetilde{\mathbf{Ric}}(p, p_0)$, in conjunction with a couple of differential identities (involving K_{ab} and K) satisfied by the VVD, which we discuss next.

2.2.2 van Vleck determinant

The van Vleck determinant, $\Delta(p, p_0)$, is an extremely important object in semi-classical physics. Geometrically, this bi-scalar governs the properties of geodesic congruences emanating from a point, say p_0, as a function of an arbitrary point p. The immense physical importance of this object certainly warrants a longer discussion than presented here (in this context, see Refs. [49, 50, 51]). In fact, as we shall see, the geometrical significance of

VVD holds the key to its relevance for the small scale structure of spacetime, a theme that will resonate constantly throughout this chapter.

The VVD is defined as follows:

$$\Delta(p,p_0) = \frac{1}{\sqrt{g(p)\,g(p_0)}} \det\left\{\nabla_a^{(p)}\nabla_b^{(p_0)}\left[\frac{\sigma^2(p,p_0)}{2}\right]\right\}. \tag{2.13}$$

Two of the most important differential identities that we shall use, connecting the VVD with the extrinsic curvature of Σ_{G,p_0}, are the following:

$$I1: \qquad \nabla_{\boldsymbol{q}} \ln\Delta = \frac{D_1}{\sqrt{\epsilon\,\sigma^2}} - K, \tag{2.14a}$$

$$I2: \qquad \nabla_{\boldsymbol{q}}\nabla_{\boldsymbol{q}} \ln\Delta = -\frac{D_1}{\epsilon\,\sigma^2} + K_{ab}^2 + R_{ab}\,q^a\,q^b, \tag{2.14b}$$

where $\nabla_{\boldsymbol{q}} \equiv q^i\,\nabla_i$ and $K_{ab}^2 \equiv K_{ab}\,K^{ab}$.

Proofs of $I1$ and $I2$: The above elementary identities follow trivially from the expression [50, 51, 52]

$$\nabla_i\left[\Delta\nabla^i\sigma^2\right] = 2\,D\,\Delta. \tag{2.15}$$

Noting that the acceleration a^i of q^i is zero since q^i represents tangents to geodesics, we can write the above identity as

$$\nabla_{\boldsymbol{q}} \ln\Delta = \frac{D_1}{\sqrt{\epsilon\,\sigma^2}} - K \tag{2.16}$$

which is $I1$. Operating once more with $\nabla_{\boldsymbol{q}}$, and using the (easily proved) differential geometric identity

$$\nabla_{\boldsymbol{q}} K = q^i\,\nabla_i\,\nabla_j q^j = -K_{ab}^2 - R_{ab}\,q^a\,q^b + \nabla_i a^i \tag{2.17}$$

with $a^i = 0$, we get $I2$.

2.2.3 An aside: The van Vleck determinant and the surface term

As an aside, let us point out the possible relevance of the VVD in the gravitational action when one focuses on an observer dependent description of gravitational dynamics based on causal structure associated with an arbitrary event ('observer') p_0. The relevance of such a description has gained increased attention since the original proposal of using local Rindler frames as probes of gravitational dynamics (in this context, see Ref. [53]). We shall focus on the equi-geodesic surfaces Σ_{G,p_0} straddling the causal boundaries of an arbitrary event p_0, and briefly comment on the null limit in the end.

The complete Einstein-Hilbert action is given by [54]

$$16\,\pi\,\mathcal{A}_{EH} = \int\limits_{\mathcal{V}} R\,\mathrm{d}V_D + 2\,\epsilon \int\limits_{\partial\mathcal{V}} (K - K_0)\,\mathrm{d}\Sigma_{D-1} \tag{2.18}$$

where $\mathrm{d}V_D, \mathrm{d}\Sigma_{D-1}$ are covariant volume elements in bulk and boundary respectively. The subtraction term, K_0, is usually taken to be the trace of extrinsic curvature of the boundary surface embedded in flat spacetime. Usually, the boundary ∂V is taken at infinity. However, given the fact that the causal structure of spacetime limits the amount of information accessible at an event p_0, it is interesting to ask for the contribution of the boundaries Σ_{G,p_0} (which, in the null limit, would make the null cone of p_0). We therefore write

$$16\,\pi\,\mathcal{A}_{EH} = \int\limits_{\mathcal{V}_{p_0}} R\,\mathrm{d}V_D + 2\,\epsilon \left(\int\limits_{\partial\mathcal{V}_\infty} + \int\limits_{\Sigma_{G,p_0}} \right) (K - K_0)\,\mathrm{d}\Sigma_{D-1}. \tag{2.19}$$

[Note the subscript p_0 on $\mathcal{V}$; we include it as a reminder that we are now focusing on quantities from the point of view of a specific event (observer) p_0.]

The trace of extrinsic curvature of Σ_{G,p_0}, as embedded in *flat* spacetime, is $K_0 = D_1/\sqrt{\epsilon\,\sigma^2}$. Recalling $I1$, this immediately implies

$$(K - K_0)_{\Sigma_{G,p_0}} = -q^i\,\nabla_i \ln\Delta. \tag{2.20}$$

Using divergence theorem, $\int_{\Sigma_{G,p_0}} q^i \nabla_i \ln\Delta = \int_V \Box \ln\Delta$. (We must include a similar contribution from $\partial\mathcal{V}_\infty$; we do not write this explicitly since we are only interested in the contribution from Σ_{G,p_0}.) Putting all this together, we get

$$16\,\pi\,\mathcal{A}_{EH} = \int\limits_{\mathcal{V}_{p_0}} (R - 2\,\epsilon\,\Box\ln\Delta)\,\mathrm{d}V_D + \mathcal{A}_{\partial\mathcal{V}_\infty}, \tag{2.21}$$

where we have dumped all contributions from $\partial\mathcal{V}_\infty$ in $\mathcal{A}_{\partial\mathcal{V}_\infty}$. Let us now comment briefly on the null limit. Since the term $\Box\ln\Delta$ is purely geometrical, we expect the null limit of the bulk term above to be straightforward. However, we must point out that the issue of boundary term for null boundaries is not completely unambiguous [55], and it might therefore require more care to repeat the above steps for a strictly null surface.

The above analysis strongly suggests that an observer dependent study of gravitational dynamics might require us to change the conventional description based on Einstein-Hilbert Lagrangian. In the rest of this chapter, we will actually present a much stronger result suggesting a very natural transmutation of the gravitational Lagrangian from R to $R_{ab}\,q^a\,q^b$ in presence of a Lorentz invariant short distance cut-off.

2.3 The idea of the qmetric

We now have the basic geometric tools using which we can implement **Q1** and **Q2** to arrive at a geometrical description of spacetime at small scales. Our aim in this section would be to construct the so called *qmetric* $q_{ab}(p, p_0; \ell_0)$ (as described in Ref. [44]), which would reduce to the background spacetime metric $g_{ab}(p)$ for $d(p, p_0) \gg \ell_0$, but which yields geodesic distances bounded from below by ℓ_0, while maintaining Lorentz invariance. As was shown earlier (see Ref. [44]), the general form of q_{ab} turns out to be (throughout this chapter, $q^a = g^{ab} q_b$)

$$q^{ab} = A^{-1} g^{ab} + \epsilon\, Q\, q^a\, q^b = A^{-1}\, h^{ab} + \epsilon\, (A^{-1} + Q)\, q^a\, q^b \tag{2.22}$$

with the corresponding covariant components q_{ab} being given by

$$q_{ab} = A\, g_{ab} - \epsilon\, B\, q_a\, q_b, \tag{2.23}$$

where $B \equiv Q\, A / \, (A^{-1} + Q)$, $h^{ab} = g^{ab} - \epsilon\, q^a\, q^b$ is the induced metric on Σ_{G,p_0}, and A and Q are functions of events p and p_0 to be fixed by **Q1** and **Q2**.

The requirement of minimal length, **Q1**, can be imposed [44, 46] using the Hamilton-Jacobi equation satisfied by $\sigma^2 = 2\,\Omega$ [52]

$$g^{ab}\, \partial_a\, \sigma^2\, \partial_b \sigma^2 = 4\, \sigma^2 \tag{2.24}$$

and requiring

$$q^{ab}\, \partial_a \mathcal{S}_{\ell_0}\, \partial_b \mathcal{S}_{\ell_0} = 4\, \mathcal{S}_{\ell_0}. \tag{2.25}$$

We make no assumptions about precisely how quantum gravity would actually affect geodesic intervals, that is, we construct q_{ab} for *arbitrary* modification of distances $\mathcal{S}_{\ell_0} :\; 2\,\Omega \to 2\,\widetilde{\Omega}$. We will only require:

1. $\mathcal{S}_{\ell_0}(0) = \ell_0^2$ (the condition of minimal length),

2. $\mathcal{S}_0$ is identity: $\mathcal{S}_0(2\Omega) = 2\Omega$,

3. $\left[|\mathcal{S}_{\ell_0}| / \mathcal{S}'^2_{\ell_0} \right](0) < \infty$.

The Hamilton-Jacobi equation, Eq. (2.25), then partially fixes the following combination in the qmetric (as was sketched in App. A of Ref. [46]):

$$\alpha \equiv A^{-1} + Q = \frac{1}{\sigma^2}\, \frac{\mathcal{S}_{\ell_0}(\sigma^2)}{\mathcal{S}'^2_{\ell_0}(\sigma^2)}. \tag{2.26}$$

We now use **Q2** to fix the qmetric completely (which is where we differ significantly with the presentation in Refs. [44, 46]). Recalling the condition **Q2** explained in detail in the introductory section of the chapter, we will require that the two point functions of the modified d'Alembartian $\widetilde{{}_{p_0}\Box_p}$ satisfy $\widetilde{G}\,[\sigma^2] = G\,[\mathcal{S}_{\ell_0}(\sigma^2)]$ in all maximally symmetric spacetimes (rather than just flat spacetime).

We start with the d'Alembartian operator corresponding to q_{ab} for arbitrary backgrounds g_{ab} (not necessarily maximally symmetric). After some algebra, we obtain:

$$\begin{aligned}\widetilde{\Box} &= A^{-1}\left(\Box_g + \frac{1}{2}D_3\, g^{ij}\partial_i \ln A\,\partial_j + \epsilon\,\not{\partial}\ln A\,\not{\partial}\right)\\ &\quad + \epsilon\,Q\left[\left(\nabla_i q^i + \frac{1}{2}\,D_1\,\not{\partial}\ln A\right]\not{\partial} + \not{\partial}^2\right] + \sqrt{\epsilon\,\sigma^2}\,\alpha'\,\not{\partial}\end{aligned} \tag{2.27}$$

where $D_k \equiv D - k$ and $\not{\partial} \equiv q^i\partial_i$. To impose **Q2**, we will analyze this operator for maximally symmetric spacetimes, in which A and Q are functions of only σ^2, and Eq. (2.27) becomes

$$\widetilde{\Box} = \alpha\,\Box + 2\,\alpha\,\sigma^2\left[\ln\left(\alpha A^{D_1}\right)\right]'\,\frac{\partial}{\partial\sigma^2}. \tag{2.28}$$

On the other hand, the d'Alembertian $\Box$ for maximally-symmetric spacetimes is given by

$$\Box = \frac{\partial^2}{\partial\sigma^2} + \left(\frac{\partial}{\partial\sigma}\ln\Delta^{-1} + \frac{D_1}{\sigma}\right)\frac{\partial}{\partial\sigma}, \tag{2.29}$$

where

$$\Delta^{-1/(D-1)} = \left\{\frac{\sin(|\sigma|/a)}{|\sigma|/a}, 1, \frac{\sinh(|\sigma|/a)}{|\sigma|/a}\right\} \tag{2.30}$$

is the exact expression of the van Vleck determinant in maximally symmetric spacetimes of positive, zero, and negative curvature, respectively (with radius of curvature a). The quantity $\Delta_{\mathcal{S}}$ below is defined as above with $\sigma^2 \to \mathcal{S}_{\ell_0}$.

We are now ready to impose **Q2**. As shown in App. A.1, the condition that $\widetilde{G}\,[\sigma^2] = G\,[\mathcal{S}_{\ell_0}(\sigma^2)]$ is the two point function corresponding to $\widetilde{\Box}$, which translates into $\widetilde{\Box}\widetilde{G}\,[\sigma^2] = 0$ when $\Box G\,[\sigma^2] = 0$ (for $p \neq p_0$), gives a differential equation

$$\frac{\mathrm{d}}{\mathrm{d}\sigma^2}\ln\left[\frac{A}{\mathcal{S}_{\ell_0}/\sigma^2}\left(\frac{\Delta_{\mathcal{S}}}{\Delta}\right)^{2/D_1}\right] = 0 \tag{2.31}$$

whose solution is

$$A = \frac{\mathcal{S}_{\ell_0}}{\sigma^2}\left(\frac{\Delta}{\Delta_{\mathcal{S}}}\right)^{2/D_1}, \tag{2.32}$$

where the constant of integration is fixed by the condition $A = 1$ when $\mathcal{S}_{\ell_0} = \sigma^2$.

We have therefore accomplished our aim of identifying the dependence of A, and hence the qmetric, on the VVD by appealing to maximally symmetric spaces and **Q2**. Equations (2.26) and (2.32) fix the final form of the qmetric as

$$\boldsymbol{q} = \frac{\mathcal{S}_{\ell_0}}{\sigma^2}\left(\frac{\Delta}{\Delta_{\mathcal{S}}}\right)^{+\frac{2}{D_1}} \boldsymbol{g} + \epsilon\left[\frac{\sigma^2 \mathcal{S}'^2_{\ell_0}}{\mathcal{S}_{\ell_0}} - \frac{\mathcal{S}_{\ell_0}}{\sigma^2}\left(\frac{\Delta}{\Delta_{\mathcal{S}}}\right)^{+\frac{2}{D_1}}\right] \boldsymbol{q} \otimes \boldsymbol{q} \tag{2.33}$$

with the inverse metric given by

$$q^{ab} = \frac{\sigma^2}{\mathcal{S}_{\ell_0}}\left(\frac{\Delta}{\Delta_{\mathcal{S}}}\right)^{-\frac{2}{D_1}} g^{ab} + \epsilon\left[\frac{\mathcal{S}_{\ell_0}}{\sigma^2 \mathcal{S}'^2_{\ell_0}} - \frac{\sigma^2}{\mathcal{S}_{\ell_0}}\left(\frac{\Delta}{\Delta_{\mathcal{S}}}\right)^{-\frac{2}{D_1}}\right] q^a\, q^b. \tag{2.34}$$

For maximally-symmetric spacetimes, it can be shown that the metrics g_{ab} and q_{ab} are related by a non-local, singular diffeomorphism. This is most easily seen from the line element corresponding to q_{ab} when g_{ab} is maximally symmetric (assuming $\sigma^2 > 0$ and constant positive curvature below for purpose of demonstration):

$$\mathrm{d}s^2 = \mathrm{d}\sigma^2 + \sigma^2 \Delta^{-2/D_1} \mathrm{d}\Omega^2_{D-1}, \tag{2.35a}$$

$$\widetilde{\mathrm{d}s^2} = q_{ab}\, \mathrm{d}x^a\, \mathrm{d}x^b = \left(\mathrm{d}\sqrt{\mathcal{S}_{\ell_0}}\right)^2 + \mathcal{S}_{\ell_0}\, \Delta_{\mathcal{S}}^{-2/D_1}\, \mathrm{d}\Omega^2_{D-1}. \tag{2.35b}$$

The above relationship between g_{ab} and q_{ab} will, of course, not hold in arbitrary curved spacetimes, and therefore the two metrics would have different curvatures.

The form derived earlier in the literature (in Refs. [44, 46]) turn out to be special cases of the one derived above if one chooses $\mathcal{S}_{\ell_0}(x) = x + \ell_0^2$ and $\Delta = 1$. As we will see, while the choice of $\mathcal{S}_{\ell_0}$ is just that, a choice, setting $\Delta = 1$ can be potentially dangerous, since one then risks missing important contributions to $\widetilde{\mathbf{Ric}}(p, p_0)$ arising from derivatives of Δ. In fact, this is just what happens.

2.4 Ricci scalar associated with the qmetric

Having found the qmetric, Eq. (2.33), in terms of modification of geodesic distances $\mathcal{S}_{\ell_0}$ and the VVD, we can now proceed to evaluate the Ricci *bi*-scalar $\widetilde{\mathbf{Ric}}(p, p_0)$ corresponding to it. This is the simplest curvature invariant associated with any spacetime, and more importantly for us, the Ricci scalar is the simplest Lagrangian describing gravitational dynamics in general theory of relativity. We can then construct a scalar from $\widetilde{\mathbf{Ric}}(p, p_0)$ by taking the coincidence limit $p \to p_0$, and compare it with $\mathbf{Ric}(p_0)$, the Ricci scalar of the background spacetime g_{ab}. Naively, one might expect that

$$\left[\widetilde{\mathbf{Ric}}\right](p_0) \stackrel{?}{=} \mathbf{Ric}(p_0) + \text{terms of order } \ell_0. \tag{2.36}$$

We will explicitly calculate $\lim_{\ell_0 \to 0} \left[\widetilde{\mathbf{Ric}}\right](p_0)$ to verify this, and show that the leading term is not equal to $\mathbf{Ric}(p_0)$. We will find an exact expression for the leading term as well as sub-leading terms in terms of the geometry of Σ_{G,p_0} and the first two derivatives of the VVD.

To proceed with the calculation, we use the following expression (derived in Ref. [48]), relating Ricci scalars of metrics related in a manner similar to q_{ab} and g_{ab}.

$$\widetilde{\mathbf{Ric}}(p, p_0) = \Omega^{-2}\, \mathbf{Ric}(p_0) + \epsilon\, \left(\alpha - \Omega^{-2}\right) \mathcal{J}_d - \epsilon\, \alpha\, \mathcal{J}_c, \tag{2.37}$$

where (borrowing notation of Ref. [48]) $\Omega^2 = A$ and

$$\begin{aligned} \mathcal{J}_c &= \epsilon\, \left[2\, D_1\, \Omega^{-1}\, \Box\Omega + D_1\, D_4\, \Omega^{-2}\, (\nabla\Omega)^2\right] + (K + D_1\, \nabla_{\boldsymbol{q}} \ln\Omega) \times \nabla_{\boldsymbol{q}} \ln\alpha\, \Omega^2, & \text{(2.38a)} \\ \mathcal{J}_d &= 2\, R_{ab}\, q^a\, q^b + K_{ab}^2 - K^2 = \epsilon\, \left(R - \mathcal{R}_{\Sigma_{G,p_0}}\right). & \text{(2.38b)} \end{aligned}$$

One can now substitute the forms of A and α from Eqs. (2.26) and (2.32) to determine the form of RHS. This is the most important, and also the most lengthy, part of the calculation. The computation is largely aided by identities $I1$ and $I2$ (Eqs. (2.14b)) satisfied by the VVD. Some of the key steps are sketched in App. A.2. The final result turns out to be

$$\begin{aligned} \widetilde{\mathbf{Ric}}(p, p_0) &= \underbrace{\left[\frac{\sigma^2}{\mathcal{S}_{\ell_0}}\, \zeta^{-2/D_1}\, \mathcal{R}_{\Sigma_{G,p_0}} - \frac{D_1\, D_2}{\mathcal{S}_{\ell_0}} + 4\,(D+1)\,(\ln\Delta_{\mathcal{S}})^\bullet\right]}_{\boldsymbol{Q_0}} \\ &\quad \underbrace{- \frac{\mathcal{S}_{\ell_0}}{\lambda^2 \mathcal{S}_{\ell_0}'^2} \left\{K_{ab}K^{ab} - \frac{1}{D_1} K^2\right\}}_{\boldsymbol{Q_K}} + \underbrace{4\, \mathcal{S}_{\ell_0} \left\{-\frac{D}{D_1}\, [(\ln\Delta_{\mathcal{S}})^\bullet]^2 + 2\,(\ln\Delta_{\mathcal{S}})^{\bullet\bullet}\right\}}_{\boldsymbol{Q_\Delta}}, \end{aligned} \tag{2.39}$$

where we have defined $\zeta = \Delta/\Delta_{\mathcal{S}}$, $(\ln\Delta_{\mathcal{S}})^\bullet = \mathrm{d}\ln\Delta_{\mathcal{S}}/\mathrm{d}\mathcal{S}_{\ell_0}$, and $(\ln\Delta_{\mathcal{S}})^{\bullet\bullet} = \mathrm{d}(\ln\Delta_{\mathcal{S}})^\bullet/\mathrm{d}\mathcal{S}_{\ell_0}$. It is not too difficult to see that for $\ell_0 = 0, \mathcal{S}_0(x) = x$, the Right Hand Side (RHS) of the above expression reduces to $\mathbf{Ric}(p_0)$. (To verify this, one has to use $I1, I2$ from Eqs. (2.14b) above along with $\nabla_{\boldsymbol{q}} \equiv 2\,\epsilon\,\lambda\,\mathrm{d}/\mathrm{d}\sigma^2$.)

It is crucial to note here that we have not used any of the covariant Taylor expansions yet; the above expression, therefore, does not assume the region of spacetime under consideration to be smooth (*i.e.* having finite curvature). This will be important for discussing the implications of our framework for cosmological and black hole singularities, which we wish to address in future work.

For the purpose of this work, however, we shall assume that we are working in smooth regions of spacetime, so that the various Taylor expansions given in Sec. 2.2 can be used. The significance of separating out the RHS into $\boldsymbol{Q_0}, \boldsymbol{Q_{\mathrm{K}}}$ and $\boldsymbol{Q_{\Delta}}$ will become evident shortly.

The above expression holds the key to understand non-perturbative effects of a covariant short distance cut-off on spacetime curvature. Let us therefore first highlight some of it's most important mathematical aspects, before taking it's $\ell_0 \to 0$ limit.

1. The expression contains no derivatives of the function $\mathcal{S}_{\ell_0}(x)$ higher than one. This is an extremely delicate mathematical point; as can be seen from the details provided in App. A.2, terms of the form $\mathcal{S}''_{\ell_0}$ do in fact appear in the intermediate steps, but they cancel out in the final expression. Since $\mathcal{S}_{\ell_0}(x)$ represents (in general, non-perturbative) effects of quantum gravity on invariant distance between spacetime events, the non-existence of higher derivatives of $\mathcal{S}_{\ell_0}$ in $\widetilde{\mathbf{Ric}}(p, p_0)$ is of deep conceptual importance — it tells us that semi-classical effects of quantum gravity can be captured only via limited information about the precise details of quantum gravity.

2. The Ricci bi-scalar $\widetilde{\mathbf{Ric}}(p, p_0)$ is completely described by the *geodesic structure of spacetime*, characterized by:

   (a) $\mathcal{R}_{\Sigma_{G,p_0}}$ (intrinsic curvature),

   (b) K_{ab} (extrinsic curvature), and

   (c) the van Vleck determinant $\Delta(p, p_0)$.

3. The extrinsic curvature of Σ_{G,p_0} appears only in a very special combination, which (as we will see in a moment), is responsible for *no coincidence limit divergences*! This is essentially a consequence of Eq. (2.12) for $\eta = 1/D_1$.

2.5 Relic of minimal length: The limit $\ell_0 \to 0$

2.5.1 The Ricci bi-scalar

The coincidence limit of $\widetilde{\mathbf{Ric}}(p, p_0)$ gives us a local scalar $\left[\widetilde{\mathbf{Ric}}\right](p_0)$ at each spacetime event p_0 which will depend on ℓ_0. We wish to examine whether this scalar gives back

$\mathbf{Ric}(p_0)$, the Ricci scalar of the background spacetime, when ℓ_0 is set to zero. The limit $\ell_0 \to 0$ must be taken with care. First of all, note that any ℓ_0 independent contribution must come from $\boldsymbol{Q}_{\mathbf{0}}$. The contribution from $\boldsymbol{Q}_{\mathbf{K}}$ and $\boldsymbol{Q}_{\boldsymbol{\Delta}}$ can only be $\mathcal{O}(\ell_0^2)$, since $\mathcal{S}_{\ell_0}(0) = \ell_0^2$. Let us therefore first focus on $\boldsymbol{Q}_{\mathbf{0}}$.

To do this, we invoke the coincidence limit expansions of various quantities given in Eqs. (2.10c), in addition to the following well known covariant Taylor expansion of the VVD:

$$\Delta^{1/2}(p, p_0) = 1 + \frac{\lambda^2}{12} R_{ab}\, q^a\, q^b + \mathcal{O}(\lambda^3) \tag{2.40}$$

from which it is easy to see that

$$\lim_{\ell_0 \to 0} \lim_{\sigma^2 \to 0} (\ln \Delta_{\mathcal{S}})^{\bullet} = \frac{\epsilon}{6} \left[R_{ab} q^a q^b\right](p_0). \tag{2.41}$$

Also, using the last of Eqs. (2.10c) for $\mathcal{R}_{\Sigma_{G,p_0}}$, and the fact that $\Delta(0) = 1$, we get

$$\lim_{\sigma^2 \to 0} \left(\frac{\sigma^2}{\mathcal{S}_{\ell_0}} \zeta^{-\frac{2}{D_1}} \mathcal{R}_{\Sigma_{G,p_0}} - \frac{D_1\, D_2}{\mathcal{S}_{\ell_0}} \right) = \frac{D_1\, D_2}{\mathcal{S}_{\ell_0}(0)} \left(\Delta_{\ell_0}^{\frac{2}{D_1}} - 1 \right), \tag{2.42}$$

where

$$\Delta_{\ell_0}^{1/2} = 1 + \frac{\epsilon}{12}\, \ell_0^2 \left[R_{ab} q^a q^b\right](p_0) + \dots . \tag{2.43}$$

The limit $\ell_0 \to 0$ limit of the RHS above is most easily evaluated using the *L'Hospital*'s rule (note that both the numerator and denominator vanish in this limit):

$$\lim_{\ell_0 \to 0} \frac{D_1\, D_2}{\mathcal{S}_{\ell_0}(0)} \left(\Delta_{\ell_0}^{2/D_1} - 1 \right) = \lim_{\ell_0 \to 0} \frac{D_1\, D_2}{\partial_{\ell_0^2}\, \mathcal{S}_{\ell_0}(0)} \partial_{\ell_0^2} \Delta_{\ell_0}^{2/D_1} = \frac{\epsilon}{3}\, D_2 \left[R_{ab} q^a q^b\right](p_0). \tag{2.44}$$

From Eqs. (2.41) and 2.44), we immediately get

$$\lim_{\ell_0 \to 0} \lim_{\sigma^2 \to 0} \boldsymbol{Q}_0 = \epsilon \left[\frac{D-2}{3} + \frac{4\,(D+1)}{6} \right] \left[R_{ab} q^a q^b\right](p_0) = \epsilon\, D \left[R_{ab} q^a q^b\right](p_0) = \epsilon\, D\, \mathcal{E}(p_0) \tag{2.45}$$

which is one of the most important results we have obtained in this investigation. The above limit, being independent of $\mathcal{S}_{\ell_0}(x)$, is precisely the relic left by the presence of a zero point length. Qualitatively, this is similar to the various quantum anomalies one encounters in quantum field theory in curved spacetimes (see Ref. [9]; also see the first reference of Refs. [46] for a much detailed conceptual discussion of this and related points).

Now consider $\boldsymbol{Q}_{\mathbf{K}}$, with the condition $\left[|\mathcal{S}_{\ell_0}|/\mathcal{S}_{\ell_0}'^2\right](0) < \infty$. This term would be divergent in the coincidence limit were it not for the fact that the combination of extrinsic curvature appearing here is $\mathcal{O}(\lambda^2)$, as is readily seen from Eq. (2.12) with $\eta = 1/D_1$. This is a very strong result. Any other combination of extrinsic curvature tensor would lead to coincidence limit divergences in $\left[\widetilde{\mathbf{Ric}}\right](p_0)$, and the reason the right combination appears here is completely due to the presence of VVD. In the absence of it, we would indeed get divergences (as can be seen from the result in Ref. [46]).

The final term, $\boldsymbol{Q}_{\boldsymbol{\Delta}}$, is a smooth function which would yield further $\mathcal{O}(\ell_0^2)$ dependent terms coupled to the background curvature. These terms can be read off from the known covariant Taylor expansions of the VVD.

To summarize, then, we have proved the following:

$$\lim_{\ell_0 \to 0} \left[\widetilde{\mathbf{Ric}}\right](p_0) = \epsilon\, D\, \left[R_{ab} q^a q^b\right](p_0). \tag{2.46}$$

For the sake of completeness, we quote below the higher order terms in ℓ_0 which can be obtained *if one further assumes that all the quantities involved allow a legitimate series expansion in ℓ_0 in the coincidence limit.* We must, however, caution that such an assumption could be highly objectionable (even wrong) in full quantum gravitational context. Nevertheless, the expansion turns out to be:

$$\begin{aligned}\left[\widetilde{\mathbf{Ric}}\right](p_0) \;&=\; \epsilon\, D\, \mathcal{E}(p_0) + \frac{2\,\epsilon\,(D+1)}{3} (\nabla_{\boldsymbol{q}} \mathcal{E})\, \ell_0 \\ &\quad + \left\{ \frac{1}{18} \left[D + 2 - \frac{2}{\mathcal{S}'(0)^2} \right] \left(\mathcal{E}_{ab}^2 - \frac{\mathcal{E}^2}{D_1} \right) + \frac{D+2}{4}\, \nabla_{\boldsymbol{q}}^2\, \mathcal{E} \right\} \ell_0^2 + \mathcal{O}(\ell_0^3).\end{aligned} \tag{2.47}$$

2.5.2 The surface term on Σ_{G,p_0}

In the previous sub-section, we analyzed the Ricci bi-scalar $\widetilde{\mathbf{Ric}}(p, p_0)$ for the qmetric and showed that it's coincidence limit becomes proportional to $R_{ab}\, q^a\, q^b$ in the limit $\ell_0 \to 0$. We now calculate the contribution of the surface term $\widetilde{K\sqrt{|h|}}$ for the equi-geodesic surfaces using the qmetric. This is a much simpler calculation than that of $\widetilde{\mathbf{Ric}}(p, p_0)$, and is along the same lines as the one given earlier (see the second reference in Refs. [46]), so we will be brief.

We start with the following relation between induced metrics and the extrinsic curvatures [48]

$$\sqrt{|\widetilde{h}|} \;=\; A^{D_1/2} \sqrt{|h|}, \tag{2.48a}$$

$$\widetilde{K} \;=\; \sqrt{\alpha} \left(K + \frac{D_1}{2} \nabla_q \ln A \right). \tag{2.48b}$$

Since by definition $K = \partial \ln \sqrt{|h|} / \partial \lambda$, the series for K in Eq. (2.10c) readily yields

$$\sqrt{|h|} = \lambda^{D_1} \left[1 - \frac{\lambda^2}{6}\, \mathcal{E}(p_0) + \frac{\lambda^3}{36}\, \nabla_{\boldsymbol{q}} \mathcal{E}(p_0) + \mathcal{O}(\lambda^4) \right]. \tag{2.49}$$

Putting everything together, we get

$$\lim_{\sigma^2\to 0} \widetilde{K\sqrt{|h|}} = \frac{\ell_0^D}{\Delta_{\ell_0}} \left(\frac{D_1}{\ell_0^2} - 2 \lim_{\sigma^2\to 0} (\ln \Delta_{\mathcal{S}})^{\bullet} \right). \tag{2.50}$$

The above limit of the surface term corresponds to the surfaces Σ_{G,p_0} straddling very close to the causal horizon of p_0. If one takes the limit $\ell_0 \to 0$ above, it gives zero, and hence there is no non-trivial effect on the surface term as was found in $\widetilde{\mathbf{Ric}}(p, p_0)$.

Again, *if one can justify a series expansion in ℓ_0*, one arrives at

$$\begin{aligned} \lim_{\sigma^2\to 0} \widetilde{K\sqrt{|h|}} &= D_1\, \ell_0^{D-2} \left[1 - \frac{D+1}{6\,(D-1)}\, \mathcal{E}(p_0)\ell_0^2 + \mathcal{O}(\ell_0^3) \right] \\ &\overset{D=4}{=} 3\,\ell_0^2 - \frac{5}{6}\, \mathcal{E}(p_0)\, \ell_0^4 + \mathcal{O}(\ell_0^5) \end{aligned} \tag{2.51}$$

in which the first two terms have the same form as obtained earlier (see the second reference in Refs. [46]), where no expansion in ℓ_0 was needed.

2.6 Discussion

As mentioned in the introductory section, one needs only a very few conceptual inputs from semi-classical gravity to deduce some basic facts about spacetime at small scales. The existence of a lower bound on spacetime intervals is one such input, and if it turns out to be a fundamental feature of quantum gravity, it makes sense to look for a geometric description of spacetime in terms of objects which are likely to be more useful in incorporating such a lower bound. Bi-tensors, then, provide a natural choice, and indeed, if one looks deeper into our theories of classical general theory of relativity and quantum field theory, some of the most important features of these theories, such as geodesic deviation, focusing of geodesics, causal structure, singularity structure of two point functions *etc.*, are characterized in terms of bi-tensors. Characterizing the small scale topology of spacetime is another aspect which would necessitate a description directly in terms of bi-tensors such as the distance function $d(p, p_0)$. This is the point of view which was stressed in Ref. [44], developed and described in much greater conceptual detail in Refs. [46], and has been put on a much more rigorous basis in this work. Our general expression (2.39) for the Ricci bi-scalar $\widetilde{\mathbf{Ric}}(p, p_0)$ of the qmetric presents a natural basis for the description of gravitational dynamics by a non-local action. This can be particularly relevant for study of spacetime singularities, where one can not use covariant Taylor expansions[1].

[1] The idea of gravity being described fundamentally by a non-local action, with geodesic distance playing the key role, seems to be *conceptually* in tune with certain ideas already discussed in the literature (in this context, see Refs. [56]).

Although mathematical complexity forced us to look at only the Ricci scalar (instead of the full Riemann tensor) for geometries with a covariant short distance cut-off, the resulting expression very elegantly and concretely expresses the key idea: curvature of spacetime might be solely expressible in terms of behaviour of it's geodesics and related bi-tensorial quantities. In absence of a lower bound on geodesic distances, such a description would coincide with the standard one in terms of local tensors such as $g_{ab}(p), R_{abcd}(p)$ *etc.*. However, if there exists a minimal length, then the non-local character of bi-tensors, combined with the non-analytic deformation of geometry necessitated by such a minimal length, might lead to a very different description of spacetime curvature at smallest of scales; in particular, it may leave a relic independent of the details or value of the short distance cut-off, thereby acting as a crucial guidepost towards our understanding of classical gravity itself [57].

The mathematical results derived here, for example, seem to strongly support the so called emergent gravity paradigm, in which gravitational dynamics is described in terms of thermodynamics of future causal horizon of an event p_0. Two of the key ideas in this context — the use of *local Rindler frames* as probes of spacetime curvature (see Ref. [53]), and a variational principle based on *entropy functional* (in this context, see Refs. [58]) — find a unified and purely geometric description in our framework in terms of equi-geodesic *surfaces* (which replace the Rindler *trajectories*) and the $\ell_0 = 0$ term of the coincidence limit of Ricci bi-scalar of the qmetric, which happens to have the same form as the entropy functional.

The possibility of description of geometry in terms of two point functions of quantum fields has also been emphasized, in a series of papers (see Refs. [59]). The connection with the work presented here is obvious: the UV behavior of two point functions is in one to one correspondence with vanishing of geodesic distances in the coincidence limit, which, of course, was the basis for our input **Q2**. In fact, there could also be a more fundamental connection at the level of geometry itself. For example, it has been pointed out that the commutation relation between position and momenta, $[\hat{\boldsymbol{x}}^\mu, \hat{\boldsymbol{p}}_\nu]$, would in general acquire a correction on a curved manifold, thereby affecting the resultant uncertainties [60]. We expect to present more details on this particular connection in a future work (which is in progress).

We hope to apply the results derived here to analyze implications of a Lorentz invariant minimal length for issues such as cosmological and black hole singularities, trans-Planckian problem in black hole physics and cosmology, and possible relevance for the cosmological constant problem.

Chapter 3

Response of a rotating detector in polymer quantum field theory

3.1 A variant of the Unruh effect

Despite decades of sustained effort, a viable quantum theory of gravity continues to elude us. In such a scenario, over the last twenty five years or so, a variety of approaches have been constructed *by hand* to investigate possible imprints of Planck scale effects on phenomena involving matter fields (see, for instance, the reviews [23]). These methods evidently involve a new scale (often assumed to be of the order of the Planck scale) and they strive to capture one or more features that are expected to arise in the complete quantum theory of gravity. An important goal is to utilize these approaches to examine whether high energy effects will modify phenomena at observably low energies.

One such phenomenological approach is the approach referred to as polymer quantization [27]. The method of polymer quantization can be said to be inspired by loop quantum gravity [6]. (We should hasten to clarify that the approach we shall consider is different from another related method, also inspired by loop quantum gravity, and often referred to by a very similar name [28]. In the approach, the configuration space is considered to be discrete, whereas in the method that we shall adopt, it remains continuous.) Using the standard Fourier decomposition of a field into oscillators and the polymer method of quantization of the oscillators [28], one can arrive at a modified propagator governing a quantum field in the Minkowski spacetime (see Ref. [27]; for a very recent discussion, see Ref. [61]). While the modified propagator is identical to the conventional propagator (in Fourier space) at low energies, it behaves differently at high energies (in this context, see Ref. [62]). It is the modified propagator which we shall utilize in this work to study a phenomenon closely related to the Unruh effect in flat spacetime.

The Unruh effect refers to the thermal nature of the Minkowski vacuum when viewed by an observer in motion along a uniformly accelerated trajectory (for the original efforts, see Refs. [13, 14, 15]; for relatively recent reviews, see Refs. [16, 17]). As we had mentioned in the introductory chapter, it has a close relation to Hawking radiation from black holes [11] and, due to this reason, the effect provides an important scenario to investigate possible quantum gravitational effects. In fact, the question of Unruh effect in polymer quantization has received some attention recently in the literature [63, 64, 65]. On the one hand, it has been claimed that, in polymer quantization, the Rindler vacuum may *not* be inequivalent to the Minkowski vacuum [63]. On the other, it has been argued that the response of a uniformly accelerated Unruh-DeWitt detector coupled to a polymer quantized field would not vanish [64]. In fact, it has been found that even an inertial detector will respond non-trivially (under certain conditions) in polymer quantization [64, 65].

It is in such a situation that we choose to study the response of a rotating Unruh-DeWitt detector that is coupled to a polymer quantized field in this work [22, 66, 67, 68]. As we shall see, the propagator in polymer quantization can be expressed as a series of propagators described by specific modified dispersion relations, along with corresponding changes to the measure of the density of the modes [27]. Since modified dispersion relations break Lorentz invariance, the corresponding propagators do not prove to be time translation invariant in the frame of a uniformly accelerated detector. This aspect makes it rather difficult to explicitly evaluate the transition probability of an accelerated detector. In contrast, since modified dispersion relations preserve rotational invariance, the corresponding propagators prove to be time translation invariant in the frame of a rotating detector, a property which allows the transition probability rate to be evaluated [68]. Actually, it is such a feature that has recently been exploited to study the response of an inertial detector that is coupled to a polymer quantized field [65].

This chapter is organized as follows. In the following section, we shall quickly review the response of inertial and rotating Unruh-DeWitt detectors that are coupled to a massless scalar field governed by the standard linear dispersion relation in Minkowski spacetime. In Sec. 3.3, we shall briefly discuss the response of these detectors when they are coupled to a scalar field characterized by a modified dispersion relation. In Sec. 3.4, we shall consider the response of detectors coupled to a scalar field described by polymer quantization. We shall conclude with a summary of the results and their implications in the final section.

At this stage, a few words on the conventions and notations that we shall adopt in this chapter are in order. We shall set $\hbar = c = 1$ and, for simplicity in notation, we shall denote the spacetime coordinates x^μ as $\tilde{x}$. We shall work in $(3{+}1)$-spacetime dimensions and with the metric signature of $(+,-,-,-)$. As far as the spatial coordinates $\boldsymbol{x}$ are concerned, we shall be working with either the Cartesian coordinates (x, y, z) or the cylindrical polar coordinates (ρ, θ, z), as convenient.

3.2 Detector coupled to the standard scalar field

In this section, we shall rapidly summarize the response of inertial and rotating Unruh-DeWitt detectors coupled to the standard, massless scalar field in flat spacetime. Since the inertial and rotating trajectories are integral curves of timelike Killing vector fields, typically, one first evaluates the Wightman function along the trajectory of the detector and attempts to Fourier transform the resulting Wightman function. It is well known that the inertial detector does not respond and, in the case of the rotating detector, while the response proves to be non-zero, the integral cannot be evaluated analytically, but can be easily computed numerically (see, for instance, Refs. [22, 68]). However, it proves to be convenient to express the Wightman function as a sum over the normal modes and evaluate the Fourier transform (with respect to the differential proper time) first before evaluating the sum. In the rotating case, though the final sum needs to be calculated numerically, this method happens to be rather effective as the sum converges very quickly. Importantly, as we shall illustrate, this method can be immediately extended to situations wherein the field is described by a modified dispersion relation [68].

3.2.1 The Unruh-DeWitt detector

A detector can be considered to be an operational tool in an attempt to define the concept of a particle in a generic situation. It corresponds to an idealized point like object, whose motion is described by a classical worldline, but which nevertheless possesses internal, quantum energy levels. The detectors are basically described by the interaction Lagrangian for the coupling between the degrees of freedom of the detector and the quantum field. The simplest of the different possible detectors is the monopole detector originally due to Unruh and DeWitt [14, 15].

Consider a Unruh-DeWitt detector that is moving along a trajectory $\tilde{x}(\tau)$, where τ is the proper time in the frame of the detector. The interaction of the Unruh-DeWitt detector with a canonical, real scalar field ϕ is described by the interaction Lagrangian

$$\mathcal{L}_{\rm int}[\phi(\tilde{x})] = \bar{c}\, m(\tau)\, \phi\left[\tilde{x}(\tau)\right], \tag{3.1}$$

where $\bar{c}$ is a small coupling constant and m is the detector's monopole moment. Let us assume that the quantum field $\hat{\phi}$ is in the vacuum state, say, $|0\rangle$, and the detector is in its ground state with zero energy. It is then straightforward to establish that the transition probability of the detector to be excited to an energy state with energy eigen value $E > 0$ can be expressed as

$$P(E) = \int_{-\infty}^{\infty} \mathrm{d}\tau \int_{-\infty}^{\infty} \mathrm{d}\tau'\, \mathrm{e}^{-i\,E\,(\tau-\tau')}\, G^{+}\left[\tilde{x}(\tau), \tilde{x}(\tau')\right], \tag{3.2}$$

where $G^{+}\left[\tilde{x}(\tau), \tilde{x}(\tau')\right]$ is the Wightman function defined as

$$G^{+}\left[\tilde{x}(\tau), \tilde{x}(\tau')\right] = \langle 0|\hat{\phi}\left[\tilde{x}(\tau)\right]\ \hat{\phi}\left[\tilde{x}(\tau')\right]|0\rangle. \tag{3.3}$$

When the Wightman function is invariant under time translations in the frame of the detector — as it can occur, for example, in cases wherein the detector is moving along the integral curves of timelike Killing vector fields — one has

$$G^{+}\left[\tilde{x}(\tau), \tilde{x}(\tau')\right] = G^{+}(\tau - \tau'). \tag{3.4}$$

In such situations, the transition probability of the detector simplifies to

$$P(E) = \lim_{T\to\infty} \int_{-T}^{T} \frac{\mathrm{d}v}{2} \int_{-\infty}^{\infty} \mathrm{d}u\, \mathrm{e}^{-i\,E\,u}\, G^{+}(u), \tag{3.5}$$

where

$$u = \tau - \tau', \quad v = \tau + \tau'. \tag{3.6}$$

The above expression then allows one to define the transition probability rate of the detector to be

$$R(E) = \lim_{T\to\infty} \frac{P(E)}{T} = \int_{-\infty}^{\infty} \mathrm{d}u\, \mathrm{e}^{-i\,E\,u}\, G^{+}(u). \tag{3.7}$$

For the case of the canonical, massless scalar field, in $(3+1)$-spacetime dimensions, the Wightman function $G^{+}(\tilde{x}, \tilde{x}')$ in the Minkowski vacuum is given by

$$G^{+}(\tilde{x}, \tilde{x}') = -\frac{1}{4\,\pi^2}\left[\frac{1}{(t - t' - i\,\epsilon)^2 - (\boldsymbol{x} - \boldsymbol{x}')^2}\right], \tag{3.8}$$

where $\epsilon \to 0^{+}$ and $(t, \boldsymbol{x})$ denote the Minkowski coordinates. Given a trajectory $\tilde{x}(\tau)$ that is an integral curve of a timelike Killing vector field, the response of the detector is usually obtained by substituting the trajectory in this Wightman function and evaluating the transition probability rate (3.7). Instead, let us express the Wightman function as a sum over the normal modes, evaluate the integral over u first, before evaluating the sum.

3.2.2 Response of the inertial detector

Before considering the case of the rotating detector, it is instructive to consider the rather simple case of an inertial detector that is moving with a constant velocity, say, $\boldsymbol{v}$. The trajectory of the detector can be expressed as $\tilde{x}(\tau) = [t(\tau),\, \boldsymbol{x}(\tau)] = (\gamma\,\tau,\, \gamma\,\boldsymbol{v}\,\tau)$, where $\gamma = (1 - |\boldsymbol{v}|^2)^{-1/2}$ is the Lorentz factor. The Wightman function evaluated in the Minkowski vacuum associated with the scalar field can be expressed as a sum over the normal modes as follows:

$$G^{+}(\tilde{x}, \tilde{x}') = \int \frac{\mathrm{d}^3\boldsymbol{k}}{(2\,\pi)^3\,(2\,\omega)}\, \mathrm{e}^{-i\,\omega\,(t-t')}\, \mathrm{e}^{i\,\boldsymbol{k}\cdot(\boldsymbol{x}-\boldsymbol{x}')}, \tag{3.9}$$

where, for the massless scalar field of our interest, $\omega = |\boldsymbol{k}| \geq 0$. Let us now substitute the trajectory for the inertial detector in the above Wightman function and use the resulting expression to calculate the transition probability rate (3.7). Upon carrying out the integral over u, we obtain that

$$R(E) = \int \frac{\mathrm{d}^3\boldsymbol{k}}{(2\,\pi)^2\,(2\,\omega)}\, \delta^{(1)}\left[E + \gamma\, \left(\omega - \boldsymbol{k}\cdot\boldsymbol{v}\right)\right]. \tag{3.10}$$

Since E is positive and $(\omega - \boldsymbol{k}\cdot\boldsymbol{v}) \geq 0$, the argument of the delta function never vanishes leading to the well known result that the inertial detector does not respond at all.

3.2.3 Response of the rotating detector

Let us now turn to the case of the rotating detector. In this case, it proves to be more convenient to work with the cylindrical polar coordinates, say, (ρ, θ, z), than the Cartesian coordinates. It is straightforward to show that the Minkowski Wightman function (3.9) can be expressed in terms of the modes associated with the cylindrical polar coordinates as follows:

$$G^{+}(\tilde{x}, \tilde{x}') = \sum_{m=-\infty}^{\infty} \int\limits_{0}^{\infty} \frac{\mathrm{d}q\, q}{(2\,\pi)^2} \int\limits_{-\infty}^{\infty} \frac{\mathrm{d}k_z}{(2\,\omega)}\, \mathrm{e}^{-i\,\omega\,(t-t')}\, J_m(q\,\rho)\, J_m(q\,\rho')\, \mathrm{e}^{i\,m\,(\theta-\theta')}\, \mathrm{e}^{i\,k_z\,(z-z')}, \tag{3.11}$$

where $J_m(x)$ denotes Bessel function of the first kind and of order m, while $\omega = k = \sqrt{q^2 + k_z^2} \geq 0$.

Consider a detector moving on a circular trajectory with a radius σ and angular velocity Ω in the $z = 0$ plane. The trajectory of the detector can be expressed in terms of the cylindrical polar coordinates and the proper time as $\tilde{x}(\tau) = [t(\tau), \boldsymbol{x}(\tau)] = (\gamma\,\tau,\, \sigma,\, \gamma\,\Omega\,\tau,\, 0)$, where $\gamma = [1 - (\sigma\,\Omega)^2]^{-1/2}$ is the Lorentz factor associated with the trajectory. The transition probability rate of the detector moving along the above trajectory can be obtained by substituting the trajectory in the expression (3.11) for the Wightman function and calculating the integral (3.7). We find that the resulting transition probability rate can be expressed as

$$R(E) = \sum_{m=-\infty}^{\infty} \int_0^{\infty} \frac{\mathrm{d}q\, q}{2\,\pi}\, J_m^2(q\,\sigma) \int_{-\infty}^{\infty} \frac{\mathrm{d}k_z}{2\,\omega}\, \delta^{(1)}[E + \gamma\ (\omega - m\,\Omega)]. \tag{3.12}$$

This integral can be rewritten as

$$R(E) = \sum_{m=-\infty}^{\infty} \int_0^{\infty} \frac{\mathrm{d}k\, k}{2\,\pi}\, \delta^{(1)}[E + \gamma\ (k - m\,\Omega)] \int_0^{\pi/2} \mathrm{d}\alpha \cos\alpha\, J_m^2(k\,\sigma\cos\alpha), \tag{3.13}$$

where, for convenience, we have used the fact that $\omega = k$, as is appropriate for positive frequency modes. The angular integral over α can be evaluated using the standard integral [69]

$$\int_0^{\pi/2} \mathrm{d}\alpha \cos\alpha\, J_m^2(z\cos\alpha) = \frac{z^{2\,m}}{\Gamma(2\,m+2)}\, {}_1F_2[m+1/2; m+3/2, 2m+1; -z^2] \tag{3.14}$$

for $\mathrm{Re.}\ z \geq 0$ and $\mathrm{Im.}\ z = 0$, where ${}_1F_2[a; b, c; x]$ represents the generalized hypergeometric function. Since E and Ω are positive definite quantities by assumption and $k \geq 0$, the delta function in the expression (3.13) will be non-zero only when $m \geq \bar{E}$, where $\bar{E} = E/(\gamma\,\Omega)$ is a dimensionless energy. Therefore, the transition probability rate of the detector reduces to

$$\begin{aligned} \bar{R}(\bar{E}) &\equiv \sigma\, R(\bar{E}) \\ &= \frac{1}{2\,\pi\,\gamma} \sum_{m\geq\bar{E}}^{\infty} \left[\frac{(\sigma\, k_*)^{2\,m+1}}{\Gamma(2\,m+2)}\right] {}_1F_2[m+1/2; m+3/2, 2\,m+1; -(\sigma\, k_*)^2], \end{aligned} \tag{3.15}$$

where $k_* = (m - \bar{E})\,\Omega$ corresponds to the value k when the argument of the delta function in Eq. (3.13) vanishes. It is interesting to note that, for a given energy $\bar{E}$, the detector seems to respond to modes whose energy $\omega\ (= k)$ are proportional to the angular frequency Ω of the detector. While it does not seem to be possible to carry out the above sum analytically, it converges very quickly and hence it is easy to evaluate numerically. In Fig. 3.1, we have plotted the transition probability rate of the rotating detector (with respect to the dimensionless energy $\bar{E}$) evaluated numerically using the above result for different values of the dimensionless velocity parameter $\sigma\,\Omega$. We should clarify that we

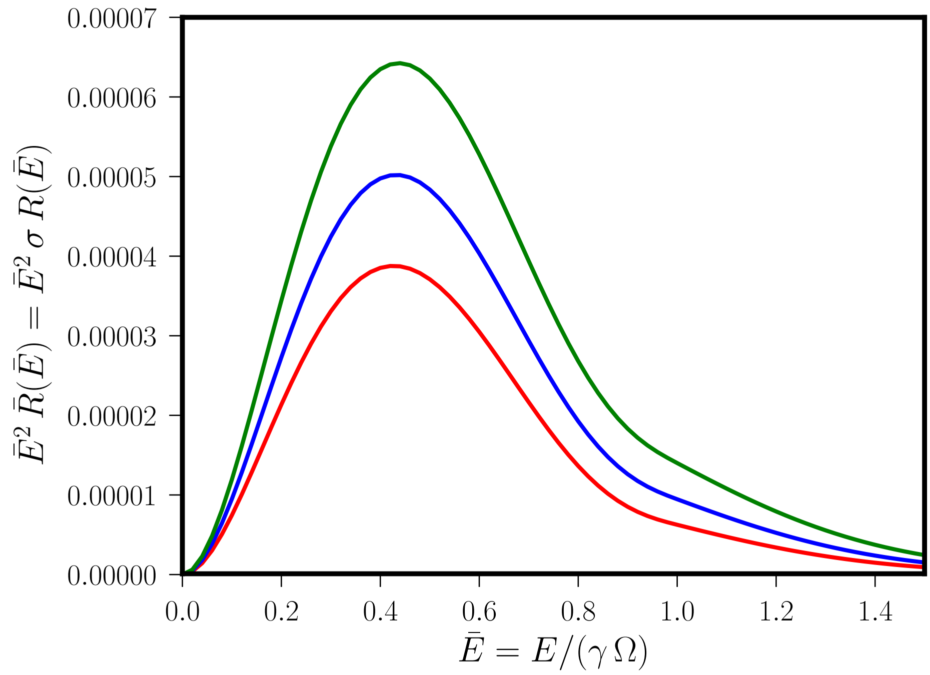

Figure 3.1: The transition probability rate of the rotating Unruh-DeWitt detector that is coupled to a massless scalar field which is governed by the standard, Lorentz invariant, linear dispersion relation. The three curves correspond to the following choices of the dimensionless velocity parameter $\sigma\,\Omega$: 0.325 (in red), 0.350 (in blue) and 0.375 (in green).

have arrived at these results by taking into account the contributions due to the first ten terms in the sum (3.15). We find that the next ten terms contribute less than 0.01%, indicating that the sum indeed converges quickly and that the contributions due to the higher terms are insignificant.

3.3 Detector coupled to a scalar field governed by a modified dispersion relation

Let us now briefly discuss the response of inertial and rotating detectors that are coupled to a scalar field governed by a dispersion relation, say, $\omega(k)$, which is no more linear. Such dispersion relations can, for instance, arise in theories which break Lorentz invariance. It can be easily shown that, in such a situation too, the Minkowski Wightman function can be expressed in the form (3.9) as in the standard case, but with the quantity $\omega(k)$ now being determined by the modified dispersion relation.

If the Wightman function is given by (3.9), it is then clear that the response of an inertial detector can also be expressed in the form (3.10), as in the standard case. Let us first consider a completely super-luminal dispersion relation wherein $\omega(k) \geq k$ for all k. Since $\boldsymbol{k} \cdot \boldsymbol{v} \leq k$ (as $|\boldsymbol{v}| < 1$), for a super-luminal dispersion relation $\boldsymbol{k} \cdot \boldsymbol{v} < \omega$ and, hence, $\omega - \boldsymbol{k} \cdot \boldsymbol{v} > 0$ for all k. Therefore, the argument of the delta function in the expression (3.10) never goes to zero, implying a vanishing detector response. In contrast, consider a field governed by a sub-luminal dispersion relation wherein $\omega(k) < k$ over some range of k. Over this domain in k, it is possible that $\omega - \boldsymbol{k} \cdot \boldsymbol{v} < 0$ for suitable values of the detector energy E and the speed $|\boldsymbol{v}|$ of the detector. These modes of the field can excite the detector, *provided the velocity of the detector is non-zero*. (In certain cases, depending on the form of the dispersion relation, there can also arise a critical velocity, only beyond which the detector would respond, as we shall encounter in the following section.) In other words, even inertial detectors with possibly a threshold velocity (which will, in general, depend on the internal energy E of the detector) may respond when they are coupled to a field that is characterized by a sub-luminal dispersion relation. This violation of Lorentz invariance should not come as a surprise as it is a characteristic of fields governed by modified dispersion relations.

In the standard case, the Wightman function (3.9) in the Minkowski vacuum could be written as (3.11) in the cylindrical polar coordinates. In fact, this proves to be true even for the case of a scalar field described by a modified dispersion relation. Hence, the transition probability rate of a rotating detector coupled to such a field is again given by (3.12), with ω [and, later, the corresponding k_* — cf. Eq. (3.15)] suitably redefined. Using these results, one can show that, while the super-luminal dispersion relations hardly affect the response of the rotating detector, sub-luminal dispersion relations — depending on their shape — can substantially alter the response (for more details and illustration of the modified response in specific cases, see Ref. [68]).

3.4 Detector coupled to the polymer quantized scalar field

Let us now turn to the primary case of our interest, *viz.* the response of a detector coupled to a polymer quantized scalar field.

3.4.1 The Wightman function in polymer quantization

As we had mentioned in the introductory section, the polymer quantized field can be considered as a series of modified dispersion relations of a specific form, along with suitable changes to the density of modes. In (3+1)-dimensions, the Wightman function evaluated under the polymer quantization procedure in the Minkowski vacuum is found to be [27, 65]

$$G_{\mathrm{P}}^{+}(\tilde{x},\tilde{x}') = \sum_{n=0}^{\infty} \int \frac{\mathrm{d}^3\boldsymbol{k}}{(2\,\pi)^3}\, |c_{4n+3}(k)|^2\, \mathrm{e}^{-i\,\omega_{4n+3}(k)(t-t')}\, \mathrm{e}^{i\,\boldsymbol{k}\cdot(\boldsymbol{x}-\boldsymbol{x}')}, \tag{3.16}$$

where, as before, $k = |\boldsymbol{k}|$, while the quantity $\omega_{4n+3}(g)$ is given by

$$\frac{\omega_{4n+3}(g)}{k_{\mathrm{P}}} = \frac{g^2}{2}\left\{B_{2n+2}\left[1/\left(4\,g^2\right)\right] - A_0\left[1/\left(4\,g^2\right)\right]\right\}, \tag{3.17}$$

with $g = k/k_{\mathrm{P}}$ and k_{P} being the polymer energy scale, which is usually assumed to be of the order of the Planck scale M_{Pl}. The quantities $A_r(x)$ and $B_r(x)$ denote the Mathieu characteristic value functions[1]. At small g, one finds that $\omega_{4n+3} \simeq (2\,n+1)\,k$, which is clear from Fig. 3.2, wherein we have plotted the quantity ω_{4n+3} as a function of g for the first few values of n. Moreover, the polymer coefficients $c_{4n+3}(k)$ are defined by the integral

$$c_{4n+3}(k) = \frac{i}{\pi\,\sqrt{k_{\mathrm{P}}}} \int_0^{2\,\pi} \mathrm{d}u\, se_{2n+2}\left[1/\left(4\,g^2\right), u\right]\, \frac{\partial\, ce_0\left[1/(4\,g^2), u\right]}{\partial u}, \tag{3.18}$$

where $se_r(x,q)$ and $ce_r(x,q)$ are the elliptic sine and cosine functions, respectively [69]. It is useful to note that for $g \ll 1$, $|c_{4n+3}(k)| \simeq 1/(\sqrt{2\,k})$, for $n = 0$, which corresponds to the standard result [27].

In summary, three new features are encountered in polymer quantization when compared to the standard case. Firstly, the quantity $\omega(k)$ in the exponential is replaced by $\omega_{4n+3}(k)$, in a fashion similar to that of a quantum field governed by a modified dispersion relation. Secondly, the standard measure in the integral over the modes — *viz.* $1/\sqrt{2\,k}$ — is replaced by $c_{4n+3}(k)$. It should be pointed out that, in the case of a field described by a modified dispersion relation, this measure would have been given by $1/\sqrt{2\,\omega(k)}$. Lastly, there occurs an infinite sum over the polymer index n, which is an aspect that is peculiar to polymer quantization.

[1]We should clarify that the Mathieu characteristic value functions were written as $A_r(g)$ and $B_r(g)$ in the original work [27]. However, in order to be consistent with the Mathieu differential equation describing the polymer quantized massless scalar field, they have to be actually written as $A_r[1/(4\,g^2)]$ and $B_r[1/(4\,g^2)]$.

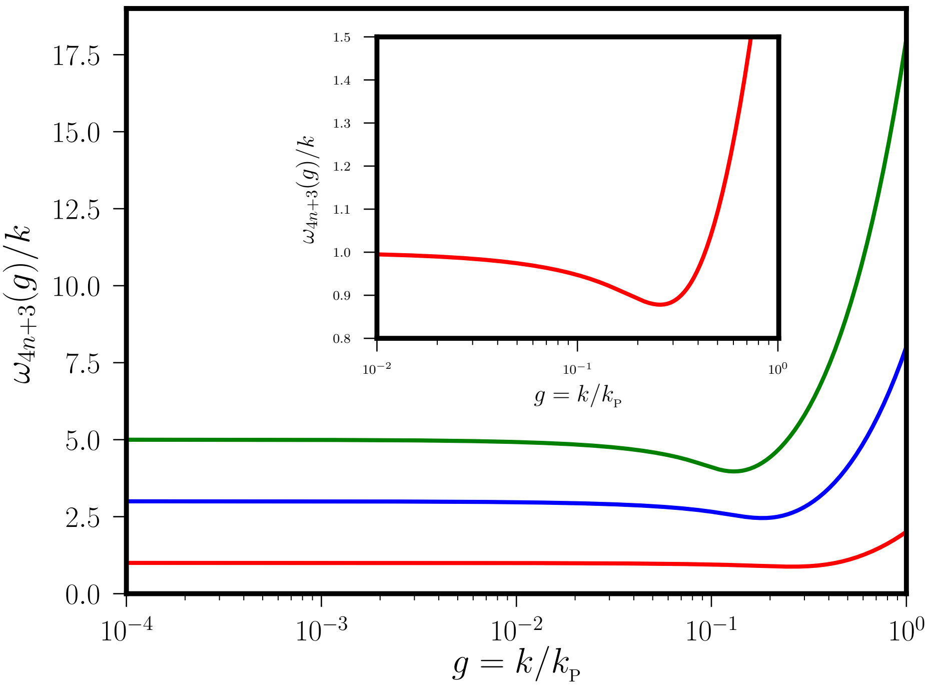

Figure 3.2: The behavior of $\omega_{4n+3}(g)/k$ has been plotted as a function of $g = k/k_{\mathrm{P}}$ for $n = 0$ (in red), $n = 1$ (in blue) and $n = 2$ (in green). The dispersion relation proves to be sub-luminal in the $n = 0$ case for a small range of k near k_{P}, while it is always super-luminal for $n > 0$. The sub-luminal behavior in the $n = 0$ case is clear from the inset in the figure.

3.4.2 The case of the inertial detector

Let us first revisit the response of the inertial detector in polymer quantization, which has been studied recently [65].

In such a case, upon considering the Wightman function (3.16) along the inertial trajectory $\tilde{x}(\tau) = (\gamma\,\tau, \gamma\,\boldsymbol{v}\,\tau)$, where $\gamma = (1 - |\boldsymbol{v}|^2)^{-1/2}$ and calculating the corresponding transition probability rate, we obtain that

$$\begin{aligned}\bar{R}_{\mathrm{P}}(\bar{E}) &= \frac{R_{\mathrm{P}}(\bar{E})}{k_{\mathrm{P}}}\\ &= \frac{1}{2\,\pi}\sum_{n=0}^{\infty}\int_{-\infty}^{\infty}\mathrm{d}^2\boldsymbol{k}_{\perp}\int_{0}^{\infty}\mathrm{d}k_{\parallel}\,k_{\parallel}\,|c_{4n+3}(k)|^2\,\delta^{(1)}\left[E + \gamma\,\omega_{4n+3}(k) - \gamma\,k_{\parallel}\,v\right], \qquad (3.19)\end{aligned}$$

where $\bar{E} = E/k_{\mathrm{P}}$ and $v = |\boldsymbol{v}|$, while $k_{\parallel}$ and $\boldsymbol{k}_{\perp}$ denote the components of $\boldsymbol{k}$ that are parallel and perpendicular to the velocity vector $\boldsymbol{v}$. Upon making the change of variables to $k_{\|} = k\cos\theta$ and $\boldsymbol{k}_{\perp} = k\sin\theta$, we obtain that

$$\bar{R}_{\rm P}(\bar{E}) \;=\; \frac{1}{2\,\pi\,\gamma\,v}\,\sum_{n=0}^{\infty}\int\limits_{0}^{\infty}{\rm d}k\,k\,\vert c_{4n+3}(k)\vert^2\int\limits_{-1}^{1}{\rm d}\,(\cos\theta)\,\delta^{(1)}\left[\cos\theta-\frac{E+\gamma\,\omega_{4n+3}(k)}{\gamma\,k\,v}\right]. \tag{3.20}$$

Note that this integral is non-zero only if

$$\vert E+\gamma\,\omega_{4n+3}(k)\vert < \gamma\,k\,v, \tag{3.21}$$

which leads to the following expression for the transition probability rate:

$$\bar{R}_{\rm P}(\bar{E}) \;=\; \frac{1}{2\,\pi\,\gamma\,v}\,\sum_{n=0}^{\infty}\int\limits_{0}^{\infty}{\rm d}k\,k\,\vert c_{4n+3}(k)\vert^2\,\Theta\big[\gamma\,k\,v-\vert E+\gamma\,\omega_{4n+3}(k)\vert\big], \tag{3.22}$$

where $\Theta(x)$ denotes the theta function. It seems difficult to evaluate the above transition probability rate analytically. Hence, we have to resort to numerics [65]. We shall first need to determine the domain in k (or, equivalently, g) over which the Θ function contributes. It is expected to contribute when $\omega_{4n+3}(k)$ behaves sub-luminally. It is clear from the plots in Fig. 3.2 that the function $\omega_{4n+3}(k)$ is always super-luminal when $n > 0$. Therefore, these terms are not expected to contribute to the response of the detector. Moreover, in the $n = 0$ case, the sub-luminal behavior occurs roughly over the small domain wherein $0.01 \lesssim g \lesssim 1$. It is these modes which we need to integrate over. We evaluate the quantity $c_{4n+3}(k)$ using the definition (3.18) before going on to carry out the integral over the relevant domain in k (determined by the Θ function) to arrive at the transition probability rate of the detector. We find that, because the integrand in Eq. (3.18) is well behaved, both the integrals can be evaluated with even the simplest of methods. We make use of the Simpson's rule to carry out these integrals. We should emphasize that we have checked the accuracy of the integrations involved by working with a larger number of steps as well as using the more accurate Bode's rule. We find that the integrations we have carried out are accurate to better than 0.01%. In Fig. 3.3, we have plotted the dimensionless transition probability rate as a function of the rapidity parameter $\beta = \tanh^{-1} v$. These curves match the results obtained earlier [65]. In Fig. 3.4, we have plotted the transition probability rate as a function of the dimensionless energy $\bar{E} = E/k_{\rm P}$ for a few different values of β. These results confirm the correctness of our numerical procedures.

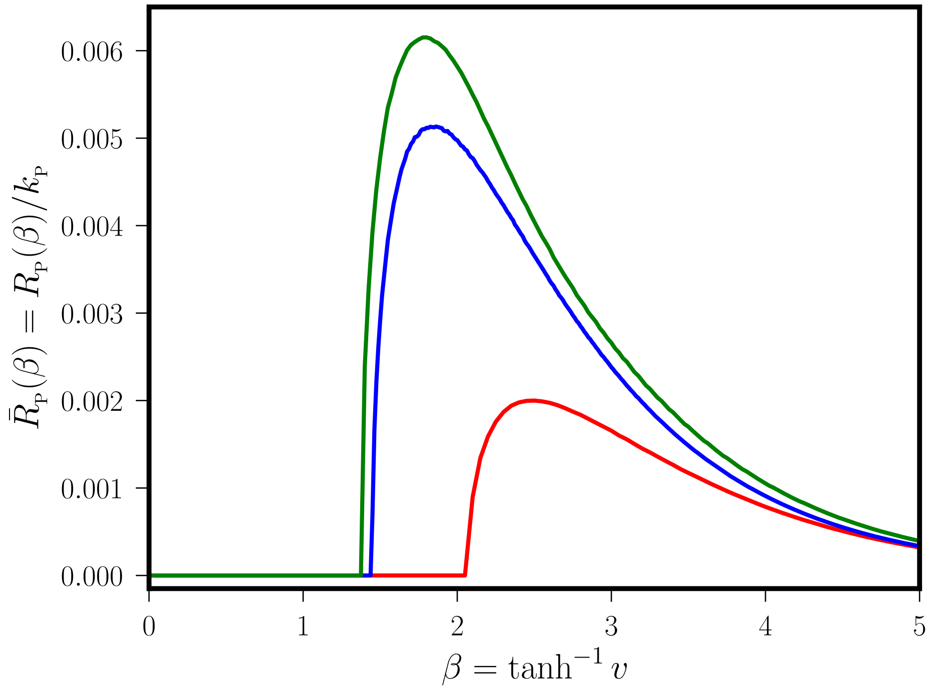

Figure 3.3: The dimensionless transition probability rate $\bar{R}_{\rm P}$ [cf. Eq. (3.22)] of an inertial detector that is coupled to a polymer quantized scalar field. We should stress that the transition probability rate has been plotted as a function of the rapidity parameter $\beta = \tanh^{-1}v$ for specific values of $\bar{E} = E/k_{\rm P}$. Also, for reasons mentioned, we have considered only the contribution due to the $n = 0$ case. The different curves correspond to $\bar{E} = 10^{-1}$ (in red), 10^{-2} (in blue) and 10^{-3} (in green). These plots match the results that have been recently obtained in the literature [65]. Note that, for a given $\bar{E}$, there is a threshold velocity for the detector to respond. The threshold velocity seems to become smaller as $\bar{E}$ decreases. The critical velocity beyond which an inertial detector begins to respond is determined by the condition that the argument of the Θ function in Eq. (3.22) turns positive. The associated critical rapidity parameter is determined by the relation $\tanh\beta_{\rm c} = \mathrm{Min.}\ [\omega_3(k)/g]$, which leads to $\beta_{\rm c} \simeq 1.3267$.

3.4.3 The case of the rotating detector

To determine the response of the rotating detector coupled to a polymer quantized field, we shall follow the same strategy that we had adopted earlier. It is straightforward to establish that, when working in the cylindrical polar coordinates, along the rotating trajectory that we had considered earlier, the polymer quantized Wightman function (3.16)

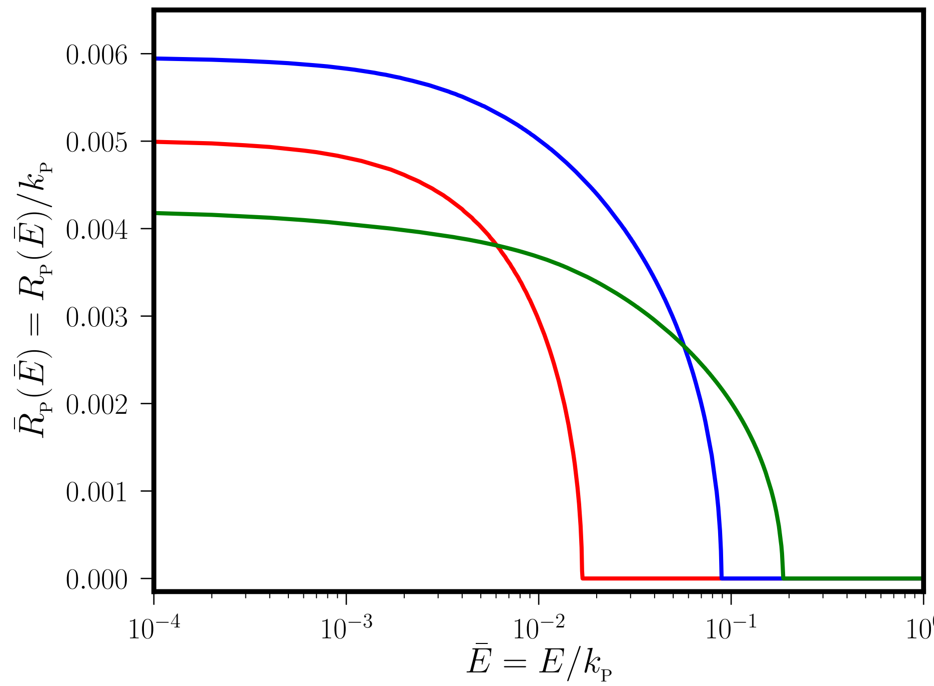

Figure 3.4: The dimensionless transition probability rate $\bar{R}_{\rm P}$ of an inertial detector that is coupled to the polymer quantized scalar field has been plotted as a function of the dimensionless energy $\bar{E} = E/k_{\rm P}$ for different values of β, which corresponds to different velocities of the detector. The different curves correspond to $\beta = 1.5$ (in red), 2.0 (in blue) and 2.5 (in green).

is given by

$$G^{+}_{\rm P}(u) = \sum_{n=0}^{\infty} \sum_{m=-\infty}^{\infty} \int_{0}^{\infty} \frac{{\rm d}q\, q}{2\,\pi} \int_{-\infty}^{\infty} \frac{{\rm d}k_z}{2\,\pi}\, |c_{4n+3}(k)|^2\, J_m^2(q\,\sigma)\, {\rm e}^{-i\,[\omega_{4n+3}(k) - \gamma\, m\, \Omega]\, u}, \tag{3.23}$$

where, as before, $k = \sqrt{q^2 + k_z^2}$. We can convert the integrals over q and k_z into integrals over k and a suitable angle α, as in the standard case. Upon doing so and carrying out the integrals over α as well as u, we find that the transition probability rate of the rotating detector can be expressed as

$$\begin{aligned} \bar{R}_{\rm P}(\bar{E}) &\equiv \sigma\, R_{\rm P}(\bar{E}) \\ &= \sum_{n=0}^{\infty} \sum_{m=-\infty}^{\infty} \int_{0}^{\infty} \frac{{\rm d}k}{2\,\pi}\, \frac{(\sigma\, k)^{2\,m+1}}{\Gamma(2\,m+2)}\, 2\,k\, |c_{4n+3}(k)|^2 \\ &\quad \times {}_1F_2[m+1/2; m+3/2, 2\,m+1; -(\sigma\, k)^2]\, \delta^{(1)}\left[E + \gamma\, \omega_{4n+3}(k) - \gamma\, m\, \Omega\right]. \end{aligned} \tag{3.24}$$

The integral over k can be evaluated immediately to arrive at

$$\begin{aligned}\bar{R}_{\mathrm{P}}(\bar{E}) &= \frac{1}{2\,\pi\,\gamma}\sum_{n=0}^{\infty}\sum_{m\geq\bar{E}}^{\infty}\frac{(\sigma\,k_*)^{2\,m+1}}{\Gamma(2\,m+2)}\,\left[\frac{2\,k_*\,|c_{4n+3}(k_*)|^2}{|\mathrm{d}\omega_{4n+3}/\mathrm{d}k|_{k=k_*}}\right]\\ &\quad\times{}_1F_2[m+1/2;m+3/2,2\,m+1;-(\sigma\,k_*)^2],\end{aligned} \tag{3.25}$$

where k_* now denote the roots of the equation

$$\omega_{4n+3}(k_*)=\left(m-\bar{E}\right)\,\Omega. \tag{3.26}$$

Since $\omega_{4n+3}(k)$ is a positive definite quantity, we need to confine ourselves to $m\geq\bar{E}$ in the above sum, exactly as in the standard case. Note that, in the standard situation, we have just the $n=0$ case, with $\omega(k)=k$, leading to $k_*=\left(m-\bar{E}\right)\,\Omega$. Also, in such a case, the quantity within the large square brackets in the above expression reduces to unity, thereby simplifying to the result (3.15) we had obtained earlier.

In order to determine the transition probability rate of the rotating detector, we need to first determine the roots k_* and evaluate the quantities $|c_{4n+3}(k)|^2$ and $|\mathrm{d}\omega_{4n+3}(k)/\mathrm{d}k|$ at these k_*. As we had mentioned in the inertial case, these seem impossible to evaluate analytically. However, we find that they can be determined numerically without much difficulty. Having determined the roots k_*, the quantity $|\mathrm{d}\omega_{4n+3}(k)/\mathrm{d}k|$ is easy to obtain. We evaluate $c_{4n+3}(k)$ just as in the inertial case, using the Simpson's rule. Once all these quantities are in hand, we also need to sum over n and m to arrive at the complete transition probability rate of the detector. The sum over m converges rapidly as in the standard case. In Fig. 3.5, we have plotted the contributions due to the the first three terms in the sum over n for specific values of the parameters involved. It is evident from the figure that the $n=0$ term dominates the contribution.

Let us now turn to examine if polymer quantization modifies the transition probability rate of the rotating detector. In Fig. 3.6, we have plotted the transition probability rate of the detector for a few different values of k_{P}. We should mention here that, as in the standard case, we have taken into account only the first ten contributions in the sum over m in Eq. (3.25) (for the $n=0$ case, as discussed above). We have also examined and confirmed that the contributions due to the higher terms are indeed completely insignificant. It is clear that, even for an extreme value of $\bar{k}_{\mathrm{P}}=\sigma\,k_{\mathrm{P}}=1$, the detector response does not differ considerably from the standard case. This suggests that polymer quantization does not alter the standard results appreciably.

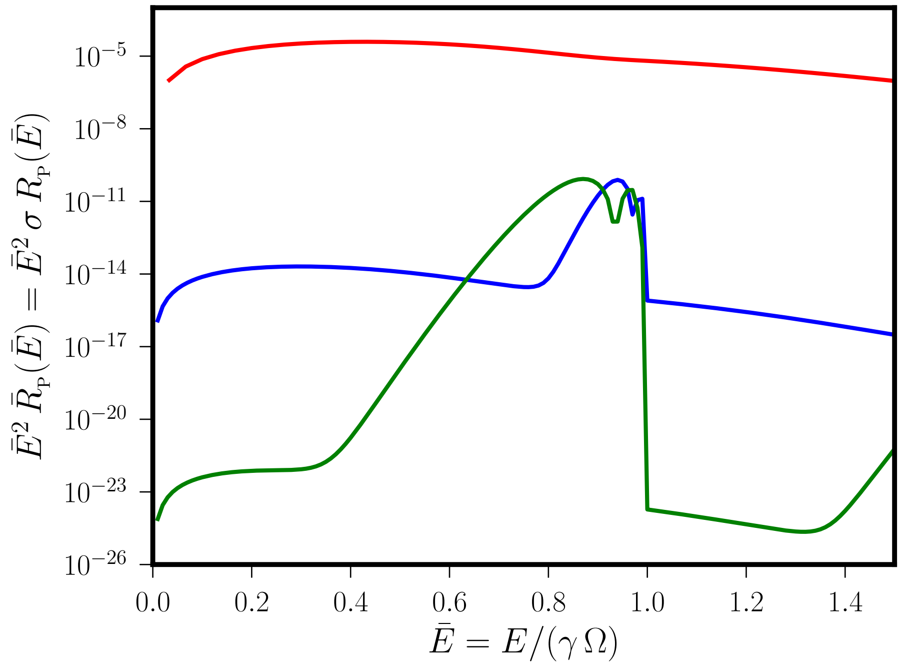

Figure 3.5: The transition probability rate of the rotating detector when it is coupled to a polymer quantized scalar field. The three curves correspond to $n = 0$ (in red), $n = 1$ (in blue) and $n = 2$ (in green). We have set $\sigma\,\Omega = 0.325$ and $\bar{k}_{\rm P} = \sigma\,k_{\rm P} = 10^2$ in plotting these curves. Note that, in order to illustrate the relative magnitude of the three terms, in contrast to Fig. 3.1, we have plotted the y-axis on a logarithmic scale. Clearly, the $n = 0$ term dominates the contributions to the transition probability rate of the rotating detector. Therefore, the higher order terms can be safely ignored.

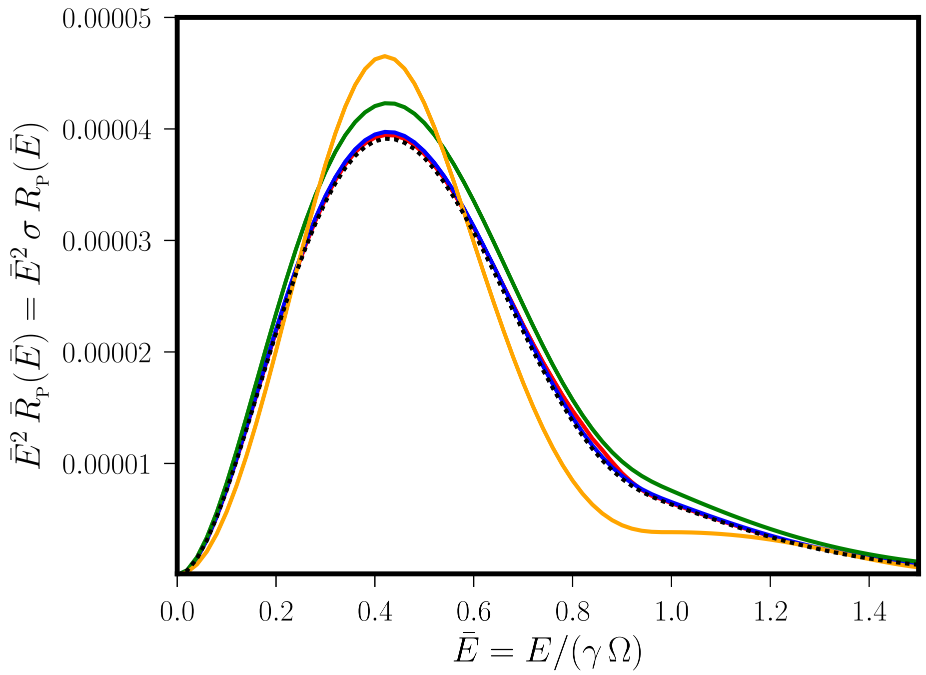

Figure 3.6: The transition probability rate of the rotating detector that is coupled to a polymer quantized field has been plotted for different values of $k_{\rm P}$. We have set $\sigma\,\Omega = 0.325$ and have taken into consideration only the $n = 0$ contribution to the response of the detector. Note that the different solid curves correspond to the following values of $\bar{k}_{\rm P} = \sigma\,k_{\rm P}$: 10^3 (in red), 10^2 (in blue), 10 (in green) and unity (in orange). The dotted black curve corresponds to the standard case we had plotted in Fig. 3.1. Evidently, the larger the $\bar{k}_{\rm P}$, the smaller is the deviation from the standard case. This indicates that the high energy modifications do not alter the response of the rotating detector considerably.

3.5 Summary

The approach due to polymer quantization takes into account certain aspects that are expected to arise in a plausible quantum theory of gravitation and arrives at a modified version of the standard Minkowski propagator. The response of the so-called detectors that are coupled to a scalar field are determined by the Fourier transform of the Wightman function governing the field. In this work, using the propagator arrived at by polymer quantization, we have investigated the effects of high energy physics on a variant of the Unruh effect [70].

It is well known that, while inertial detectors do not respond in the Minkowski vacuum (when coupled to the standard quantum field), rotating detectors exhibit a non-zero response. But, it proves to be difficult to calculate the response of the rotating detector analytically and one needs to resort to numerics to evaluate the transition probability rate of the detector. These two results are easy to understand. As the standard Wightman function in the Minkowski vacuum is Lorentz invariant, it is not surprising that inertial detectors do not respond in such a situation. In contrast, it seems natural to expect that detectors in non-inertial motion will, in general, respond non-trivially in the Minkowski vacuum (in this context, see, for instance, Ref. [17]). In this work, we have studied the response of detectors that are coupled to a scalar field which is quantized through the method of polymer quantization. After revisiting the case of the inertial detector which has been studied recently, we had investigated the response of a rotating detector. It has been shown earlier that the response of detectors which are coupled to a quantum field that is described by super-luminal dispersion relations are hardly affected. Also, it is known that the response of the detectors can be altered considerably if they are coupled to a field characterized by sub-luminal dispersion relations. In the case of a polymer quantized field, one of the dispersion relations governing the field behaves sub-luminally over a limited domain in wavenumber. It is this behavior that is expected to alter the standard response of the rotating detector [68]. However, in polymer quantization, since the sub-luminal modification to the dispersion relation is small, we find that, the corresponding change in the response of the detector is also not considerable. Our results confirm similar conclusions concerning the sub-luminal and super-luminal dispersion relations that have been arrived at earlier. Specifically, as we had pointed out earlier, two phenomena where the effects due to trans-Planckian physics have been investigated to a considerable extent are Hawking radiation from black holes and the inflationary perturbation spectra. In both these cases, it has been found that, while super-luminal dispersion relations hardly affect the conventional results, sub-luminal relations can, in principle, alter (depending on the details of the dispersion relation) the standard results to a good extent (in this context, see the reviews [24, 25]).

A couple of additional points need to be clarified concerning the responses of the inertial and rotating detectors that are coupled to a polymer quantized field. While the response of an inertial detector that is coupled to the standard quantum field vanishes identically, the detector coupled to a polymer quantized field exhibits a non-zero response. Specifically, the modifications of the inertial detector seem to be significant for a range of the parameters involved. In contrast, the response of the rotating detector coupled to a polymer quantized field seems hardly different from the standard case. In fact, it is also possible to construct a situation that is analogous to the inertial detector in the rotating case. Note that there exists a static limit in the rotating frame. It has been shown that a rotating detector coupled to the standard field ceases to respond when one imposes a boundary condition on the field at the static limit [67]. However, it is easy to argue that a rotating detector coupled to a polymer quantized field will respond non-trivially (due to the sub-luminal nature of the dispersion relation) in the same situation [68]. The significance of these modifications and their dependence on the parameters needs to be investigated in greater detail.

Needless to add, it will be interesting to evaluate the response of a uniformly accelerated detector that is coupled to a polymer quantized field. However, as we had pointed out in the introductory section, the polymer Wightman function does not prove to be translation invariant in terms of the proper time in the frame of the accelerated detector. This poses difficulty in evaluating the corresponding transition probability rate of the detector. One possible way to deal with this problem is to evaluate the response of the detector for a finite proper time interval and examine the behavior of the response when the duration for which the detector is kept switched on is much larger than the time scale associated with the acceleration [71]. We are currently investigating this issue.

Chapter 4

Moving mirrors and the fluctuation-dissipation theorem

4.1 A point mirror as a Brownian particle

Brownian motion refers to the random motion of small particles immersed in a large bath. Classic examples of Brownian motion would include the random motion of particles floating in a liquid and the motion of dust particles illuminated by a ray of sunlight. The motion of a Brownian particle is effectively described by the Langevin equation (see, for instance, Ref. [33]). In the Langevin equation, the force experienced by the particle is decomposed into two components: one, an averaged force which is dissipative in nature, and another that is rapidly fluctuating. The combination of the dissipative and the fluctuating forces leads to the diffusion of the Brownian particle through the bath.

The amplitudes of the dissipative force and the correlation function describing the fluctuating component are related by the fluctuation-dissipation theorem (see, for example, Refs. [34]). The theorem can also be utilized to evaluate the mean-squared displacement of the Brownian particle and thereby illustrate the diffusive nature of the particle. It is well known that, in a bath maintained at a finite temperature, the mean-squared displacement of the Brownian particle grows linearly with time at late times. An interesting question that seems worth addressing is whether the Brownian particle diffuses even at zero temperature (in this context, see Refs. [35]).

A point mirror moving in a thermal bath provides a splendid example for studying these issues and, in fact, the system has been considered earlier in different contexts (see, for instance, Refs. [72, 73, 74]; also see the following reviews [32]). Our goal in this work is to reconsider the random motion of the mirror immersed in a thermal bath. Specifically, our aims can be said to be two-fold. Our first goal is to evaluate the average force on the moving mirror as well as the correlation function characterizing the fluctuating component and explicitly establish the fluctuation-dissipation theorem relating these quantities. Our second aim is to utilize the fluctuation-dissipation theorem to calculate the mean-squared displacement of the mirror both at finite and zero temperature and, in particular, examine the nature of diffusion at zero temperature. In order for the problem to be analytically tractable, as is usually done in this context, we shall work in $(1+1)$-spacetime dimensions and assume that the mirror is interacting with a massless scalar field (for the original discussions, see Refs. [29, 30, 75]). Importantly, one finds that, under these simplifying assumptions, it proves to be possible to calculate all the quantities involved explicitly using the standard methods of quantum field theory.

A few clarifying remarks concerning the prior efforts in these directions are in order at this stage of our discussion. The earliest efforts in the literature had primarily focused on carrying out the quantum field theory of a massless scalar field in the presence of a moving mirror in $(1+1)$-spacetime dimensions [29]. It was immediately followed by efforts to evaluate the regularized stress-energy tensor associated with the quantum field in the vacuum state, *i.e.* at zero temperature [30, 75]. These efforts had also arrived at the corresponding radiation reaction force on the moving mirror. About a decade after these initial efforts, it was recognized that the system provides a tractable scenario to examine the validity of the fluctuation-dissipation theorem and the behavior of the mean-squared displacement of the mirror. The fluctuation-dissipation theorem at zero temperature was established in this context and the behavior of the mean-squared displacement of the mirror at large times was also arrived at [72]. More recently, the radiation reaction force on the moving mirror at a finite temperature has been calculated as well (in this context, see Ref. [74]). However, to the best of our knowledge, this is the first time that the correlation function governing the radiation reaction force is being evaluated and the associated fluctuation-dissipation theorem is being explicitly established for the case of the moving mirror at a finite temperature (though we should clarify that the possibility has been briefly discussed in the last reference in Refs. [35]). Moreover, we believe this is the first effort towards obtaining complete analytical expressions for the mean-squared displacements of the mirror that is valid at all times.

This chapter is organized as follows. In the following section, we shall quickly review the quantization of a massless scalar field in the presence of a moving mirror in $(1+1)$-spacetime dimensions, and evaluate the regularized stress-energy tensor of the scalar field at a finite temperature. We shall use the result to arrive at the radiation reaction force on the moving mirror. In Sec. 4.3, we shall evaluate the correlation function governing the fluctuating component of the radiation reaction force. Using the radiation reaction force and the correlation function characterizing the fluctuating component, we shall establish the fluctuation-dissipation theorem in Sec. 4.4. In Secs. 4.5 and 4.6, using the fluctuation-dissipation theorem, we shall calculate the mean-squared displacement of the mirror at finite and zero temperature. Finally, in Sec. 4.7, we shall close with a brief discussion on the results we have obtained. We shall relegate the details concerning some of the calculations to the four appendices A.3–A.6. Specifically, in the final appendix A.6, we shall clarify a subtle point concerning the zero temperature limit of the finite temperature result for the mean-squared displacement of the mirror.

Note that, in this chapter, we shall work in units such that $c = \hbar = k_{\mathrm{B}} = 1$. Also, we shall be working in $(1+1)$-spacetime dimensions with the metric signature of $(+,-)$. An overdot shall denote differentiation with respect to the Minkowski time coordinate. Unless we mention otherwise, overprimes above functions shall represent differentiation of the functions with respect to their arguments. Angular brackets shall, in general, denote expectation values evaluated at a finite temperature, barring in Sec. 4.6, where it shall represent expectation values at zero temperature (*i.e.* in the quantum vacuum). Lastly, subscripts and superscripts R and L shall denote quantities to the right and the mirror, respectively.

4.2 Radiation reaction on a mirror moving in a thermal bath

In this section, we shall first discuss the quantization of a massless scalar field in $(1+1)$-spacetime dimensions in the presence of a moving mirror. We shall impose Dirichlet or Neumann boundary conditions on the mirror and evaluate the regularized stress-energy tensor for the scalar field at a finite temperature. From this result, we shall obtain the radiation reaction force on the mirror.

4.2.1 Boundary conditions, modes and quantization

Consider a massless scalar field, say, ϕ, which is governed by the following equation in $(1+1)$-dimensional flat spacetime:

$$\frac{\partial^2\phi}{\partial t^2} - \frac{\partial^2\phi}{\partial x^2} = 0. \tag{4.1}$$

Let a mirror be moving along the trajectory $x = z(t)$, such that $|\dot{z}(t)| < 1$, and let us assume that the scalar field ϕ satisfies either the Dirichlet or the Neumann boundary conditions on the moving mirror. In the case of the Dirichlet boundary condition, we require that

$$\phi\,[t, x = z(t)] = 0, \tag{4.2}$$

whereas, in the case of the (covariant) Neumann condition, we shall require

$$n^i\,\nabla_i\phi\Big|_{x=z(t)} = \left(\frac{\partial\phi}{\partial x} + \dot{x}\,\frac{\partial\phi}{\partial t}\right)_{x=z(t)} = 0, \tag{4.3}$$

where $n^i = \left[1 - \dot{z}^2(t)\right]^{-1/2}\,[\dot{z}(t), 1]$ is the vector normal to the mirror trajectory $z(t)$. The mirror divides the spacetime into two completely *independent* regions, to the left (L) and the right (R) of the mirror.

Let $u_\omega^{\mathrm{R}}(t, x)$ and $u_\omega^{\mathrm{L}}(t, x)$ denote the normalized modes of the scalar field in the regions to the right and the left of the mirror, respectively. These modes can be expressed in terms of the null coordinates $u = t - x$ and $v = t + x$ as follows [29, 30, 74]:

$$u_\omega^{\mathrm{R}}(t, x) \;=\; \frac{1}{\sqrt{4\,\pi\,\omega}}\,\left[\kappa\,\mathrm{e}^{-i\,\omega\,v} + \kappa^*\,\mathrm{e}^{-i\,\omega\,p_1(u)}\right], \tag{4.4a}$$

$$u_\omega^{\mathrm{L}}(t, x) \;=\; \frac{1}{\sqrt{4\,\pi\,\omega}}\,\left[\kappa\,\mathrm{e}^{-i\,\omega\,u} + \kappa^*\,\mathrm{e}^{-i\,\omega\,p_2(v)}\right]. \tag{4.4b}$$

The functions $p_1(u)$ and $p_2(v)$ are given by

$$p_1(u) \;=\; 2\,\tau_u - u, \tag{4.5a}$$

$$p_2(v) \;=\; 2\,\tau_v - v, \tag{4.5b}$$

where τ_u and τ_v denote the times at which the null lines u and v intersect the mirror's trajectory to the right and the left of the mirror (see Fig. 4.1). The quantities τ_u and τ_v are determined by the conditions $\tau_u - z(\tau_u) = u$ and $\tau_v + z(\tau_v) = v$. The quantity κ is a constant and its value depends on the boundary condition, with $\kappa = i$ and $\kappa = 1$ corresponding to the Dirichlet and the Neumann conditions.

On quantization, the scalar field operator $\hat{\phi}$ to the right and the left of the mirror can be decomposed in terms of the corresponding normal modes as follows:

$$\hat{\phi}(t, x) = \int_0^\infty \mathrm{d}\omega\,\left[\hat{a}_\omega\,u_\omega(t, x) + \hat{a}_\omega^\dagger\,u_\omega^*(t, x)\right], \tag{4.6}$$

where $\hat{a}_\omega$ and $\hat{a}_\omega^\dagger$ are the annihilation and the creation operators which obey the standard commutation relations. It should be emphasized that there exist a separate set of operators defining the vacuum state and characterizing the corresponding Fock space on either side of the mirror.

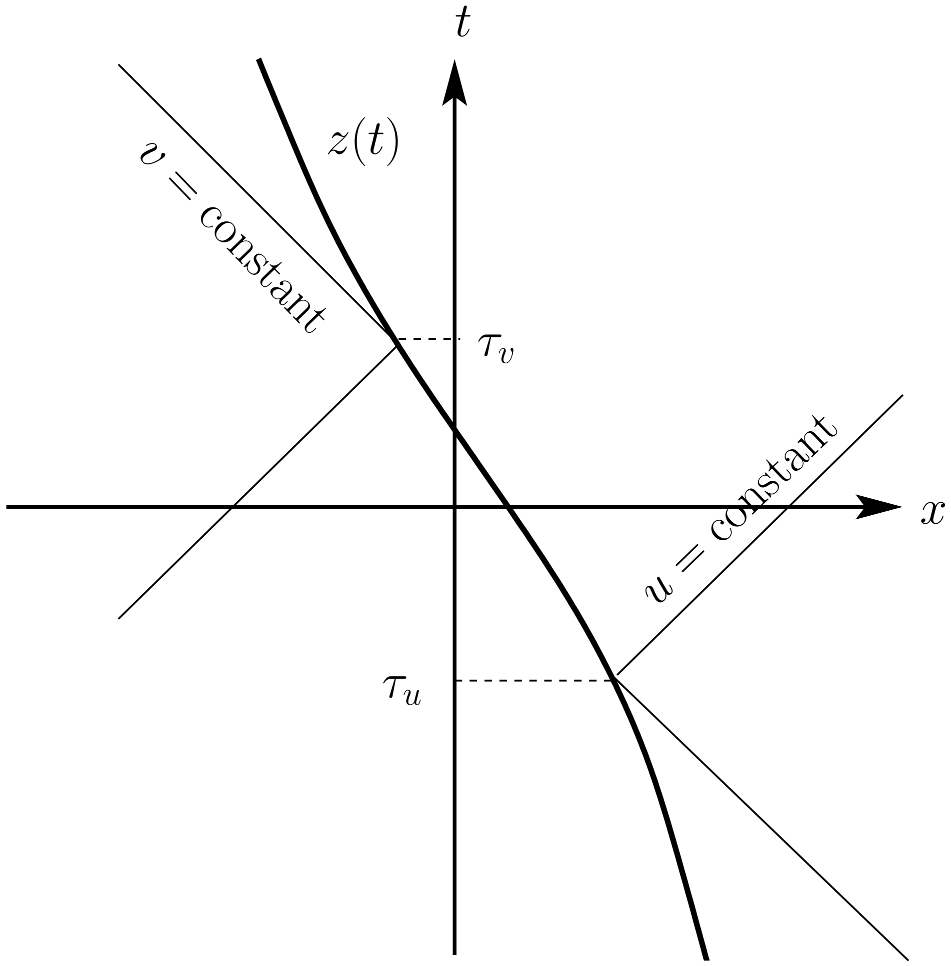

Figure 4.1: The mirror moving along the trajectory $z(t)$ divides the spacetime into two distinct regions to the right and the left of the mirror. Note that τ_u and τ_v denote the times when the incoming waves are reflected by the mirror and converted into outgoing waves to the right and the left of the mirror, respectively.

4.2.2 Stress-energy tensor at finite temperature

Let us now turn to the evaluation of the expectation value of the stress-energy tensor of the quantum scalar field at a finite temperature T. In $(1+1)$-dimensions, the different components of stress-energy tensor are given by

$$T_{00} = T_{11} = \frac{1}{2}\left[\left(\frac{\partial\phi}{\partial t}\right)^2 + \left(\frac{\partial\phi}{\partial x}\right)^2\right], \tag{4.7a}$$

$$T_{01} = T_{10} = \frac{1}{2}\left[\frac{\partial\phi}{\partial t}\,\frac{\partial\phi}{\partial x} + \frac{\partial\phi}{\partial x}\,\frac{\partial\phi}{\partial t}\right], \tag{4.7b}$$

with the indices $(0,1)$ and corresponding to the spacetime coordinates (t,x). It is now a matter of substituting the decomposition (4.6) of the quantum scalar field in the above expression for the stress-energy tensor and evaluating the expectation values at a finite temperature T on either side of the mirror. All the expectation values can be arrived at from the basic result (see, for instance, Refs. [2])

$$\langle \hat{a}_\omega^\dagger\, \hat{a}_{\omega'}\rangle = \frac{\delta^{(1)}(\omega-\omega')}{\mathrm{e}^{\beta\,\omega}-1}, \tag{4.8}$$

where $\beta = 1/T$ denotes the inverse temperature.

Since the stress-energy tensor involves two-point functions in the coincidence limit, as is well known, one will encounter divergences in calculating the quantity [9]. In flat spacetime, these divergences correspond to contributions due to the Minkowski vacuum and they can be easily identified and regularized using, say, the method of point-splitting regularization [30]. The method involves keeping the spacetime points in the two-point functions initially separate and taking the coincidence limit after removing the divergent contributions. The regularized stress-energy tensor to the right and the left of the mirror can be obtained to be

$$\langle \hat{T}^{00}_{\mathrm{R}}\rangle = -\frac{1}{24\,\pi}\left[\frac{p_1'''(u)}{p_1'(u)} - \frac{3}{2}\left(\frac{p_1''(u)}{p_1'(u)}\right)^2\right] + \frac{\pi}{12\,\beta^2}\,\left[1+p_1'^2(u)\right], \tag{4.9a}$$

$$\langle \hat{T}^{01}_{\mathrm{R}}\rangle = -\frac{1}{24\,\pi}\left[\frac{p_1'''(u)}{p_1'(u)} - \frac{3}{2}\left(\frac{p_1''(u)}{p_1'(u)}\right)^2\right] - \frac{\pi}{12\,\beta^2}\,\left[1-p_1'^2(u)\right], \tag{4.9b}$$

$$\langle \hat{T}^{00}_{\mathrm{L}}\rangle = -\frac{1}{24\,\pi}\left[\frac{p_2'''(v)}{p_2'(v)} - \frac{3}{2}\left(\frac{p_2'''(v)}{p_2'(v)}\right)^2\right] + \frac{\pi}{12\,\beta^2}\,\left[1+p_2'^2(v)\right], \tag{4.9c}$$

$$\langle \hat{T}^{01}_{\mathrm{L}}\rangle = \frac{1}{24\,\pi}\left[\frac{p_2'''(v)}{p_2'(v)} - \frac{3}{2}\left(\frac{p_2''(v)}{p_2'(v)}\right)^2\right] + \frac{\pi}{12\,\beta^2}\,\left[1-p_2'^2(v)\right], \tag{4.9d}$$

where, recall that, the overprimes denote differentiation of the functions with respect to the arguments. Three points concerning the above expressions require emphasis. To begin with, note that, the first terms in the above expressions for the components of the stress-energy tensor are independent of β. These terms represent the vacuum contribution [30], while the second terms (involving β) are the contributions arising due to the finite temperature. It should be mentioned here that the finite temperature terms include the contributions that arise even in the absence of the mirror. Secondly, note that the stress-energy tensor is a function only of u and v to the right and the left of the mirror, respectively. The moving mirror excites the scalar field and the terms that depend on $p_1(u)$ and $p_2(v)$ describe the stress-energy associated with the radiation emitted by the mirror due to its motion. Evidently, the vacuum contribution can be considered as spontaneous emission by the mirror, while the finite temperature contributions can be treated as stimulated emission. Thirdly, one finds that the stress-energy tensor is completely independent of the boundary condition (actually it depends on $|\kappa|^2$, which is unity for the Dirichlet and the Neumann conditions).

The quantities $p_1(u)$ and $p_2(v)$ and their derivatives with respect to their arguments can be expressed in terms of the velocity of the mirror and its two time derivatives. It can be shown that the components of the stress-energy tensor can be expressed in terms of $\dot{z}$, $\ddot{z}$ and $\dddot{z}$ as follows:

$$\langle \hat{T}^{00}_{\rm R} \rangle = -\frac{1}{12\,\pi}\left[\frac{\dddot{z}}{(1-\dot{z})^2\,(1-\dot{z}^2)} + \frac{3\,\dot{z}\,\ddot{z}^2}{(1-\dot{z})^2\,(1-\dot{z}^2)^2}\right] + \frac{\pi}{6\,\beta^2}\,\frac{1+\dot{z}^2}{(1-\dot{z})^2}, \tag{4.10a}$$

$$\langle \hat{T}^{01}_{\rm R} \rangle = -\frac{1}{12\,\pi}\left[\frac{\dddot{z}}{(1-\dot{z})^2\,(1-\dot{z}^2)} + \frac{3\,\dot{z}\,\ddot{z}^2}{(1-\dot{z})^2\,(1-\dot{z}^2)^2}\right] + \frac{\pi}{3\,\beta^2}\,\frac{\dot{z}}{(1-\dot{z})^2}, \tag{4.10b}$$

$$\langle \hat{T}^{00}_{\rm L} \rangle = \frac{1}{12\,\pi}\left[\frac{\dddot{z}}{(1+\dot{z})^2\,(1-\dot{z}^2)} + \frac{3\,\dot{z}\,\ddot{z}^2}{(1+\dot{z})^2\,(1-\dot{z}^2)^2}\right] + \frac{\pi}{6\,\beta^2}\,\frac{1+\dot{z}^2}{(1+\dot{z})^2}, \tag{4.10c}$$

$$\langle \hat{T}^{01}_{\rm L} \rangle = -\frac{1}{12\,\pi}\left[\frac{\dddot{z}}{(1+\dot{z})^2\,(1-\dot{z}^2)} + \frac{3\,\dot{z}\,\ddot{z}^2}{(1+\dot{z})^2\,(1-\dot{z}^2)^2}\right] + \frac{\pi}{3\,\beta^2}\,\frac{\dot{z}}{(1+\dot{z})^2}, \tag{4.10d}$$

where the velocity and its time derivatives are to be evaluated at the retarded times (*i.e.* at τ_u or τ_v) when the radiation was emitted by the mirror. At this stage, it is useful to note that, while the vacuum terms depend on the velocity $\dot{z}$, the acceleration $\ddot{z}$ as well as the time derivative of the acceleration $\dddot{z}$ [30, 75], the finite temperature term involves only the velocity $\dot{z}$.

4.2.3 Radiation reaction force on the moving mirror

The energy emitted by the moving mirror due to its interaction with the scalar field leads to a radiation reaction force on the mirror. The radiation reaction force can be obtained from the conservation of the total momentum of the mirror and the scalar field. The operator describing the radiation reaction force on the mirror can be expressed as [75]

$$\hat{F}_{\rm rad} = -\frac{{\rm d}\hat{P}^x}{{\rm d}t}, \tag{4.11}$$

where $\hat{P}^x$ is the momentum operator associated with the scalar field and is given by

$$\hat{P}^x \equiv \int_{-\infty}^{z(t)} {\rm d}x\, \hat{T}^{01}_{\rm L} + \int_{z(t)}^{\infty} {\rm d}x\, \hat{T}^{01}_{\rm R}. \tag{4.12}$$

The mean value of the radiation reaction force, evaluated at a finite temperature, can be arrived at from the expectation values of the stress-energy tensor we have obtained above. One finds that, the mean radiation reaction force can be expressed as

$$\langle \hat{F}_{\rm rad}\rangle \;=\; \frac{1}{6\,\pi}\,\frac{1}{(1-\dot{z}^2)^{1/2}}\,\frac{\rm d}{{\rm d}t}\left[\frac{\ddot{z}}{(1-\dot{z}^2)^{3/2}}\right] - \frac{2\,\pi}{3\,\beta^2}\,\frac{\dot{z}}{1-\dot{z}^2}, \tag{4.13}$$

with the first term representing the vacuum contribution [32, 75] and the second term characterizing the finite temperature contribution.

Let us emphasize here a few points regarding the radiation reaction force that we have obtained above. The procedure that we have adopted to arrive at the radiation reaction force is the same as the method that had been considered earlier (in this context, see Ref. [75]). The earlier effort had arrived at the radiation reaction force in the quantum vacuum (*i.e.* at zero temperature), which matches with our result (provided a suitable Lorentz factor is accounted for). As is well known, the radiation reaction force on the mirror in the quantum vacuum has exactly the same form as the radiation reaction force on a non-uniformly moving charge that one encounters in electromagnetism [32, 75]. We should point out here that the procedure we have adopted and the complete relativistic result we have obtained for the radiation reaction force is different from another prior effort in this direction (see Ref. [74]). Nevertheless, we find that the results for the radiation reaction force match in the non-relativistic limit [30, 35, 74], which is the domain of our primary interest in the latter part of this article.

Until now, the results have been exact, and we have made no assumptions on the magnitude of the velocity of mirror. When analyzing the Brownian motion of the mirror in the latter sections, we shall be working in the non-relativistic limit. In such a limit (*i.e.* when $|\dot{z}| \ll 1$), the above mean radiation reaction force simplifies to

$$\langle \hat{F}_{\rm rad} \rangle = \frac{1}{6\,\pi}\, \dddot{z} - \frac{2\,\pi}{3\,\beta^2}\, \dot{z}, \tag{4.14}$$

where we have ignored factors of order $\dot{z}^2$. Note that, at large temperatures, it is the second term that proves to be the dominant one. The term describes the standard dissipative force proportional to the velocity that is expected to arise as a particle moves through a thermal bath.

4.3 Correlation function describing the fluctuating component

As we discussed in the introductory section, apart from the dissipative component, a particle moving through a thermal bath also experiences a fluctuating force. We have evaluated the dissipative force on the moving mirror in the last section. Let us now turn to the calculation of the correlation function that governs the fluctuating component of the radiation reaction force.

The fluctuating component of the force on the moving mirror is clearly given by the deviations from the mean value. The operator describing the random force on the mirror can be defined as

$$\hat{\mathcal{R}}(t) \equiv \hat{F}_{\rm rad} - \langle \hat{F}_{\rm rad} \rangle\, \hat{\mathbb{I}} = -\frac{{\rm d}\hat{P}^x}{{\rm d}t} + \frac{{\rm d}\langle \hat{P}^x \rangle}{{\rm d}t}\, \hat{\mathbb{I}}, \tag{4.15}$$

where $\hat{P}_x$ is the momentum operator associated with the scalar field [as given by Eq. (4.12)] and $\hat{\mathbb{I}}$ denotes the identity operator. Using the expression (4.12) for the momentum operator, we obtain that

$$\frac{{\rm d}\hat{P}^x}{{\rm d}t} = -\dot{z}(t)\, \left[\hat{T}^{01}_{\rm R}(t,z) - \hat{T}^{01}_{\rm L}(t,z)\right] + \int_{z(t)}^{\infty} {\rm d}x\, \frac{\partial \hat{T}^{01}_{\rm R}(t,x)}{\partial t} + \int_{-\infty}^{z(t)} {\rm d}x\, \frac{\partial \hat{T}^{01}_{\rm L}(t,x)}{\partial t}. \tag{4.16}$$

Upon using the operator version of the conservation of the stress-energy tensor, one can show that the random force acting on the moving mirror can be expressed in terms of the components of the stress-energy tensor as follows:

$$\hat{\mathcal{R}}(t) = -\dot{z}(t)\, \left[\hat{\mathcal{T}}^{01}_{\rm R}(t,z) - \hat{\mathcal{T}}^{01}_{\rm L}(t,z)\right] + \hat{\mathcal{T}}^{00}_{\rm R}(t,z) - \hat{\mathcal{T}}^{00}_{\rm L}(t,z), \tag{4.17}$$

where the quantity $\hat{\mathcal{T}}^{ab}(t,x)$ is defined as

$$\hat{\mathcal{T}}^{ab}(t,x) = \hat{T}^{ab}(t,x) - \langle \hat{T}^{ab}(t,x) \rangle\, \hat{\mathbb{I}}. \tag{4.18}$$

Therefore, the correlation function describing the fluctuating force $\hat{\mathcal{R}}(t)$ can be written as

$$\begin{aligned}
\langle \hat{\mathcal{R}}(t)\, \hat{\mathcal{R}}(t')\rangle \;=\; & \dot{z}\,\dot{z}'\, \left[\langle \hat{\mathcal{T}}^{01}_{\rm R}(t,z)\, \hat{\mathcal{T}}^{01}_{\rm R}(t',z')\rangle + \langle \hat{\mathcal{T}}^{01}_{\rm L}(t,z)\, \hat{\mathcal{T}}^{01}_{\rm L}(t',z')\rangle\right] \\
& - \dot{z}\, \left[\langle \hat{\mathcal{T}}^{01}_{\rm R}(t,z)\, \hat{\mathcal{T}}^{00}_{\rm R}(t',z')\rangle + \langle \hat{\mathcal{T}}^{01}_{\rm L}(t,z)\, \hat{\mathcal{T}}^{00}_{\rm L}(t',z')\rangle\right] \\
& - \dot{z}'\, \left[\langle \hat{\mathcal{T}}^{00}_{\rm R}(t,z)\, \hat{\mathcal{T}}^{01}_{\rm R}(t',z')\rangle + \langle \hat{\mathcal{T}}^{00}_{\rm L}(t,z)\, \hat{\mathcal{T}}^{01}_{\rm L}(t',z')\rangle\right] \\
& + \langle \hat{\mathcal{T}}^{00}_{\rm R}(t,z)\, \hat{\mathcal{T}}^{00}_{\rm R}(t',z')\rangle + \langle \hat{\mathcal{T}}^{00}_{\rm L}(t,z)\, \hat{\mathcal{T}}^{00}_{\rm L}(t',z')\rangle,
\end{aligned} \tag{4.19}$$

where $z = z(t)$ and $z' = z(t')$.

The quantity $\langle \hat{\mathcal{T}}^{ab}(t,x)\, \hat{\mathcal{T}}^{cd}(t',x')\rangle$ is essentially the so-called noise kernel corresponding to the stress-energy tensor of the scalar field (in this context, see, for instance, Refs. [76]). Upon using the decomposition (4.6), the modes (4.4) and the expressions (4.7) for the stress-energy tensor, the noise kernel in the regions to the right and the left of the mirror can be calculated to be

$$\begin{aligned}
\langle \hat{\mathcal{T}}^{ab}_{\rm R}(t,x)\, \hat{\mathcal{T}}^{cd}_{\rm R}(t',x')\rangle \;=\; & \frac{\pi^2}{8\,\beta^4} \biggl\{(-1)^{a+b+c+d}\, {\rm cosech}^4\left[\pi\,(v-v')/\beta\right] \\
& + (-1)^{a+b}\, p_1'^2(u')\, {\rm cosech}^4\left[\pi\, \left[v-p_1(u')\right]/\beta\right] \\
& + (-1)^{c+d}\, p_1'^2(u)\, {\rm cosech}^4\left[\pi\, \left[p_1(u)-v'\right]/\beta\right] \\
& + p_1'^2(u)\, p_1'^2(u')\, {\rm cosech}^4\left[\pi\, \left[p_1(u)-p_2(u')\right]/\beta\right]\biggr\},
\end{aligned} \tag{4.20}$$

$$\begin{aligned}
\langle \hat{\mathcal{T}}^{ab}_{\rm L}(t,x)\, \hat{\mathcal{T}}^{cd}_{\rm L}(t',x')\rangle \;=\; & \frac{\pi^2}{8\,\beta^4} \biggl\{{\rm cosech}^4\left[\pi\,(u-u')/\beta\right] \\
& + (-1)^{c+d}\, p_2'^2(v')\, {\rm cosech}^4\left[\pi\, \left[u-p_2(v')\right]/\beta\right] \\
& + (-1)^{a+b}\, p_2'^2(v)\, {\rm cosech}^4\left[\pi\, \left[p_2(v)-u'\right]/\beta\right] \\
& + (-1)^{a+b+c+d}\, p_2'^2(v)\, p_2'^2(v')\, {\rm cosech}^4\left[\pi\, \left[p_2(v)-p_2(v')\right]\beta\right]\biggr\},
\end{aligned} \tag{4.21}$$

where, as we had defined, $u = t - x$ and $v = t + x$, while $u' = t' - x'$ and $v' = t' + x'$. Note that the indices (a, b, c, d) take on the values zero and unity corresponding to t and x, respectively. Along the trajectory of the mirror $z(t)$, the noise kernels to the right and the left of the mirror simplify to

$$\begin{aligned}
\langle\hat{\mathcal{T}}^{ab}_{\rm R}(t,z)\,\hat{\mathcal{T}}^{cd}_{\rm R}(t',z')\rangle &= \frac{\pi^2}{8\,\beta^4}\left[(-1)^{a+b+c+d} + (-1)^{a+b}\left(\frac{1+\dot{z}'}{1-\dot{z}'}\right)^2 + (-1)^{c+d}\left(\frac{1+\dot{z}}{1-\dot{z}}\right)^2\right.\\
&\quad \left. + \left(\frac{1+\dot{z}}{1-\dot{z}}\right)^2\left(\frac{1+\dot{z}'}{1-\dot{z}'}\right)^2\right]\,{\rm cosech}^4\left[\pi\,\left(\Delta t + \Delta z\right)/\beta\right], \qquad (4.22a)\\
\langle\hat{\mathcal{T}}^{ab}_{\rm L}(t,z)\,\hat{\mathcal{T}}^{cd}_{L}(t',z')\rangle &= \frac{\pi^2}{8\beta^4}\left[1 + (-1)^{a+b}\left(\frac{1-\dot{z}}{1+\dot{z}}\right)^2 + (-1)^{c+d}\left(\frac{1-\dot{z}'}{1+\dot{z}'}\right)^2\right.\\
&\quad \left. + (-1)^{a+b+c+d}\left(\frac{1-\dot{z}}{1+\dot{z}}\right)^2\left(\frac{1-\dot{z}'}{1+\dot{z}'}\right)^2\right]\,{\rm cosech}^4\left[\pi\,\left(\Delta t - \Delta z\right)/\beta\right],\\
&\qquad (4.22b)
\end{aligned}$$

where $\Delta t = t - t'$ and $\Delta z = z - z'$. These quantities can be used in the expression (4.19) to arrive at the correlation function describing the fluctuating component of the radiation reaction force. Until now, the expressions we have obtained are exact. Our aim is to arrive at the correlation function when the mirror is moving non-relativistically. If one consistently ignores terms of order $\dot{z}^2$, it can be shown that the correlation function simplifies to (for details, see App. A.3)

$$\langle\hat{\mathcal{R}}(t)\,\hat{\mathcal{R}}(t')\rangle = \frac{\pi^2}{\beta^4}\,{\rm cosech}^4\left[\pi\,(t-t')/\beta\right]. \qquad (4.23)$$

This correlation function is a sharply peaked function about $t = t'$ with a width of the order of β. In the limit $\beta \to \infty$ (*i.e.* in the quantum vacuum), this correlation function reduces to

$$\langle\hat{\mathcal{R}}(t)\,\hat{\mathcal{R}}(t')\rangle = \frac{1}{\pi^2}\,\frac{1}{(t-t')^4}, \qquad (4.24)$$

which is what can be expected from general arguments in $(1+1)$-spacetime dimensions.

4.4 Establishing the fluctuation-dissipation theorem

Having obtained the average radiation reaction force on the moving mirror and having evaluated the correlation function describing the fluctuating component, let us now turn to establishing the fluctuation-dissipation theorem relating these quantities. In this section, we shall first explicitly establish the theorem for the problem of the moving mirror in the frequency domain and then go on to also establish it in the time domain.

4.4.1 The fluctuation-dissipation theorem in the frequency domain

Fluctuation-dissipation theorem is a general result in statistical mechanics, which is a relation between the generalized resistance and the fluctuations of the generalized forces in linear dissipative systems [34]. Before discussing the fluctuation-dissipation theorem let us define some essential quantities which are needed to state the fluctuation-dissipation theorem.

Let us define the correlation function of an operator $\hat{A}$ as

$$C_A(t) \equiv \langle \hat{A}(t_0)\, \hat{A}(t_0 + t) \rangle. \tag{4.25}$$

The symmetric and anti-symmetric correlation functions, *i.e.* $C_A^+(t)$ and $C_A^-(t)$, of the operator $\hat{A}$ can be defined to be [34]

$$C_A^+(t) \equiv \frac{1}{2}\left(\langle \hat{A}(t_0)\, \hat{A}(t_0+t)\rangle + \langle \hat{A}(t_0+t)\, \hat{A}(t_0)\rangle\right) = \frac{1}{2}\left[C_A(t) + C_A(-t)\right], \tag{4.26a}$$
$$C_A^-(t) \equiv \frac{1}{2}\left(\langle \hat{A}(t_0)\, \hat{A}(t_0+t)\rangle - \langle \hat{A}(t_0+t)\, \hat{A}(t_0)\rangle\right) = \frac{1}{2}\left[C_A(t) - C_A(-t)\right]. \tag{4.26b}$$

Given a function $f(t)$, let the Fourier transform $\widetilde{f}(\omega)$ be defined as

$$\widetilde{f}(\omega) = \int_{-\infty}^{\infty} \mathrm{d}t\, f(t)\, \mathrm{e}^{-i\,\omega\, t}. \tag{4.27}$$

The fluctuation-dissipation theorem describing the random function $\hat{A}(t)$ can be stated as the following relation between the Fourier transforms $\widetilde{C}_A^+(\omega)$ and $\widetilde{C}_A^-(\omega)$ [34]:

$$\widetilde{C}_A^+(\omega) = \coth(\beta\,\omega/2)\, \widetilde{C}_A^-(\omega), \tag{4.28}$$

with $\omega > 0$.

In the rest of this section, our aim will be to establish the relation (4.28) for the fluctuating component of the radiation reaction force on the moving mirror, *viz.* $\hat{\mathcal{R}}(t)$. Note that the quantity $C_{\mathcal{R}}(t)$ can be written as [cf. Eq. (4.23)]

$$C_{\mathcal{R}}(t) = \frac{\pi^2}{\beta^4}\, \mathrm{cosech}^4\left[\pi\,(t + i\,\epsilon)/\beta\right], \tag{4.29}$$

where, as is usually done in the context of quantum field theory, we have suitably introduced an $i\,\epsilon$ factor (with $\epsilon \to 0^+$) to regulate the two-point function in the coincidence limit. The Fourier transform of the correlation function $C_{\mathcal{R}}(t)$ is, evidently, given by

$$\widetilde{C}_{\mathcal{R}}(\omega) = \frac{\pi^2}{\beta^4} \int_{-\infty}^{\infty} \mathrm{d}t\, \mathrm{cosech}^4\left[\pi\,(t + i\,\epsilon)/\beta\right]\, \mathrm{e}^{-i\,\omega\, t}. \tag{4.30}$$

To evaluate this integral, it proves to be convenient to express the function $C_{\mathcal{R}}(t)$ as a series in the following fashion (for details, see App. A.4):

$$\begin{aligned} C_{\mathcal{R}}(t) &= \frac{\pi^2}{\beta^4}\,\mathrm{cosech}^4\left[\pi\,(t+i\,\epsilon)/\beta\right] \\ &= -\frac{2}{3\,\beta^2}\left[\frac{1}{(t+i\,\epsilon)^2}+\sum_{n=1}^{\infty}\frac{1}{(t+i\,n\,\beta)^2}+\sum_{n=1}^{\infty}\frac{1}{(t-i\,n\,\beta)^2}\right] \\ &\quad +\frac{1}{\pi^2}\left[\frac{1}{(t+i\,\epsilon)^4}+\sum_{n=1}^{\infty}\frac{1}{(t+i\,n\,\beta)^4}+\sum_{n=1}^{\infty}\frac{1}{(t-i\,n\,\beta)^4}\right]. \end{aligned} \tag{4.31}$$

Upon using this series representation, the integral (4.30) can be carried out as a contour integral in the complex ω-plane. Since $\omega > 0$, the contour has to be closed in the lower half plane. The contour encloses the poles at $-i\,\epsilon$ and $-i\,n\,\beta$, so that only the first two terms within the square brackets in the above series representation for $C_{\mathcal{R}}(t)$ contribute. Their contributions can be summed over to obtain that [32, 35, 74]

$$\widetilde{C}_{\mathcal{R}}(\omega) = \frac{2}{(1-\mathrm{e}^{-\beta\,\omega})}\left(\frac{\omega^3}{6\,\pi}+\frac{2\,\pi\,\omega}{3\,\beta^2}\right). \tag{4.32}$$

The quantities $\widetilde{C}_{R}^{+}(\omega)$ and $\widetilde{C}_{R}^{-}(\omega)$ can be determined from the above expression for $\widetilde{C}_{\mathcal{R}}(\omega)$, and they are found to be

$$\widetilde{C}_{\mathcal{R}}^{+}(\omega) = \coth\left(\beta\,\omega/2\right)\left(\frac{\omega^3}{6\,\pi}+\frac{2\,\pi\,\omega}{3\,\beta^2}\right), \tag{4.33a}$$

$$\widetilde{C}_{\mathcal{R}}^{-}(\omega) = \frac{\omega^3}{6\,\pi}+\frac{2\,\pi\,\omega}{3\,\beta^2}. \tag{4.33b}$$

The first term in the above expression for $\widetilde{C}_{\mathcal{R}}^{-}(\omega)$ is the vacuum contribution, while the second term arises at a finite temperature. These can be attributed to the $\dddot{z}$ and the $\dot{z}$ terms that arise in the mean radiation reaction force at zero and finite temperature, respectively [cf. Eq. (4.14)]. It is evident from these expressions that the quantities $\widetilde{C}_{R}^{+}(\omega)$ and $\widetilde{C}_{R}^{-}(\omega)$ are related as

$$\widetilde{C}_{\mathcal{R}}^{+}(\omega) = \coth\left(\beta\,\omega/2\right)\,\widetilde{C}_{R}^{-}(\omega), \tag{4.34}$$

exactly as required by the fluctuation-dissipation theorem.

4.4.2 The fluctuation-dissipation theorem in the time domain

Let us now consider the fluctuation-dissipation theorem in the time domain. In the time domain, the theorem relates the correlation function $C_{\mathcal{R}}(t)$ of the fluctuating force to the amplitude of the coefficient, say, $m\,\gamma$, of the mean dissipative force (proportional to velocity) arising at a finite temperature as follows [34]:

$$m\,\gamma = \beta \int_0^\infty \mathrm{d}t\, C_{\mathcal{R}}(t). \tag{4.35}$$

In the case of the moving mirror, we have $m\,\gamma = 2\,\pi/(3\,\beta^2)$ [cf. Eq. (4.14)]. Since the above integral corresponds to the $\omega \to 0$ of $\widetilde{C}_{\mathcal{R}}(\omega)/2$, we find that

$$\beta \int_0^\infty \mathrm{d}t\, C_{\mathcal{R}}(t) = \beta \lim_{\omega\to 0} \frac{\widetilde{C}_{\mathcal{R}}(\omega)}{2} = \beta\, \frac{2\,\pi}{3\,\beta^3} = m\,\gamma, \tag{4.36}$$

as required, implying the validity of the fluctuation-dissipation theorem in the time domain as well.

4.5 Diffusion of the mirror at finite temperature

In this section, we shall utilize the fluctuation-dissipation theorem to determine the mean-squared displacement in the position of the mirror due to the combination of the mean radiation reaction force on the mirror as well as the fluctuating component. We shall also discuss the different limiting behavior of the mean-squared displacement of the mirror.

4.5.1 The mean-squared displacement of the mirror at finite temperature

The mean-squared displacement $\sigma_z^2(t)$ in the position of the mirror is defined as

$$\sigma_z^2(t) \equiv \langle [\hat{z}(t) - \hat{z}(0)]^2 \rangle = 2\,\left[C_z^+(0) - C_z^+(t)\right], \tag{4.37}$$

where $\hat{z}(t)$ represents the stochastic nature of the position of the mirror, which are induced due to the fluctuations in the radiation reaction force. When we take into account the mean radiation reaction force (4.14) and the fluctuating component (4.15), the Langevin equation governing the motion of the moving mirror is given by

$$m\,\frac{\mathrm{d}^2\hat{z}}{\mathrm{d}t^2} - \frac{1}{6\,\pi}\,\frac{\mathrm{d}^3\hat{z}}{\mathrm{d}t^3} + \frac{2\,\pi}{3\,\beta^2}\,\frac{\mathrm{d}\hat{z}}{\mathrm{d}t} = \hat{\mathcal{R}}(t). \tag{4.38}$$

Let $\widetilde{z}(\omega)$ and $\widetilde{\mathcal{R}}(\omega)$ denote the Fourier transforms of the position of the mirror $\hat{z}(t)$ and the fluctuating component $\hat{\mathcal{R}}(t)$ of the radiation reaction force. The above Langevin equation relates these two quantities as follows:

$$\widetilde{z}(\omega) = \widetilde{\chi}(\omega)\,\widetilde{\mathcal{R}}(\omega), \tag{4.39}$$

where $\widetilde{\chi}(\omega)$ is a complex quantity known as the generalized susceptibility. It can be expressed as

$$\widetilde{\chi}(\omega) = \frac{6\,\pi}{i\,\omega\,(\omega + i\,\alpha_1)\,(\omega - i\,\alpha_2)} \tag{4.40}$$

with α_1 and α_2 being given by

$$\alpha_1 = 3\,\pi\,\omega_{\rm c}\left[\sqrt{1 + \left(\frac{2\,r}{3}\right)^2} + 1\right], \tag{4.41a}$$

$$\alpha_2 = 3\,\pi\,\omega_{\rm c}\left[\sqrt{1 + \left(\frac{2\,r}{3}\right)^2} - 1\right], \tag{4.41b}$$

where we have set $\omega_{\rm c} = m$ and $r = (\beta\,m)^{-1}$. The quantity $\omega_{\rm c}$ is essentially the Compton frequency associated with the mirror, while r is the dimensionless ratio of the average energy associated with a single degree of freedom in the thermal bath and the rest mass energy of the mirror.

Let us write the generalized susceptibility as $\chi(\omega) = \widetilde{\chi}'(\omega) - i\,\widetilde{\chi}''(\omega)$, where $\widetilde{\chi}'(\omega)$ and $\widetilde{\chi}''(\omega)$ are real quantities. (The single and the double primes above $\widetilde{\chi}(\omega)$ are the conventional notations to denote the real and the imaginary parts of the generalized susceptibility. It should be clarified that these primes *do not* represent derivatives of these quantities.) According to the fluctuation-dissipation theorem, the quantity $\widetilde{C}_z^{+}(\omega)$ is related to the quantity $\widetilde{\chi}''(\omega)$ as follows [34]:

$$\widetilde{C}_z^{+}(\omega) = \coth\left(\beta\,\omega/2\right)\,\widetilde{\chi}''(\omega). \tag{4.42}$$

Note that the mean-squared displacement $\sigma_z^2(t)$ of the mirror is related to the correlation function $C_z^{+}(t)$ [cf. Eq. (4.37)]. The correlation function $C_z^{+}(t)$ can be arrived at by inverse Fourier transforming the above expression for $\widetilde{C}_z^{+}(\omega)$. Clearly, the quantity $C_z^{+}(t)$ is the convolution of the inverse Fourier transforms of $\coth\left(\beta\,\omega/2\right)$ and $\widetilde{\chi}''(\omega)$, so that we have

$$C_z^{+}(t) = \frac{i}{\beta}\int_{-\infty}^{\infty} {\rm d}t'\,\coth\left(\pi\,t'/\beta\right)\,\chi''(t-t'), \tag{4.43}$$

where $\chi''(t)$ is described by the integral

$$\chi''(t) = \frac{1}{2\,\pi}\int_{-\infty}^{\infty} {\rm d}\omega\,\widetilde{\chi}''(\omega)\,{\rm e}^{i\,\omega\,t}. \tag{4.44}$$

The imaginary part of complex susceptibility $\widetilde{\chi}(\omega)$ is found to be

$$\widetilde{\chi}''(\omega) = \frac{6\,\pi\,(\omega^2 + \alpha_1\,\alpha_2)}{(\omega - i\,\epsilon)\,(\omega^2 + \alpha_1^2)\,(\omega^2 + \alpha_2^2)}, \tag{4.45}$$

where we have introduced an $i\,\epsilon$ factor suitably to ensure the convergence of $\tilde{\chi}(\omega)$ [34]. The integral (4.44), with $\widetilde{\chi}''(\omega)$ given by the above expression, can be carried out easily as a contour integral in the complex ω-plane, and one obtains that

$$\chi''(t) = 3\,i\,\pi\left\{\frac{2\,\Theta(t)}{\alpha_1\,\alpha_2} - \mathrm{sgn}(t)\,\left[\frac{\mathrm{e}^{-\alpha_1\,|t|}}{\alpha_1\,(\alpha_1+\alpha_2)} + \frac{\mathrm{e}^{-\alpha_2\,|t|}}{\alpha_2\,(\alpha_1+\alpha_2)}\right]\right\}, \tag{4.46}$$

where $\Theta(t)$ is the theta function, while the function $\mathrm{sgn(t)}$ is given by

$$\mathrm{sgn}(t) = \begin{cases} 1 & \text{when} \quad t > 0, \\ -1 & \text{when} \quad t < 0. \end{cases} \tag{4.47}$$

Upon using the above expression for $\chi''(t)$ in Eq. (4.43), we find that we can write $C_z^{+}(t)$ as follows:

$$\begin{aligned} C_z^{+}(t) \;=\; & -\frac{6\,\pi}{\alpha_1\,\alpha_2\,\beta}\int_{-\infty}^{t}\mathrm{d}t'\,\coth\left[\pi\,(t'+i\epsilon)/\beta\right] \\ & +\frac{3\,\pi}{\alpha_1\,(\alpha_1+\alpha_2)\,\beta}\,\left[\mathrm{e}^{-\alpha_1\,t}\,I_1(\alpha_1,t) - \mathrm{e}^{\alpha_1\,t}\,I_2(\alpha_1,t)\right] \\ & +\frac{3\,\pi}{\alpha_2\,(\alpha_1+\alpha_2)\,\beta}\,\left[\mathrm{e}^{-\alpha_2\,t}\,I_1(\alpha_2,t) - \mathrm{e}^{\alpha_2\,t}\,I_2(\alpha_2,t)\right], \end{aligned} \tag{4.48}$$

where the quantities $I_1(\alpha,t)$ and $I_2(\alpha,t)$ are described by the integrals

$$I_1(\alpha,t) \;=\; \int_{-\infty}^{t}\mathrm{d}t'\,\mathrm{e}^{\alpha\,t'}\,\coth\left[\pi\,(t'+i\,\epsilon)/\beta\right], \tag{4.49a}$$

$$I_2(\alpha,t) \;=\; \int_{t}^{\infty}\mathrm{d}t'\,\mathrm{e}^{-\alpha\,t'}\,\coth\left[\pi\,(t'+i\epsilon)/\beta\right]. \tag{4.49b}$$

On substituting the above expression for $C_z^{+}(t)$ in Eq. (4.37), we obtain the mean-squared displacement of the mirror to be

$$\begin{aligned} \sigma_z^2(t) \;=\; & \frac{12\,\pi}{\alpha_1\,\alpha_2\,\beta}\int_0^t\mathrm{d}t'\,\coth\left[\pi\,(t'+i\epsilon)/\beta\right] \\ & -\frac{6\,\pi}{\alpha_1\,(\alpha_1+\alpha_2)\,\beta}\,\left[\mathrm{e}^{-\alpha_1\,t}\,I_1(\alpha_1,t) - \mathrm{e}^{\alpha_1\,t}\,I_2(\alpha_1,t) - I_1(\alpha_1,0) + I_2(\alpha_1,0)\right] \\ & -\frac{6\,\pi}{\alpha_2\,(\alpha_1+\alpha_2)\,\beta}\,\left[\mathrm{e}^{-\alpha_2\,t}\,I_1(\alpha_2,t) - \mathrm{e}^{\alpha_2\,t}\,I_2(\alpha_2,t) - I_1(\alpha_2,0) + I_2(\alpha_2,0)\right]. \end{aligned} \tag{4.50}$$

The integrals $I_1(\alpha,t)$ and $I_2(\alpha,t)$ can be evaluated in terms of the hypergeometric functions (for details, see App. A.5), and the final result can be expressed as

$$\begin{aligned} \sigma_z^2(t) \;=\; & \frac{12}{\alpha_1\,\alpha_2}\left\{\gamma_{\mathrm{E}} + \ln\left[2\sinh(\pi\,t/\beta)\right]\right\} + \frac{12}{\alpha_1\,(\alpha_1+\alpha_2)}\,F(p_1,t) \\ & +\frac{12}{\alpha_2\,(\alpha_1+\alpha_2)}\,F(p_2,t), \end{aligned} \tag{4.51}$$

where $\gamma_{\rm E} \simeq 0.5772$ is the Euler-Mascheroni constant [77]. The function $F(p,t)$ is given by

$$\begin{aligned} F(p,t) &= \frac{\pi}{2}\cot(\pi\, p)\, {\rm e}^{-2\,\pi\, p\, t/\beta} + \frac{{\rm e}^{-2\,\pi\, t/\beta}}{2\,(1-p)}\, {}_2F_1\left[1, 1-p; 2-p; {\rm e}^{-2\,\pi\, t/\beta}\right] \\ &\quad + \frac{1}{2\,p}\, {}_2F_1\left[1, p; p+1; {\rm e}^{-2\pi\, t/\beta}\right] + \psi_0(p), \end{aligned} \tag{4.52}$$

where ${}_2F_1[a, b, c, ; z]$ denotes the hypergeometric function, and $\psi_n(z)$ is known as the polygamma function [77]. The quantities p_1 and p_2 are defined as

$$p_1 = \frac{\alpha_1\, \beta}{2\,\pi}, \quad p_2 = \frac{\alpha_2\, \beta}{2\,\pi}, \tag{4.53}$$

with α_1 and α_2 being given by Eqs. (4.41). Note that the mean-squared displacement (4.51) depends on three time scales, *viz.* t, $\omega_{\rm c}^{-1}$ and β. Let us now consider the limiting forms of the mean-squared displacement of the mirror in the different regimes of interest.

4.5.2 The different limiting behavior of the mean-squared displacement of the mirror

As mentioned above, the mean-squared displacement $\sigma_z^2(t)$ depends on three time scales t, ω_c^{-1} and β. Using these time scales one can construct the following three dimensionless variables: $\omega_{\rm c}\, t$, t/β and $\beta\, \omega_c$. Notice that the expression (4.51) for the mean-squared displacement at a finite temperature depends on time only through the following dimensionless combination: $\tilde{t} \equiv t/\beta$. It also depends on the dimensionless quantity $r = (\beta\, \omega_{\rm c})^{-1}$, which we had introduced earlier [cf. Eq. (4.41)]. Typically, we will be interested in the behavior of the mean-squared displacement at small and large times, *i.e.* for $\tilde{t} \ll 1$ and $\tilde{t} \gg 1$. But, because of the presence of the additional dimensionless quantity r, the different possible limits that one can actually consider are as follows:

$$\begin{aligned} &\lim_{r\to 0}\lim_{\tilde{t}\to 0}\, \sigma_z^2(t), \quad \lim_{\tilde{t}\to 0}\lim_{r\to 0}\, \sigma_z^2(t), \\ &\lim_{r\to \infty}\lim_{\tilde{t}\to 0}\, \sigma_z^2(t), \quad \lim_{\tilde{t}\to 0}\lim_{r\to \infty}\, \sigma_z^2(t), \end{aligned}$$

for small $\tilde{t}$, and

$$\begin{aligned} &\lim_{r\to 0}\lim_{\tilde{t}\to \infty}\, \sigma_z^2(t), \quad \lim_{\tilde{t}\to \infty}\lim_{r\to 0}\, \sigma_z^2(t), \\ &\lim_{r\to \infty}\lim_{\tilde{t}\to \infty}\, \sigma_z^2(t), \quad \lim_{\tilde{t}\to \infty}\lim_{r\to \infty}\, \sigma_z^2(t), \end{aligned}$$

for large $\tilde{t}$. In other words, a priori, one can consider the limits of small and large r before or after considering the small and large limits of $\tilde{t}$. However, we find that, as $r \to 0$ (or, as $r \to \infty$) the limiting values of the mean-squared displacement are not numerically equal to the dominant term in the series expansion of $\sigma_z^2(t)$ around $r = 0$ (and $r = \infty$, respectively) for all values of $\tilde{t}$. Therefore, we shall take the small and large limits of $\tilde{t}$, before considering the limiting cases of r.

We find that, in the limit of $\tilde{t} \ll 1$, $\sigma_z^2(t)$ can be expressed as

$$\sigma_z^2(t) = 6\, t^2 \left\{\frac{3}{2} - \gamma_{\mathrm{E}} - \ln\left(2\,\pi\, t/\beta\right) - \frac{1}{(p_1 + p_2)}\, \left[1 + p_1\, \psi_0(p_1) + p_2\, \psi_0(p_2)\right]\right\}. \tag{4.54}$$

Whereas, when $\tilde{t} \gg 1$, it reduces to

$$\sigma_z^2(t) = \frac{3\,\beta\, t}{\pi} + \frac{6\,\beta^2}{2\,\pi^2} \left\{\gamma_{\mathrm{E}} + \frac{p_2}{(p_1 + p_2)}\, \left[\frac{1}{2\, p_1} + \psi_0(p_1)\right] + \frac{p_1}{(p_1 + p_2)}\, \left[\frac{1}{2\, p_2} + \psi_0(p_2)\right]\right\}. \tag{4.55}$$

Let us now consider the different limits of r of the above two expressions. For convenience and clarity, we have listed these forms in the table below and have commented appropriately on their behavior.

<table>
<tr><th>Relevant limits</th><th>Limiting behavior of $\sigma_z^2(t)$</th><th>Remarks</th></tr>
<tr><td>$t \ll \omega_{\rm c}^{-1} \ll \beta$</td><td>$6\,t^2\,\left[(3/2) - \gamma_{\rm E} - \,\ln(6\,\pi\,\omega_c\,t)\right]$</td><td rowspan="2">Although we quote it for the sake of completeness, this limit corresponds to $\omega_{\rm c}\,t \ll 1$, i.e. when the times involved are much smaller than the Compton time scale. The quantum nature of the mirror cannot be ignored in such a domain. Since our analysis assumes a classical, non-relativistic description for the mirror, it might be unjustified to attach any significance to this limit for the mean-squared displacement of the mirror.</td></tr>
<tr><td>$t \ll \beta \ll \omega_{\rm c}^{-1}$</td><td>$6\,t^2\,\left[1 - \,\ln\left(2\pi\,t/\beta\right)\right]$</td></tr>
<tr><td>$\beta \ll t \ll \omega_{\rm c}^{-1}$</td><td rowspan="2">$\dfrac{2\,t}{m\,\gamma\,\beta} + \dfrac{3\,\beta^2}{2\,\pi^2} \simeq \dfrac{2\,t}{m\,\gamma\,\beta}$</td><td rowspan="2">This limit demonstrates that, as long as $t \gg \beta$, the limiting behavior of $\sigma_z^2(t)$ does not depend on $\omega_{\rm c}\,t$ (although the same comment as above applies to the case $\omega_{\rm c}\,t \ll 1$). Moreover, as is evident from the expression in the last row (below), this limit is also independent of r. One can therefore see that, for $t \gg \beta$, the mirror exhibits the standard random walk with $\sigma_z^2(t) \propto t$. (To highlight this behavior, we have expressed the final result in terms of the parameter γ to facilitate comparison with standard discussions of random walk [33].)</td></tr>
<tr><td>$\beta \ll \omega_{\rm c}^{-1} \ll t$</td></tr>
<tr><td>$\omega_{\rm c}^{-1} \ll t \ll \beta$</td><td>$t^2/(\beta\,m)$</td><td rowspan="2">In these limits, the mirror behaves exactly like a Brownian particle. For $t \ll \beta$, we have $\sigma_z^2(t) \propto t^2$, and the mirror diffuses like a free particle with velocity $1/\sqrt{m\,\beta}$. This result suggests that the thermal length scale (β) can be the mean free path of the mirror. For $t \gg \beta$, we recover the standard random walk result, viz. $\sigma_z^2(t) \propto t$.</td></tr>
<tr><td>$\omega_{\rm c}^{-1} \ll \beta \ll t$</td><td>$\dfrac{2}{m\,\gamma\,\beta}\,\left[t - \gamma^{-1}\right] \simeq \dfrac{2\,t}{m\,\gamma\,\beta}$</td></tr>
</table>

4.6 Diffusion of the mirror at zero temperature

Let us now study the nature of diffusion of the mirror at zero temperature.

4.6.1 The mean-squared displacement of the mirror at zero temperature

At zero temperature, evidently, the finite temperature contribution will be absent and the Langevin equation governing the motion of the mirror simplifies to

$$m\,\frac{\mathrm{d}^2\hat{z}}{\mathrm{d}t^2} - \frac{1}{6\,\pi}\,\frac{\mathrm{d}^3\hat{z}}{\mathrm{d}t^3} = \hat{\mathcal{R}}. \tag{4.56}$$

In such a case, the complex susceptibility $\widetilde{\chi}(\omega)$ is given by [cf. Eq. (4.39)]

$$\widetilde{\chi}(\omega) = \frac{6\,\pi}{i\,\omega^2\,(\omega + 6\,\pi\,i\,\omega_{\mathrm{c}})}, \tag{4.57}$$

and the imaginary part of the complex susceptibility $\widetilde{\chi}(\omega)$ can be determined to be

$$\widetilde{\chi}''(\omega) = \frac{6\,\pi}{\omega\,[\omega^2 + (6\,\pi\,\omega_{\mathrm{c}})^2]}. \tag{4.58}$$

At zero temperature, the fluctuation-dissipation relation (4.42) reduces to

$$\widetilde{C}_z^+(\omega) = [\Theta(\omega) - \Theta(-\omega)]\,\widetilde{\chi}''(\omega), \tag{4.59}$$

where $\Theta(\omega)$ denotes the theta function. The inverse Fourier transform of this function yields $C_z^+(t)$, which is, evidently, a convolution described by the integral

$$C_z^+(t) = \frac{i}{\pi}\int_{-\infty}^{\infty}\frac{\mathrm{d}t'}{t'}\,\chi''(t-t'). \tag{4.60}$$

The quantity $\chi''(t)$ can be easily evaluated from $\widetilde{\chi}''(\omega)$ above [cf. Eq. (4.58)] as a contour integral in the complex ω-plane. It can be obtained to be

$$\chi''(t) = \frac{3\,\pi\,i}{(6\,\pi\,\omega_c)^2}\,\left[2\,\Theta(t) - \mathrm{sgn}(t)\,\mathrm{e}^{-6\,\pi\,\omega_{\mathrm{c}}\,|t|}\right], \tag{4.61}$$

where $\mathrm{sgn}(t)$ is defined in Eq. (4.47). On using this expression, we find that $C_z^+(t)$ can be written as

$$C_z^+(t) = \frac{-3}{(6\,\pi\,\omega_{\mathrm{c}})^2}\left[2\int_{-\infty}^{t}\frac{dt'}{t'} - \mathrm{e}^{-6\,\pi\,\omega_{\mathrm{c}}\,t}\,\mathrm{Ei}\,(6\,\pi\,\omega_{\mathrm{c}}\,t) - \mathrm{e}^{6\,\pi\,\omega_{\mathrm{c}}\,t}\,\mathrm{Ei}\,(-6\,\pi\,\omega_{\mathrm{c}}\,t)\right], \tag{4.62}$$

where $\mathrm{Ei}(x)$ is the exponential integral function [77]. Upon using the above result, one can show that the mean-squared displacement of the mirror can be expressed as follows:

$$\sigma_z^2(t) = \frac{6}{(6\,\pi\,\omega_{\mathrm{c}})^2}\left[2\ln(6\,\pi\,\omega_{\mathrm{c}}\,t) + 2\,\gamma_E - \mathrm{e}^{-6\,\pi\,\omega_{\mathrm{c}}\,t}\,\mathrm{Ei}(6\,\pi\,\omega_{\mathrm{c}}\,t) - \mathrm{e}^{6\,\pi\,\omega_{\mathrm{c}}\,t}\,\mathrm{Ei}(-6\,\pi\,\omega_{\mathrm{c}}\,t)\right], \tag{4.63}$$

where, as we have pointed out before, γ_{E} is Euler-Mascheroni constant.

4.6.2 The different limiting behavior of the mean-squared displacement of the mirror

We find that, when $\omega_{\mathrm{c}}\, t \ll 1$, the mean-squared displacement of the mirror behaves as

$$\sigma_z^2(t) = 6\, t^2\, \left[\frac{3}{2} - \gamma_{\mathrm{E}} - \ln\left(6\,\pi\,\omega_{\mathrm{c}}\, t\right)\right]. \tag{4.64}$$

Whereas, when $\omega_{\mathrm{c}}\, t \gg 1$, $\sigma_z^2(t)$ is found to behave as

$$\sigma_z^2(t) = \frac{12}{(6\,\pi\,\omega_{\mathrm{c}})^2}\, \left[\gamma_{\mathrm{E}} + \ln\left(6\,\pi\,\omega_{\mathrm{c}}\, t\right)\right]. \tag{4.65}$$

This implies that, at zero temperature, the mirror diffuses logarithmically rather than linearly as it does at a finite temperature. It should be mentioned that such a logarithmic diffusive behavior has been arrived at earlier and it seems to be a general characteristic of Brownian motion at zero temperature (in this context, see Refs. [35]).

4.7 Discussion

In this work, we have studied the random motion of a mirror that is immersed in a thermal bath [78]. We have explicitly evaluated the correlation function describing the fluctuating component of the radiation reaction force on the moving mirror and have established the fluctuation-dissipation theorem relating the correlation function to the amplitude of the finite temperature contribution to the radiation reaction force. Also, utilizing the fluctuation-dissipation theorem, we have calculated the mean-squared displacement of the moving mirror both at a finite as well as at zero temperature. We should stress that, in contrast to the earlier efforts, we have been able to arrive at a complete expression for the mean-squared displacement of the mirror that is valid at all times. While we recover the standard results in the required limits at finite temperature, interestingly, we find that the mirror diffuses logarithmically at zero temperature, a result which confirms similar conclusions that have been arrived at earlier.

Finally, we find that the mean-squared displacement in the quantum vacuum cannot be obtained by blindly considering the zero temperature limit of the final expression for the mean-squared displacement at finite temperature. This is essentially because of the following reason: the integral representations leading to the hypergeometric functions that arise in the finite temperature case [cf. Eq. (4.51)] do not apply at zero temperature, thereby rendering the subsequent expressions invalid in this limit. (We have discussed this issue more quantitatively in App. A.6.) It is for this reason that, to analyze the zero temperature case, we have returned to the Langevin equation and then proceeded with the derivation by making use of the corresponding fluctuation-dissipation theorem [see Eq. (4.59)].

Chapter 5

Quantum-to-classical transition in bouncing universes

5.1 Introduction

The current cosmological observations seem to be well described by the so-called standard model of cosmology, which consists of the ΛCDM model, supplemented by the inflationary paradigm [79, 80]. The primary role played by inflation is to provide a causal mechanism for the generation of the primordial perturbations [81], which later lead to the anisotropies in the Cosmic Microwave Background (CMB) and eventually to the inhomogeneities in the Large Scale Structure (LSS) [36]. The nearly scale invariant power spectrum of primordial perturbations predicted by inflation has been corroborated by the state of the art observations of the CMB anisotropies by the Planck mission [80]. Despite the fact that inflation has been successful in helping to overcome some of the problems faced within the hot big bang model, the issue of the big bang singularity still remains to be addressed. Moreover, the remarkable efficiency of the inflationary scenario has led to a situation wherein, despite the constant improvement in the accuracy and precision of the cosmological observations, there seem to exist too many inflationary models that remain consistent with the data [80]. This situation has even provoked the question of whether, as a paradigm, inflation can be falsified at all (in this context, see the popular articles [82]). Due to these reasons, it seems important, even imperative, to systematically explore alternatives to inflation. One such alternative that has drawn a lot of attention in the literature are the bouncing scenarios [38].

In bouncing models, the universe goes through an initial phase of contraction, until the scale factor reaches a minimum value, and it undergoes expansion thereafter [38]. Driving a bounce often requires one to violate the null energy condition and hence, unlike inflation, they cannot be driven by simple, canonical scalar fields. In fact, the exact content of the universe which is responsible for the bounce remains to be satisfactorily understood. Also, concerns may arise whether quantum gravitational effects can become important at the bounce [83]. To avoid such concerns, one often considers completely classical bounces wherein the energy densities of the matter fields driving the bounce always remain much smaller than the Planckian energy densities. In a fashion similar to slow roll inflation, certain bouncing models referred to as near-matter bounces, can also generate nearly scale invariant power spectra [84, 85], as is demanded by the observations [79, 80]. However, while proposing an inflationary model seems to be a rather easy task (which is reflected in the multitude of such models), a variety of problems (such as the need for fine tuned initial conditions and the rapid growth of anisotropies, to name just two) plague the bouncing models [38]. It would be fair to say that a satisfactory classical bouncing scenario that is devoid of these various issues is yet to be constructed.

The generation of primordial perturbations in the early universe, whether in a bouncing or in an inflationary scenario, is a result of an interplay between quantum and gravitational physics [12, 40, 86]. Since it is the quantum perturbations that lead to anisotropies in the CMB and inhomogeneities in the LSS, it provides a unique window to probe fundamental issues pertaining to quantum and gravitational physics. One such issue of interest is the mechanism underlying the transition of the quantum perturbations generated in the early universe to the LSS that can be completely described in terms of correlations involving classical stochastic variables, in other words, the quantum-to-classical transition of the primordial perturbations.

While the issue of the quantum-to-classical transition of primordial perturbations has been studied to a good extent in inflation [12, 40, 86], we find that there has been hardly any effort in this direction in the context of bouncing scenarios (see, however, Ref. [87] which addresses issues similar to what we shall consider here). In this work, we shall investigate this problem for the case of tensor perturbations produced in a class of bouncing scenarios. We shall approach the problem from two different perspectives. Firstly, we shall examine the extent of squeezing of the quantum state associated with the tensor perturbations using the Wigner function [40]. It has been found that, in the context of inflation, the primordial quantum perturbations become strongly squeezed once the modes leave the Hubble radius [12, 86]. In strongly squeezed states, the quantum expectation values can be indistinguishable from classical stochastic averages of the correlation functions, such as those used to characterize the anisotropies in the CMB and the LSS [40]. Specifically, we shall investigate if the Wigner function and the parameter describing the extent of squeezing behave in a similar manner in the bouncing scenarios.

Secondly, we shall study the issue from the perspective of a quantum measurement problem. The quantum measurement problem concerns the phenomenon by which a quantum state upon measurement collapses to one of the eigenstates of the observable under measurement. In the cosmological context, this problem translates to as to how the quantum state of the primordial perturbations collapse into the eigenstate, say, corresponding to the CMB observed today. This problem is aggravated in the cosmological context due to the fact that there were no observers in the early universe to carry out any measurements [88]. One of the proposals which addresses the quantum measurement problem is the so-called Continuous Spontaneous Localization (CSL) model [89]. The advantage of using the CSL model to study the quantum measurement problem in the context of cosmology is that, in this model, the collapse of the wavefunction occurs without the presence of an observer. In the CSL model, the Schrödinger equation is modified by adding non-linear and stochastic terms which suppress the quantum effects in the classical domain, and also reproduce the predictions of quantum mechanics in the quantum regime (for reviews, see Refs. [90]). In the context of inflation, there have been attempts to understand the quantum measurement problem by employing the CSL model [41, 91]. Motivated by these efforts in the context of inflation, in this work, we shall investigate the quantum-to-classical transition in bouncing scenarios from the two perspectives described above.

The remainder of this chapter is organized as follows. In Sec. 5.2, working in the Schrödinger picture, we shall quickly review the quantization of the tensor perturbations in an evolving universe and arrive at the wavefunction governing the perturbations. In Sec. 5.3, we shall describe the evolution of the tensor perturbations in a specific matter bounce scenario and obtain the resulting tensor power spectrum. In Sec. 5.4, using the Wigner function, we shall examine the squeezing of the quantum state describing the tensor modes as they evolve in a matter bounce. In Sec. 5.5, after a brief summary of the essential aspects of the CSL mechanism, we shall study its imprints on the tensor power spectrum produced in a matter bounce. In Sec. 5.6, we shall discuss the evolution of the tensor perturbations in a more generic bounce and evaluate the corresponding tensor power spectrum, including the effects due to CSL. Finally, in Sec. 5.7, we shall conclude with a brief summary of the main results.

Note that, in this chapter, we shall work with natural units wherein $\hbar = c = 1$, and define the Planck mass to be $M_{_{\rm Pl}} = (8\,\pi\,G)^{-1/2}$. Working in $(3+1)$-spacetime dimensions, we shall adopt the metric signature of $(+,-,-,-)$. Also, overprimes shall denote differentiation with respect to the conformal time coordinate η.

5.2 Quantization of the tensor perturbations in the Schrödinger picture

We shall consider a spatially flat Friedmann-Lemaître-Robertson-Walker (FLRW) universe which is described by the line element

$$\mathrm{d}s^2 = a^2(\eta)\,\left(\mathrm{d}\eta^2 - \delta_{ij}\,\mathrm{d}x^i\,\mathrm{d}x^j\right), \tag{5.1}$$

where $a(\eta)$ denotes the scale factor, with η being the conformal time coordinate. Upon taking into account the tensor perturbations, say, h_{ij}, the FLRW metric assumes the form

$$\mathrm{d}s^2 = a^2(\eta)\,\left[\mathrm{d}\eta^2 - (\delta_{ij} + h_{ij})\,\mathrm{d}x^i\,\mathrm{d}x^j\right], \tag{5.2}$$

where h_{ij} satisfies the traceless and transverse conditions (*i.e.* $h^i_i = 0$ and $\partial_j h^{ij} = 0$).

The second order action governing the tensor perturbations h_{ij} is given by (see the following reviews [81])

$$\delta_2 S = \frac{M_{_{\mathrm{Pl}}}^2}{8}\int \mathrm{d}\eta \int \mathrm{d}^3\boldsymbol{x}\; a^2(\eta)\,\left[h'^2_{ij} - (\partial h_{ij})^2\right]. \tag{5.3}$$

The homogeneity and isotropy of the background metric permits the following Fourier decomposition of the tensor perturbations:

$$h_{ij}(\eta, \boldsymbol{x}) = \sum_{s=1}^{2} \int \frac{\mathrm{d}^3\boldsymbol{k}}{(2\,\pi)^{3/2}}\,\varepsilon^s_{ij}(\boldsymbol{k})\,h_{\boldsymbol{k}}(\eta)\,\mathrm{e}^{i\,\boldsymbol{k}\cdot\boldsymbol{x}}, \tag{5.4}$$

where $\varepsilon^s_{ij}(\boldsymbol{k})$ denotes the polarization tensor, with s representing the helicity. The polarization tensor satisfies the normalization condition: $\varepsilon^r_{ij}(\boldsymbol{k})\,\varepsilon^{s*}_{ij}(\boldsymbol{k}) = 2\,\delta^{rs}$ [81]. In terms of the Fourier modes $h_{\boldsymbol{k}}$, the second order action (5.3) can be expressed as

$$\delta_2 S = \frac{M_{_{\mathrm{Pl}}}^2}{2}\int \mathrm{d}\eta \int \mathrm{d}^3\boldsymbol{k}\; a^2(\eta)\,\left[h'_{\boldsymbol{k}}(\eta)\,h'^*_{\boldsymbol{k}}(\eta) - k^2\,h_{\boldsymbol{k}}(\eta)\,h^*_{\boldsymbol{k}}(\eta)\right], \tag{5.5}$$

where $k = |\boldsymbol{k}|$. Note that, since $h_{ij}(\eta, \boldsymbol{x})$ is real, the integral over $\boldsymbol{k}$ runs over only half of the Fourier space, *i.e.* $\mathbb{R}^{3+}$.

It proves to be convenient to express the tensor modes in terms of the so-called Mukhanov-Sasaki variable $u_{\boldsymbol{k}}$ as $h_{\boldsymbol{k}} = (\sqrt{2}/M_{_{\mathrm{Pl}}})\,(u_{\boldsymbol{k}}/a)$ [81]. In terms of the Mukhanov-Sasaki variable, the second order action (5.3) takes the form

$$\delta_2 S = \int \mathrm{d}\eta \int \mathrm{d}^3\boldsymbol{k}\;\left[u'_{\boldsymbol{k}}\,u'^*_{\boldsymbol{k}} - \omega_k^2(\eta)\,u_{\boldsymbol{k}}\,u^*_{\boldsymbol{k}}\right], \tag{5.6}$$

where

$$\omega_k^2(\eta) = k^2 - \frac{a''}{a}. \tag{5.7}$$

It should be noted that, upon varying the action with respect to $u_{\boldsymbol{k}}$, one obtains the following equation of motion governing $u_{\boldsymbol{k}}$:

$$u_{\boldsymbol{k}}'' + \omega_k^2(\eta)\, u_{\boldsymbol{k}} = 0. \tag{5.8}$$

The momenta associated with the variables $u_{\boldsymbol{k}}$ and $u_{\boldsymbol{k}}^*$ are given by

$$p_{\boldsymbol{k}} = u_{\boldsymbol{k}}'^*, \quad p_{\boldsymbol{k}}^* = u_{\boldsymbol{k}}'. \tag{5.9}$$

The Hamiltonian associated with the above second order action can be determined to be

$$\mathsf{H} = \int \mathrm{d}^3\boldsymbol{k}\ \left[p_{\boldsymbol{k}}\, p_{\boldsymbol{k}}^* + \omega_k^2(\eta)\, u_{\boldsymbol{k}}\, u_{\boldsymbol{k}}^*\right]. \tag{5.10}$$

To carry out the quantization procedure, we need to deal with real variables (see, for instance, Refs. [40, 12]). Hence, let us write the variables $u_{\boldsymbol{k}}$ and $p_{\boldsymbol{k}}$ as

$$u_{\boldsymbol{k}} = \frac{1}{\sqrt{2}}\left(u_{\boldsymbol{k}}^{\mathrm{R}} + i\, u_{\boldsymbol{k}}^{\mathrm{I}}\right), \quad p_{\boldsymbol{k}} = \frac{1}{\sqrt{2}}\left(p_{\boldsymbol{k}}^{\mathrm{R}} + i\, p_{\boldsymbol{k}}^{\mathrm{I}}\right), \tag{5.11}$$

where the superscripts R and I denote the real and imaginary parts of the corresponding quantities. In terms of these new variables, the Hamiltonian H is given by

$$\mathsf{H} = \int \mathrm{d}^3\boldsymbol{k}\ \mathsf{H}_{\boldsymbol{k}} = \int \mathrm{d}^3\boldsymbol{k}\ \left(\mathsf{H}_{\boldsymbol{k}}^{\mathrm{R}} + \mathsf{H}_{\boldsymbol{k}}^{\mathrm{I}}\right), \tag{5.12}$$

where

$$\mathsf{H}_{\boldsymbol{k}}^{\mathrm{R,I}} = \frac{1}{2}\,(p_{\boldsymbol{k}}^{\mathrm{R,I}})^2 + \frac{1}{2}\,\omega_k^2(\eta)\,(u_{\boldsymbol{k}}^{\mathrm{R,I}})^2. \tag{5.13}$$

It is evident from the structure of the Hamiltonian H that each variable $u_{\boldsymbol{k}}^{\mathrm{R,I}}$ evolves independently as a parametric oscillator with the time-dependent frequency $\omega_k(\eta)$. Therefore, the complete quantum state of the system, say, $\Psi(u_{\boldsymbol{k}}, \eta)$, can be written as a product of the wavefunctions of the individual modes, say, $\psi_{\boldsymbol{k}}(u_{\boldsymbol{k}}, \eta)$, in the following form:

$$\Psi(u_{\boldsymbol{k}}, \eta) = \prod_{\boldsymbol{k}} \psi_{\boldsymbol{k}}(u_{\boldsymbol{k}}, \eta) = \prod_{\boldsymbol{k}} \psi_{\boldsymbol{k}}^{\mathrm{R}}(u_{\boldsymbol{k}}^{\mathrm{R}}, \eta)\ \psi_{\boldsymbol{k}}^{\mathrm{I}}(u_{\boldsymbol{k}}^{\mathrm{I}}, \eta). \tag{5.14}$$

Quantization of the tensor perturbations can be achieved by promoting the variables $u_{\boldsymbol{k}}^{\mathrm{R,I}}$ and $p_{\boldsymbol{k}}^{\mathrm{R,I}}$ to quantum operators which satisfy the following non-trivial canonical commutation relations:

$$\left[\hat{u}_{\boldsymbol{k}}^{\mathrm{R}},\, \hat{p}_{\boldsymbol{k}'}^{\mathrm{R}}\right] = i\,\delta^{(3)}(\boldsymbol{k} - \boldsymbol{k}'), \quad \left[\hat{u}_{\boldsymbol{k}}^{\mathrm{I}}, \hat{p}_{\boldsymbol{k}'}^{\mathrm{I}}\right] = i\,\delta^{(3)}(\boldsymbol{k} - \boldsymbol{k}'). \tag{5.15}$$

The Schrödinger equation governing the evolution of the quantum state $\psi_{\boldsymbol{k}}^{\mathrm{R,I}}$ corresponding to the mode $\boldsymbol{k}$ is given by

$$i\,\frac{\partial\psi_{\boldsymbol{k}}^{\mathrm{R,I}}}{\partial\eta} = \hat{\mathsf{H}}_{\boldsymbol{k}}^{\mathrm{R,I}}\,\psi_{\boldsymbol{k}}^{\mathrm{R,I}}. \tag{5.16}$$

Upon using the following representation for $\hat{u}_{\boldsymbol{k}}^{\mathrm{R,I}}$ and $\hat{p}_{\boldsymbol{k}}^{\mathrm{R,I}}$:

$$\hat{u}_{\boldsymbol{k}}^{\mathrm{R,I}}\,\Psi = u_{\boldsymbol{k}}^{\mathrm{R,I}}\,\Psi, \quad \hat{p}_{\boldsymbol{k}}^{\mathrm{R,I}}\,\Psi = -i\frac{\partial\Psi}{\partial u_{\boldsymbol{k}}^{\mathrm{R,I}}}, \tag{5.17}$$

one can write the Hamiltonian operator in Fourier space $\hat{\mathsf{H}}_{\boldsymbol{k}}^{\mathrm{R,I}}$ as

$$\hat{\mathsf{H}}_{\boldsymbol{k}}^{\mathrm{R,I}} = -\frac{1}{2}\,\frac{\partial^2}{\partial(u_{\boldsymbol{k}}^{\mathrm{R,I}})^2} + \frac{1}{2}\,\omega_k^2(\eta)\,(\hat{u}_{\boldsymbol{k}}^{\mathrm{R,I}})^2. \tag{5.18}$$

It is well known that the wavefunction characterizing a time-dependent oscillator evolving from an initial ground state can be expressed as (see, for instance, Refs. [40])

$$\psi_{\boldsymbol{k}}^{\mathrm{R,I}}(u_{\boldsymbol{k}}^{\mathrm{R,I}},\eta) = N_k(\eta)\,\exp-\left[\Omega_k(\eta)\,(u_{\boldsymbol{k}}^{\mathrm{R,I}})^2\right], \tag{5.19}$$

where N_k is the normalization constant which can be determined (up to a phase) to be $N_k = \left(2\,\Omega_k^{\mathrm{R}}/\pi\right)^{1/4}$, with Ω_k^{R} denoting the real part of Ω_k. If we now write $\Omega_k = -(i/2)\,f_k'/f_k$ and substitute the above wave function in the Schrödinger equation (5.16), then one finds that the function f_k satisfies the same classical equation of motion [*i.e.* Eq. (5.8)] as the Mukhanov-Sasaki variable $u_{\boldsymbol{k}}$. In other words, if we know the solution to the classical Mukhanov-Sasaki equation, then we can arrive at the complete wavefunction $\psi_{\boldsymbol{k}}^{\mathrm{R,I}}$ [cf. Eq. (5.19)] describing the tensor modes. (Note that, since the equation governing f_k and $u_{\boldsymbol{k}}$ are the same, hereafter, we shall often refer to f_k as the tensor mode.)

5.3 Tensor modes and power spectrum in a matter bounce

We shall be interested in bouncing scenarios where the scale factor $a(\eta)$ is of the form

$$a(\eta) = a_0\,\left[1+(\eta/\eta_0)^2\right]^p = a_0\,\left[1+(k_0\,\eta)^2\right]^p, \tag{5.20}$$

where a_0 is the minimum value of the scale factor at the bounce (*i.e.* at $\eta = 0$), p is a positive real number, and $\eta_0 = {k_0}^{-1}$ is the time scale associated with the bounce. It is clear from the form of the scale factor that the universe starts in a contracting phase at large negative η with the scale factor reaching a minimum at $\eta = 0$, and expands thereafter.

Before we discuss the case of evolution of the tensor modes in a bouncing universe characterized by an arbitrary value of p, it is instructive to consider the simpler case of

$p = 1$. Such a bounce is often referred to as a matter bounce, since, at early times, far away from the bounce, the scale factor behaves in the same manner as in a matter dominated era, *i.e.* as $a(\eta) \propto \eta^2$. The evolution of the tensor modes and the resulting power spectrum in such a matter bounce has been discussed before (see for instance, Refs. [92, 93, 94]). For the sake of completeness, we shall briefly present the essential derivation here.

We need to evolve the modes from early times during the contracting phase, across the bounce until a suitable time after the bounce, when we have to evaluate the power spectrum. In order to arrive at an analytical expression for the tensor modes, it is convenient to divide this period of interest into two domains. Let the time range $-\infty < \eta < -\alpha\,\eta_0$ be the first domain, where the parameter α is a large number, say, 10^5. This period is far away from the bounce and corresponds to very early times, Since, in this domain, $\eta \ll -\eta_0$, the scale factor behaves as $a(\eta) \simeq a_0\,(k_0\,\eta)^2$. Therefore, the differential equation describing the tensor modes in the first domain reduces to

$$f_k'' + \left(k^2 - \frac{2}{\eta^2}\right) f_k \simeq 0. \tag{5.21}$$

This is exactly the equation of motion satisfied by the tensor modes in de Sitter inflation, whose solutions are well known [93].

If we assume that, at very early times during the contracting phase, the oscillator corresponding to each tensor mode is in its ground state, then, we require that $\Omega_k = k/2$ for $\eta \ll -\eta_0$. This, in turn, corresponds to demanding that, for $\eta \ll -\eta_0$, the tensor mode f_k behaves as

$$f_k(\eta) \simeq \frac{1}{\sqrt{2\,k}}\,\mathrm{e}^{i\,k\,\eta}, \tag{5.22}$$

which essentially corresponds to the Bunch-Davies initial condition, had we been working in the Heisenberg picture [95]. Let η_k be the time when $k^2 = a''/a$, *i.e.* when the modes leave the Hubble radius during the contracting phase. For cosmological modes such that $k/k_0 \ll 1$, $\eta_k \simeq -\sqrt{2}/k$. (If, say, $k_0/a_0 \simeq M_{_{\rm Pl}}$, one finds that k/k_0 is of the order of 10^{-28} or so for scales of cosmological interest.) The Bunch-Davies initial condition can be imposed when $\eta \ll \eta_k$. We shall assume that $\eta_k \ll -\alpha\,\eta_0$, which corresponds to $k \ll k_0/\alpha$. Since, as we mentioned, Eq. (5.21) resembles that of the equation in de Sitter inflation, the tensor mode f_k satisfying the Bunch-Davies initial condition can be immediately written down to be [92, 93, 94]

$$f_k^{(\mathrm{I})}(\eta) = \frac{1}{\sqrt{2\,k}}\,\left(1 + \frac{i}{k\,\eta}\right)\,\mathrm{e}^{i\,k\,\eta}. \tag{5.23}$$

The solution $f_k^{(\mathrm{I})}$ we have obtained above corresponds to the first domain, *i.e.* over $-\infty < \eta < -\alpha\,\eta_0$. Let us now turn to the evolution of the mode during the second domain, which covers the period of bounce. The domain corresponds $-\alpha\,\eta_0 < \eta < \beta\,\eta_0$, where we shall assume β to be of the order of 10^2. Over this domain, for scales of our interest (*i.e.* $k \ll k_0/\alpha$), we can ignore the k^2 term in Eq. (5.8) which governs f_k. In such a case, the equation simplifies to

$$f_k'' - \frac{a''}{a} f_k \simeq 0 \tag{5.24}$$

or, equivalently, in terms of the original variable h_k, to

$$h_k'' + 2\,\frac{a'}{a}\,h_k' \simeq 0. \tag{5.25}$$

Using the exact form (5.20) of the scale factor, this equation can be immediately integrated to obtain the following solution in the second domain [94]:

$$f_k^{(\mathrm{II})}(\eta) = a(\eta)\ \left[A_k + B_k\, g(k_0\,\eta)\right], \tag{5.26}$$

where A_k and B_k are constants, and the function $g(x)$ is given by

$$g(x) = \frac{x}{1+x^2} + \tan^{-1}(x). \tag{5.27}$$

The constants A_k and B_k are arrived at by matching the solutions $f_k^{(\mathrm{I})}$ and $f_k^{(\mathrm{II})}$ and their derivatives with respect to η at $-\alpha\,\eta_0$. We find that A_k and B_k are given by

$$A_k = \frac{1}{\sqrt{2\,k}}\left(\frac{1}{a_0\,\alpha^2}\right)\left(1 - \frac{i\,k_0}{\alpha\,k}\right)\mathrm{e}^{-i\,\alpha\,k/k_0} + B_k\,g(\alpha), \tag{5.28a}$$

$$B_k = \frac{1}{\sqrt{2\,k}}\,\frac{\left(1+\alpha^2\right)^2}{2\,a_0\,\alpha^2}\left(\frac{i\,k}{k_0} + \frac{3}{\alpha} - \frac{3\,i\,k_0}{\alpha^2\,k}\right)\mathrm{e}^{-i\,\alpha\,k/k_0}. \tag{5.28b}$$

Assuming that the universe transits to the conventional radiation dominated epoch at the end of the second domain, we evaluate the tensor power spectrum at $\eta = \beta\,\eta_0$ (where $\beta \simeq 10^2$) after the bounce [94]. Recall that the tensor power spectrum is defined in terms of the mode function $f_k(\eta)$ as [81]

$$\mathcal{P}_{\mathrm{T}}(k) = \frac{8}{M_{\mathrm{Pl}}^2}\,\frac{k^3}{2\,\pi^2}\,\frac{|f_k(\eta)|^2}{a^2(\eta)}. \tag{5.29}$$

On using the solution $f_k^{(\mathrm{II})}$ above, the tensor power spectrum at $\eta = \beta/k_0$ can be expressed as

$$\mathcal{P}_{\mathrm{T}}(k) = \frac{8}{M_{\mathrm{Pl}}^2}\,\frac{k^3}{2\,\pi^2}\,|A_k + B_k\,g(\beta)|^2. \tag{5.30}$$

We have plotted the resulting tensor power spectrum as a function of k/k_0 in Fig. 5.1 for a set of values of the parameters. Note that our analytical expressions and the resulting

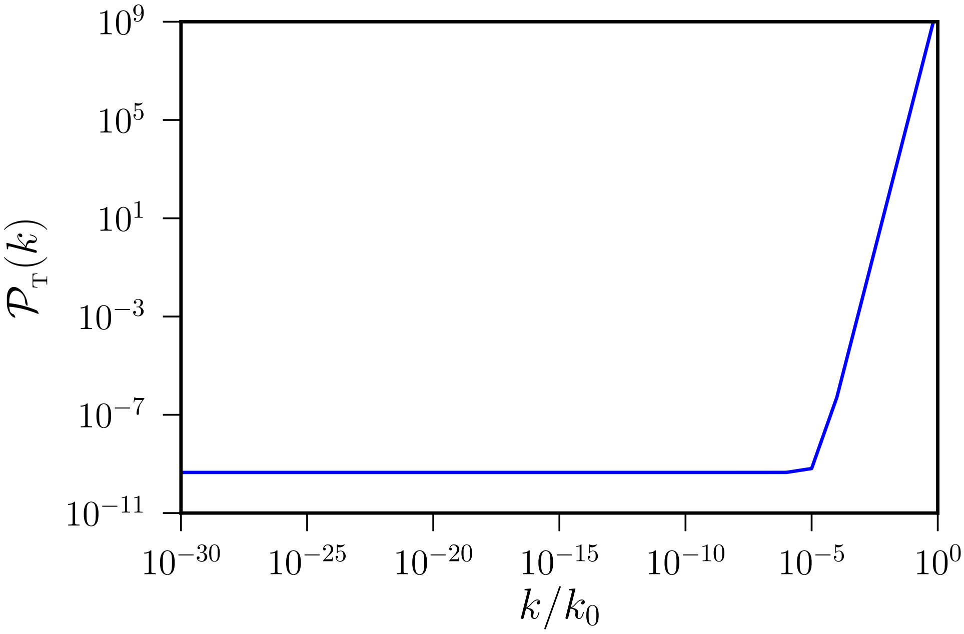

Figure 5.1: The tensor power spectrum in the matter bounce scenario [*i.e.* when $p = 1$ in Eq. (5.20)] has been plotted as a function of k/k_0. Actually, we find that the power spectrum depends only on the combination k_0/a_0. We have set $k_0/(a_0\, M_{_{\rm Pl}}) = 10^{-5}$, $\alpha = 10^5$ and $\beta = 10^2$ in plotting this figure. As expected, the power spectrum is scale invariant for modes such that $k/(k_0/\alpha) \ll 1$, the range over which our analytical approximations are valid.

power spectrum are valid only for modes such that $k \ll (k_0/\alpha)$. It is clear that the power spectrum is scale invariant over this range of wavenumbers. Such a scale invariant spectrum is indeed expected to arise in a matter bounce as the scenario is 'dual' to de Sitter inflation (in this context, see Ref. [93]).

5.4 Squeezing of quantum states associated with tensor modes in the matter bounce

Having discussed the evolution of the tensor modes through a matter bounce, let us turn our attention to the behavior of the quantum state $\psi_{\boldsymbol{k}}$. We shall essentially follow the approach adopted in the context of perturbations generated during inflation [40, 41, 86, 91].

In classical mechanics, a rather pictorial approach for analyzing the evolution of a system is to examine its behavior in phase space. However, since canonically conjugate variables cannot be measured simultaneously in quantum mechanics, a method needs to be devised in order to compare the evolution of a quantum system with its classical behavior in phase space. As is well known, one of the ways to understand the evolution of a quantum state is to examine the behavior of the so-called Wigner function, which is a quasi-probability distribution in phase space that can be constructed from a given wave function. Recall that the wave function corresponding to a tensor mode can be expressed as

$$\psi_{\boldsymbol{k}}(u_{\boldsymbol{k}},\eta) = \psi_{\boldsymbol{k}}^{\mathrm{R}}(u_{\boldsymbol{k}}^{\mathrm{R}},\eta)\, \psi_{\boldsymbol{k}}^{\mathrm{I}}(u_{\boldsymbol{k}}^{\mathrm{I}},\eta) = N_k^2 \exp -\left(2\,\Omega_k\, u_{\boldsymbol{k}}\, u_{\boldsymbol{k}}^{*}\right), \tag{5.31}$$

where, as mentioned before, $N_k = (2\,\Omega_k^{\mathrm{R}}/\pi)^{1/4}$, $\Omega_k = -(i/2)\, f_k'/f_k$ and f_k satisfies the differential equation (5.8). The Wigner function associated with the quantum state (5.31) is defined as [40, 41, 91]

$$\begin{aligned} W(u_{\boldsymbol{k}}^{\mathrm{R}}, u_{\boldsymbol{k}}^{\mathrm{I}}, p_{\boldsymbol{k}}^{\mathrm{R}}, p_{\boldsymbol{k}}^{\mathrm{I}}, \eta) &= \frac{1}{(2\,\pi)^2}\int_{-\infty}^{\infty}\mathrm{d}x \int_{-\infty}^{\infty}\mathrm{d}y\; \psi_{\boldsymbol{k}}\left(u_{\boldsymbol{k}}^{\mathrm{R}}+\frac{x}{2}, u_{\boldsymbol{k}}^{\mathrm{I}}+\frac{y}{2},\eta\right)\\ &\quad\times \psi_{\boldsymbol{k}}^{*}\left(u_{\boldsymbol{k}}^{\mathrm{R}}-\frac{x}{2}, u_{\boldsymbol{k}}^{\mathrm{I}}-\frac{y}{2},\eta\right)\, \exp -i\,\left(p_{\boldsymbol{k}}^{\mathrm{R}}\,x + p_{\boldsymbol{k}}^{\mathrm{I}}\,y\right). \end{aligned} \tag{5.32}$$

The integrals over x and y can be easily evaluated to arrive at the following form for the Wigner function [41]

$$\begin{aligned} W(u_{\boldsymbol{k}}^{\mathrm{R}}, u_{\boldsymbol{k}}^{\mathrm{I}}, p_{\boldsymbol{k}}^{\mathrm{R}}, p_{\boldsymbol{k}}^{\mathrm{I}}, \eta) &= \frac{\left|\psi_{\boldsymbol{k}}(u_{\boldsymbol{k}},\eta)\right|^2}{2\,\pi\,\Omega_k^{\mathrm{R}}}\, \exp -\left[\frac{1}{2\,\Omega_k^{\mathrm{R}}}\,\left(p_{\boldsymbol{k}}^{\mathrm{R}} + 2\,\Omega_{\boldsymbol{k}}^{\mathrm{I}}\,u_{\boldsymbol{k}}^{\mathrm{R}}\right)^2\right]\\ &\quad\times \exp -\left[\frac{1}{2\,\Omega_k^{\mathrm{R}}}\,\left(p_{\boldsymbol{k}}^{\mathrm{I}} + 2\,\Omega_{\boldsymbol{k}}^{\mathrm{I}}u_{\boldsymbol{k}}^{\mathrm{I}}\right)^2\right]. \end{aligned} \tag{5.33}$$

Since we know the mode functions f_k, we can evaluate Ω_k^{R} and Ω_k^{I} and thereby determine the above Wigner function as a function of time. Note that, in inflation, to cover a wide range in time, one often works with e-folds, say, N, as the time variable. The e-folds are defined through the relation $a(N) = a_{\mathrm{i}}\exp\left(N - N_{\mathrm{i}}\right)$, where, evidently, $a = a_{\mathrm{i}}$ at

$N = N_{\rm i}$. However, the exponential function e^N is a monotonically growing function and hence does not seem appropriate to describe bounces. In the context of bounces, particularly the symmetric ones of our interest, it seems more suitable to introduce a new variable $\mathcal{N}$ known as e-$\mathcal{N}$-folds, which is defined through the relation $a(\mathcal{N}) = a_0 \exp(\mathcal{N}^2/2)$ [96]. In the matter bounce, the conformal time coordinate η is related to e-$\mathcal{N}$-folds as

$$\eta(\mathcal{N}) = \pm k_0^{-1} \left(e^{\mathcal{N}^2/2} - 1\right)^{1/2}, \tag{5.34}$$

with $\mathcal{N}$ being zero at the bounce, while it is negative before the bounce and positive after. Using the above relation $\eta(\mathcal{N})$, we have converted the Wigner function as a function of $\mathcal{N}$. In Fig. 5.2, we have illustrated the behavior of the function in terms of contour plots in the $(u_{\boldsymbol{k}}^{\rm R}, p_{\boldsymbol{k}}^{\rm R})$-plane as a tensor mode (corresponding to a scale of cosmological interest) evolves across the bounce.

In a time-dependent background, the modes associated with quantum fields are generally expected to get increasingly squeezed as time evolves [86]. Let us now try to understand the extent to which the tensor modes are squeezed in the matter bounce scenario. If we define f_k as [41]

$$f_k = \frac{1}{\sqrt{2\,k}}\,(\tilde{u}_k + \tilde{v}_k^*), \tag{5.35}$$

then the second order differential equation (5.8) governing f_k can be written as two coupled first order differential equations as follows:

$$\tilde{u}_k' = i\,k\,\tilde{u}_k + \frac{a'}{a}\,\tilde{v}_k^*, \quad \tilde{v}_k' = i\,k\,\tilde{v}_k + \frac{a'}{a}\,\tilde{u}_k^*. \tag{5.36}$$

The Wronskian, say, W, corresponding to the equation governing f_k is defined as $\mathsf{W} = f_k'\,f_k^* - f_k'^*\,f_k$. It can be readily shown using equation (5.8) that $\mathrm{d}\mathsf{W}/\mathrm{d}\eta = 0$ or, equivalently, W is a constant. If we assume that the modes f_k satisfy the Bunch-Davies initial condition (5.22), then one finds that $\mathsf{W} = i$.

In terms of $\tilde{u}_k$ and $\tilde{v}_k$, the Wronskian can be expressed as $\mathsf{W} = i\,(|\tilde{u}_k|^2 - |\tilde{v}_k|^2)$. Since $\mathsf{W} = i$, we can parametrize the variables $\tilde{u}_k$ and $\tilde{v}_k$ as [12, 41]

$$\tilde{u}_k = \mathrm{e}^{i\,\theta_k}\cosh(r_k), \quad \tilde{v}_k = \mathrm{e}^{-i\,\theta_k + 2\,i\,\phi_{\boldsymbol{k}}}\sinh(r_k), \tag{5.37}$$

where r_k, θ_k and ϕ_k are known as the squeezing parameter, the rotation and squeezing angles, respectively. On substituting the expressions (5.37) in Eqs. (5.36), one can arrive at a set of coupled differential equations which determine the behavior of the parameters r_k, θ_k and ϕ_k with respect to η [41]. The coupled differential equations governing these

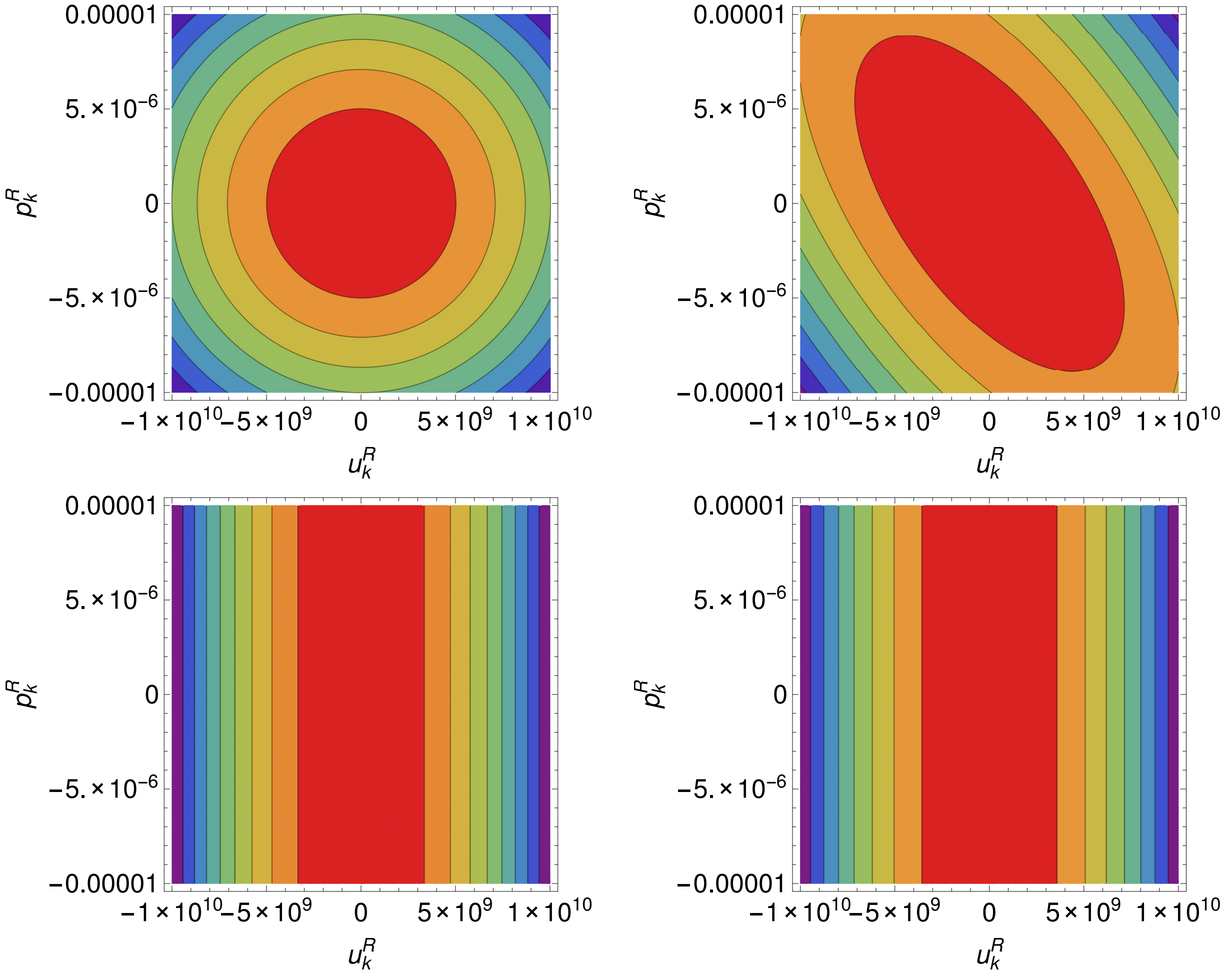

Figure 5.2: The evolution of the Wigner function $W(u_{\boldsymbol{k}}^{\mathrm{R}}, u_{\boldsymbol{k}}^{\mathrm{I}}, p_{\boldsymbol{k}}^{\mathrm{R}}, p_{\boldsymbol{k}}^{\mathrm{I}}, \eta)$ associated with the quantum state that describes a tensor mode of cosmological interest. Out of the two independent sets of variables $(u_{\boldsymbol{k}}^{\mathrm{R}}, p_{\boldsymbol{k}}^{\mathrm{R}})$ and $(u_{\boldsymbol{k}}^{\mathrm{I}}, p_{\boldsymbol{k}}^{\mathrm{I}})$, we have chosen the set $(u_{\boldsymbol{k}}^{\mathrm{R}}, p_{\boldsymbol{k}}^{\mathrm{R}})$ and have fixed $(u_{\boldsymbol{k}}^{\mathrm{I}}, p_{\boldsymbol{k}}^{\mathrm{I}}) = (0, 0)$ to illustrate the behavior of the quantity $\ln\left[W(u_{\boldsymbol{k}}^{\mathrm{R}}, u_{\boldsymbol{k}}^{\mathrm{I}}, p_{\boldsymbol{k}}^{\mathrm{R}}, p_{\boldsymbol{k}}^{\mathrm{I}}, \eta)\right]$. In plotting these figures, we have set $k_0/(a_0\, M_{_{\mathrm{Pl}}}) = 10^{-5}$ as in the previous figure, and have chosen the mode corresponding to $k/k_0 = 10^{-15}$. The plots correspond to the times $\mathcal{N} = -13$ (top left), $\mathcal{N} = -12.1$ (top right), $\mathcal{N} = 0$ (bottom left) and $\mathcal{N} = 5$ (bottom right). The first two instances (*viz.* when $\mathcal{N} = -13$ and $\mathcal{N} = -12.1$) correspond to situations when the mode is in the strongly sub-Hubble domain and close to Hubble exit during the contracting phase, respectively. Note that, as time evolves, the Gaussian state that is initially symmetric in $u_{\boldsymbol{k}}^{\mathrm{R}}$ and $p_{\boldsymbol{k}}^{\mathrm{R}}$ (top left) gets increasingly squeezed about about $u_{\boldsymbol{k}} = 0$ (top right, bottom left) as one approaches the bounce, and remains so (bottom right) as the universe begins to expand. This largely reflects the behavior that occurs in the inflationary scenario.

parameters are given by

$$r_k' = \frac{a'}{a}\cos(2\phi_k), \tag{5.38a}$$

$$\phi_k' = k - \frac{a'}{a}\coth(2r_k)\sin(2\,\phi_k), \tag{5.38b}$$

$$\theta_k' = k - \frac{a'}{a}\tanh(r_k)\sin(2\,\phi_k). \tag{5.38c}$$

Our primary quantity of interest is the parameter r_k which characterizes the extent of squeezing of the quantum state $\psi_{\boldsymbol{k}}(u_{\boldsymbol{k}}, \eta)$ as the universe evolves [86].

By assuming the scale factor of interest, one can attempt to solve the differential equations (5.38) to arrive at the behavior of the squeezing parameter. These equations essentially stem from the original equation (5.8) that determines the evolution of the Mukhanov-Sasaki variable u_k or f_k. Since, we already know the solution to f_k across the bounce, it would be simpler to express the parameters r_k, θ_k and ϕ_k in terms of f_k. To begin with, we find that the variables $\tilde{u}_k$ and $\tilde{v}_k$ can be expressed in terms of f_k and its derivative f_k' as follows:

$$\tilde{u}_k = \sqrt{\frac{k}{2}}\left(1 + \frac{i}{k}\,\frac{a'}{a}\right) f_k - \frac{i}{\sqrt{2\,k}}\, f_k', \quad \tilde{v}_k = \sqrt{\frac{k}{2}}\left(1 + \frac{i}{k}\,\frac{a'}{a}\right) f_k^* - \frac{i}{\sqrt{2\,k}}\, f_k'^* \tag{5.39}$$

and it is straightforward to examine that $|\tilde{u}_k|^2 - |\tilde{v}_k|^2 = 1$, as required. Once we have these two quantities at hand, we can obtain the squeezing parameters r_k, ϕ_k and θ_k from the relations

$$r_k = \sinh^{-1}(|\tilde{v}_k|)\,, \quad \phi_k = \frac{1}{2}\,\mathrm{Arg}\,(\tilde{u}_k\tilde{v}_k), \quad \theta_k = \mathrm{Arg}\,(\tilde{u}_k). \tag{5.40}$$

Using the solutions for f_k we have obtained in the case of the matter bounce in the previous section, we have plotted the behavior of the squeezing parameter r_k as a function of e-$\mathcal{N}$-folds in Fig. 5.3. We have also independently solved the differential equations (5.38) using *Mathematica* [97] to check the validity of the analytical solution for r_k. The numerical solution has also been plotted in the figure. The agreement between the solutions clearly indicate the extent of accuracy of the analytical solutions. It is evident from the figure that the wave function associated with the quantum state $\psi_{\boldsymbol{k}}$ is increasingly squeezed as the universe evolves, reaching a maximum at the bounce. In fact, it is this behavior which was reflected in the behavior of the Wigner function (which had peaked about $u_{\boldsymbol{k}} = 0$) we had considered earlier. While there are similarities in the behavior with what occurs in inflation, there are some crucial differences as well. In inflation, the parameter r_k increases indefinitely with the duration of inflation [41]. For a duration corresponding to

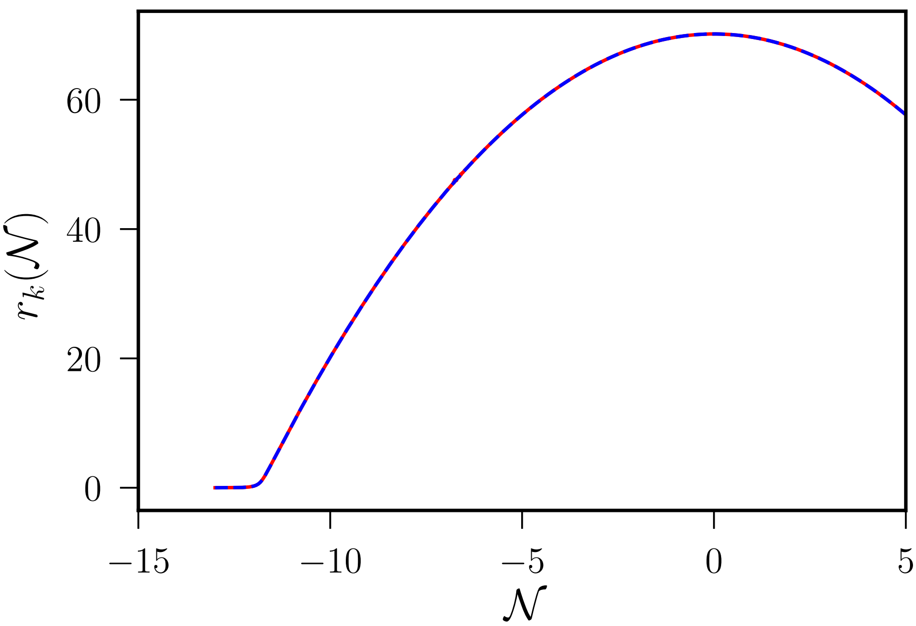

Figure 5.3: The analytical (in red) and the numerical (in blue) solutions for the squeezing parameter r_k have been plotted as a function of e-$\mathcal{N}$-folds, for a mode corresponding to $k/k_0 = 10^{-15}$ and values of the parameters of the model mentioned in the earlier figures. Since we begin with the Bunch-Davies initial condition at very early times, the squeezing parameter r_k is close to zero. As the universe contracts, r_k increases till it reaches a maximum at the bounce. Then it decreases to some extent after the bounce, before the universe is assumed to enter the radiation dominated era.

about 60 e-folds of inflation, as is typically required to overcome the horizon problem, r_k is found to grow to about 10^2 or so. We find that r_k grows to the same order of magnitude in the matter bounce as well. In accordance with the Heisenberg's uncertainty principle, squeezing of the quantum state about $u_{\boldsymbol{k}} = 0$ gives infinite possibilities of the momentum variable $p_{\boldsymbol{k}}$. Hence, a squeezed state is not strictly a classical state. But, it has been argued that in a strongly squeezed quantum state, the vacuum expectation values and the stochastic mean are indistinguishable, if the perturbations are assumed to be realizations of a classical stochastic process [40]. In such a sense, one can argue that in the extreme squeezed limit the quantum state 'turns' classical. However, in contrast to inflation where the growth seems indefinite, in the matter bounce, the parameter r_k begins to decrease as the universe starts to expand. This interesting behavior may point to crucial differences between the quantum-to-classical transition in inflation and bounces and seem to require further study.

5.5 CSL modified tensor modes and power spectrum in the matter bounce

As we had described in the introduction, one can also view the transition of primordial quantum perturbations into the classical LSS as a quantum measurement problem. In other words, we need to understand as to how the mechanism by which the original state of the primordial perturbations collapsed into a particular eigenstate which corresponds to the realization of the CMB observed today. One of the proposals which addresses this issue is known as the CSL model [89]. The crucial advantage of this model is that a specific realization can be attained without the presence of an observer. In the rest of the chapter we will focus on understanding the effects of CSL on the tensor perturbations in bouncing universes.

5.5.1 CSL in brief

The CSL model proposes a unified dynamical description which suppresses the quantum effects, such as the superposition of states in the macroscopic regime, and reproduces the predictions of quantum mechanics in the microscopic regime. In CSL, a unified dynamical description is achieved by appropriately modifying the Schrödinger equation. This modification is carried out by adding nonlinear terms and a stochastic behavior which is encoded through a Wiener process [89]. The modified Schrödinger equation encompasses an amplification mechanism which makes the new terms negligible in the quantum regime, hence retrieving the dynamics predicted by quantum mechanics. At the same time, it should make the new terms dominant in the classical regime, so that the classical-like behavior of the system is attained in the classical domain (for reviews, see Refs. [90]). Although, it should be clarified that, in the implementation of CSL for the case of primordial perturbations [41], the above mentioned amplification mechanism does not arise. Upon taking into account such modifications, the modified Schrödinger equation is given by

$$\mathrm{d}\psi_{\boldsymbol{k}}^{\mathrm{R,I}} = \left[-i\,\hat{\mathsf{H}}_{\boldsymbol{k}}^{\mathrm{R,I}}\,\mathrm{d}\eta + \sqrt{\gamma}\,\left(\hat{u}_{\boldsymbol{k}}^{\mathrm{R,I}} - \bar{u}_{\boldsymbol{k}}^{\mathrm{R,I}}\right)\,\mathrm{d}\mathcal{W}_\eta - \frac{\gamma}{2}\,\left(\hat{u}_{\boldsymbol{k}}^{\mathrm{R,I}} - \bar{u}_{\boldsymbol{k}}^{\mathrm{R,I}}\right)^2\,\mathrm{d}\eta\right]\,\psi_{\boldsymbol{k}}^{\mathrm{R,I}}, \tag{5.41}$$

where $\hat{\mathsf{H}}_{\boldsymbol{k}}$ is the original Hamiltonian operator (5.18), γ is the CSL parameter, which is a measure of the strength of the collapse and $\mathcal{W}_\eta$ denotes a real Wiener process, which is responsible for the stochastic behavior. If the CSL modified wavefunction $\psi_{\boldsymbol{k}}^{\mathrm{R,I}}$ is assumed to be of the following form [41, 91, 98]

$$\psi_{\boldsymbol{k}}^{\mathrm{R,I}}(u_{\boldsymbol{k}}^{\mathrm{R},I},\eta) = N_k(\eta)\ \exp - \left[\Omega_k(\eta)\ \left(u_{\boldsymbol{k}}^{\mathrm{R,I}} - \bar{u}_{\boldsymbol{k}}^{\mathrm{R,I}}\right)^2 + i\,\chi_{\boldsymbol{k}}^{\mathrm{R,I}}(\eta)\,u_{\boldsymbol{k}}^{\mathrm{R,I}} + i\,\sigma_{\boldsymbol{k}}^{\mathrm{R,I}}(\eta)\right], \tag{5.42}$$

then the functions $\Omega_k(\eta)$, $\chi_{\boldsymbol{k}}(\eta)$ and $\sigma_{\boldsymbol{k}}(\eta)$ have to satisfy the following set of differential equations

$$\Omega_k' = -2\,i\,\Omega_k^2 + \frac{i}{2}\,\omega_k^2 + \frac{\gamma}{2}, \tag{5.43a}$$

$$\frac{N_k'}{N_k} = \Omega_k^{\mathrm{I}}, \tag{5.43b}$$

$$\left(\bar{u}_{\boldsymbol{k}}^{\mathrm{R,I}}\right)' = \chi_{\boldsymbol{k}}^{\mathrm{R,I}} + \frac{\sqrt{\gamma}}{2\,\Omega_k^{\mathrm{R}}}\,\mathcal{W}_\eta{}', \tag{5.43c}$$

$$\left(\chi_{\boldsymbol{k}}^{\mathrm{R,I}}\right)' = -\omega_k^2\,\bar{u}_{\boldsymbol{k}}^{\mathrm{R,I}} - \sqrt{\gamma}\,\frac{\Omega_k^{\mathrm{I}}}{\Omega_k^{\mathrm{R}}}\,\mathcal{W}_\eta{}', \tag{5.43d}$$

$$\left(\sigma_{\boldsymbol{k}}^{\mathrm{R,I}}\right)' = \frac{\omega_k^2}{2}\,\left(\bar{u}_{\boldsymbol{k}}^{\mathrm{R,I}}\right)^2 - \frac{1}{2}\,\left(\chi_{\boldsymbol{k}}^{\mathrm{R,I}}\right)^2 - \Omega_k^{\mathrm{R}} + \sqrt{\gamma}\,\frac{\Omega_k^{\mathrm{I}}}{\Omega_k^{\mathrm{R}}}\,\bar{u}_{\boldsymbol{k}}^{\mathrm{R,I}}\,\mathcal{W}_\eta{}', \tag{5.43e}$$

where ω_k^2 is given by Eq. (5.7).

In principle, one needs to solve the above set of stochastic differential equations in order to arrive at a complete understanding of the effects of CSL. However, recall that, our primary concern is the imprints of CSL on the tensor power spectrum. Note that, earlier, we had defined $\Omega_k = -(i/2)\,f_k'/f_k$ and the original Schrödinger equation had led to f_k satisfying the Mukhanov-Sasaki equation (5.8). If we now substitute the same expression for Ω_k in the CSL corresponding modified equation (5.43a), we find that f_k now satisfies the differential equation [41]

$$f_k'' + \left(k^2 - i\,\gamma - \frac{a''}{a}\right) f_k = 0, \tag{5.44}$$

i.e. the effects of CSL is essentially to replace k^2 by $k^2 - i\,\gamma$. In the following sub-section, we shall solve this equation in a matter bounce and evaluate the effects of CSL on the tensor power spectrum.

5.5.2 CSL modified tensor power spectrum

In this sub-section we shall focus on the evaluation of CSL modified tensor power spectrum in the matter bounce scenario.

We find that, under certain conditions, even the CSL modified modes can be arrived at using the approximations we had worked with earlier. If we divide the period of our interest into two domains, we find that the CSL modified modes in the first domain (*i.e.* over

$-\infty < \eta < -\alpha\,\eta_0$), which satisfy the Bunch-Davies initial conditions, can be expressed as (for a discussion on the initial conditions for the case of CSL modified tensor modes, see Ref. [41])

$$f_k^{(\mathrm{I})}(\eta) = \frac{1}{\sqrt{2\,z_k\,k}}\left(1+\frac{i}{z_k\,k\,\eta}\right)\,\mathrm{e}^{i\,z_k\,k\,\eta}, \tag{5.45}$$

where $z_k = (1 - i\,\gamma/k^2)^{1/2}$.

In the second domain, *i.e.* in the time range $-\alpha\,\eta_0 < \eta < \beta\,\eta_0$, the term a''/a in Eq. (5.44) behaves as $a''/a \geq 2\,k_0^2/(1+\alpha^2)$. Recall that the modes of cosmological interest are assumed to be very small compared to k_0/α. Hence, if the CSL parameter γ is also assumed to be very small when compared to k_0^2, then Eq. (5.44) can be approximated to be

$$f_k'' - \frac{a''}{a}\,f_k \simeq 0, \tag{5.46}$$

exactly as in the unmodified case. Upon integrating this equation, we obtain that

$$f_k^{(\mathrm{II})}(\eta) = a(\eta)\,\left[A_k^{(\gamma)} + B_k^{(\gamma)}\,g(k_0\eta)\right], \tag{5.47}$$

where $g(x)$ is the same function (5.27) we had encountered earlier, while $A_k^{(\gamma)}$ and $B_k^{(\gamma)}$ are given by

$$A_k^{(\gamma)} = \frac{1}{\sqrt{2\,z_k\,k}}\,\frac{1}{a_0\,\alpha^2}\,\left(1-\frac{i\,k_0}{\alpha\,z_k\,k}\right)\,\mathrm{e}^{-i\,\alpha\,z_k\,k/k_0} + B_k^{(\gamma)}\,g(\alpha), \tag{5.48a}$$

$$B_k^{(\gamma)} = \frac{1}{\sqrt{2\,z_k\,k}}\,\frac{(1+\alpha^2)^2}{2\,a_0\,\alpha^2}\,\left(\frac{i\,z_k\,k}{k_0}+\frac{3}{\alpha}-\frac{3\,i\,k_0}{\alpha^2\,z_k\,k}\right)\,\mathrm{e}^{-i\,\alpha\,z_k\,k/k_0}. \tag{5.48b}$$

Note that we have arrived at these expressions for $A_k^{(\gamma)}$ and $B_k^{(\gamma)}$ by matching the solution $f_k^{(\mathrm{II})}$ [cf. Eq. (5.45)] and its derivative with the corresponding quantities in the first domain (*i.e.* $f_k^{(\mathrm{I})}$ and its derivative) at $\eta = -\alpha\,\eta_0$. We evaluate the tensor power spectrum after the bounce at $\eta = \beta\,\eta_0$ (with $\beta = 10^2$), as we had done earlier. It can be expressed as

$$\mathcal{P}_{\mathrm{T}}^{(\gamma)}(k) = \frac{8}{M_{\mathrm{Pl}}^2}\frac{k^3}{2\,\pi^2}\,|A_k^{(\gamma)} + B_k^{(\gamma)}\,g(\beta)|^2. \tag{5.49}$$

In Fig. 5.4 we have plotted logarithm of the ratio of the CSL modified power spectrum to the unmodified power spectrum, *i.e.*$\log\,[\mathcal{P}_{\mathrm{T}}^{(\gamma)}(k)/\mathcal{P}_{\mathrm{T}}(k)]$, as a function of k/k_0, for the same set of parameters we have worked with earlier and for a few different choices of γ/k_0^2. It is evident from the figure that, just as in the case of inflation [41], the effect of CSL on the power spectrum in the matter bounce is to suppress its power at large scales. We find that the power spectrum behaves as k^3 in its suppressed part, exactly

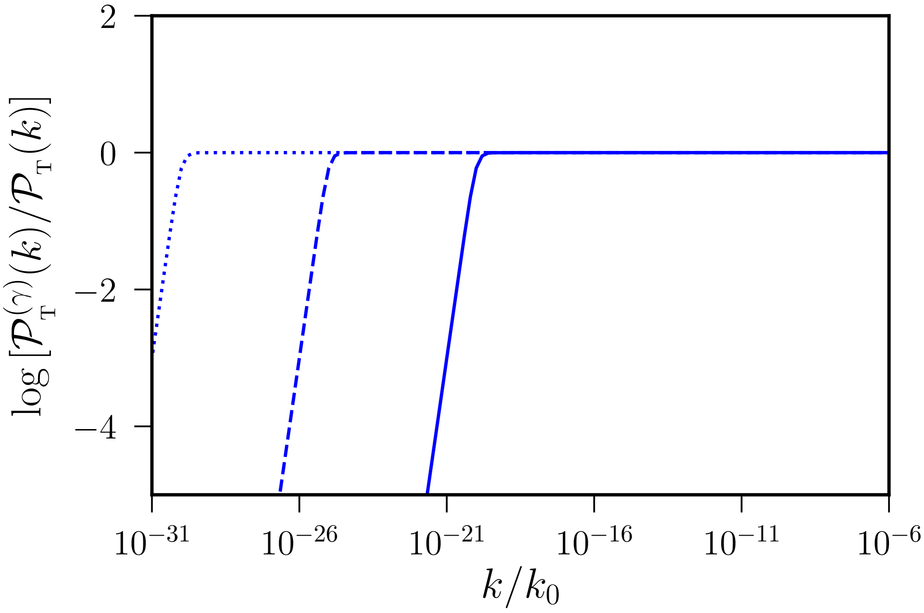

Figure 5.4: The logarithm of the ratio of the CSL modified tensor power spectrum to the standard power spectrum has been plotted as a function of k/k_0 for the matter bounce ($p = 1$) scenario. We have set $k_0/(a_0\, M_{\mathrm{Pl}}) = 10^{-5}$, $\alpha = 10^5$ and $\beta = 10^2$, as we had done in Fig. 5.1. The solid, dashed and dotted lines correspond to γ/k_0^2 of 10^{-40}, 10^{-50} and 10^{-60}, respectively. Note that the introduction of a CSL parameter γ leads to a suppression of power in the power spectrum at large scales. In the suppressed part, the power spectrum behaves as k^3, which is similar to what occurs in the case of inflation [41].

as observed in inflation [41]. We also note that, larger the value of the dimensionless parameter γ/k_0^2, smaller is the scale at which the power gets suppressed. Since, the scales of cosmological interest lie in the range $k/k_0 \simeq 10^{-30}$–10^{-25}, if we demand a nearly scale invariant power spectrum for the tensor modes, the value of the dimensionless parameter γ/k_0^2 is constrained to be $\gamma/k_0^2 \lesssim 10^{-60}$.

5.6 Tensor power spectrum in a generic bouncing model

Until now, our discussions have focused on the particular case of the bounce referred to as the matter bounce scenario described by the scale factor (5.20), with p set to unity. In this section, we shall turn our attention to a more generic case where p is any positive real number. In order to arrive at the tensor power spectrum in these models, our approach would be the same as in Sec. 5.3, *viz.* to solve Eq. (5.8) to obtain f_k and then evaluate the power spectrum using the definition (5.29).

5.6.1 Tensor modes and power spectrum

Following the discussion in Sec. 5.3, we obtain the tensor modes f_k by dividing the time of interest into two domains and working under suitable approximations [99]. In the first domain, *i.e.* over $-\infty < \eta < -\alpha\,\eta_0$, where $\alpha \gg 1$, the scale factor simplifies to the power law form $a(\eta) \simeq a_0\,(k_0\,\eta)^{2\,p}$. In such a case, the differential equation (5.8) reduces to

$$f_k'' + \left[k^2 - \frac{2\,p\,(2\,p-1)}{\eta^2}\right]\,f_k = 0, \tag{5.50}$$

and it is well known that the corresponding solutions can be written in terms of Bessel functions. Upon imposing the Bunch-Davies initial conditions at very early times, we obtain the modes to be

$$f_k^{(\mathrm{I})}(\eta) = \frac{i}{2}\,\sqrt{\frac{\pi}{k}}\,\frac{\mathrm{e}^{-i\,p\,\pi}}{\sin\,(n\,\pi)}\,(-k\,\eta)^{1/2}\,\left[J_{-n}(-k\,\eta) - \mathrm{e}^{i\,n\,\pi}\,J_n(-k\,\eta)\right], \tag{5.51}$$

where $n = 2\,p - 1/2$, while $J_n(z)$ is the Bessel function of first kind [77].

In the second domain, *i.e.* over $-\alpha\,\eta_0 < \eta < \beta\,\eta_0$, we can ignore the k^2 term in Eq. (5.8) for reasons discussed earlier. For any arbitrary value of the parameter p, upon integrating the resulting equation, we find that we can express the modes f_k in the domain as follows:

$$f_k^{(\mathrm{II})}(\eta) = a(\eta)\,\left[C_k + D_k\,\tilde{g}(k_0\,\eta)\right], \tag{5.52}$$

where the function $\tilde{g}(x)$ is given in terms of the hypergeometric function ${}_2F_1[a,b;c;z]$ as

$$\tilde{g}(x) = x\, {}_2F_1\left[2\,p, \tfrac{1}{2}; \tfrac{3}{2}; -x^2\right]. \tag{5.53}$$

The constants C_k and D_k are obtained by matching the solutions in the two domains and their derivatives at $\eta = -\alpha\,\eta_0$. They can be determined to be

$$\begin{aligned} C_k &= \frac{i}{2\,a_0\,\alpha^n}\sqrt{\frac{\pi}{k_0}}\,\frac{\mathrm{e}^{-i\,p\,\pi}}{\sin{(n\,\pi)}} \\ &\quad\times\left[J_{-n}(\alpha\,k/k_0) - \mathrm{e}^{i\,n\,\pi}\,J_n(\alpha\,k/k_0)\right] + D_k\,\tilde{g}(\alpha), \end{aligned} \tag{5.54a}$$

$$\begin{aligned} D_k &= -\frac{i}{2\,a_0\,\alpha^n}\left(\frac{k}{k_0}\right)\sqrt{\frac{\pi}{k_0}}\,\frac{\mathrm{e}^{-i\,p\,\pi}}{\sin{(n\,\pi)}}\left(1+\alpha^2\right)^{2\,p} \\ &\quad\times\left[J_{-(n+1)}(\alpha\,k/k_0) + \mathrm{e}^{i\,n\,\pi}\,J_{n+1}(\alpha\,k/k_0)\right]. \end{aligned} \tag{5.54b}$$

Upon using these expressions in the definition (5.29) of the tensor power spectrum and evaluating the spectrum after the bounce at $\eta = \beta/k_0$, we obtain that

$$\mathcal{P}_{\mathrm{T}}(k) = \frac{8}{M_{\mathrm{Pl}}^2}\,\frac{k^3}{2\pi^2}\,|C_k + D_k\,\tilde{g}(\beta)|^2. \tag{5.55}$$

In Fig. 5.5 we have plotted the tensor power spectrum for a set of values p as a function of k/k_0 for the same choice of parameters as in Fig. 5.1. As expected, deviations from $p = 1$ introduces a tilt to the tensor power spectrum. It is useful to note that the power spectrum is red for $p > 1$, as one would expect in inflation.

5.6.2 Imprints of CSL

We can now readily compute the effect of CSL mechanism on the tensor power spectrum in a more generic bouncing scenario. In order to calculate the tensor power spectrum, we need to solve the differential equation (5.44) governing f_k in the presence of CSL mechanism, which effectively replaces k^2 in the governing equation by $k^2 - i\,\gamma$. All our previous arguments go through for a general p and hence we shall quickly present the essential results.

We find that the CSL modified tensor mode in the first domain is given by

$$f_k^{(\mathrm{I})}(\eta) = \frac{i}{2}\sqrt{\frac{\pi}{z_k\,k}}\,\frac{\mathrm{e}^{-i\,p\,\pi}}{\sin(n\,\pi)}\,\frac{1}{\sqrt{-z_k\,k\,\eta}}\,\left[J_{-n}(-z_k\,k\,\eta) - \mathrm{e}^{i\,n\,\pi}\,J_n(-z_k\,k\,\eta)\right], \tag{5.56}$$

where n and z_k are given by the same expressions as before. Similarly, in the second domain, the CSL modified tensor mode can be found to be

$$f_k^{(\mathrm{II})}(\eta) = a(\eta)\,\left[C_k^{(\gamma)} + D_k^{(\gamma)}\,\tilde{g}(k_0\eta)\right], \tag{5.57}$$

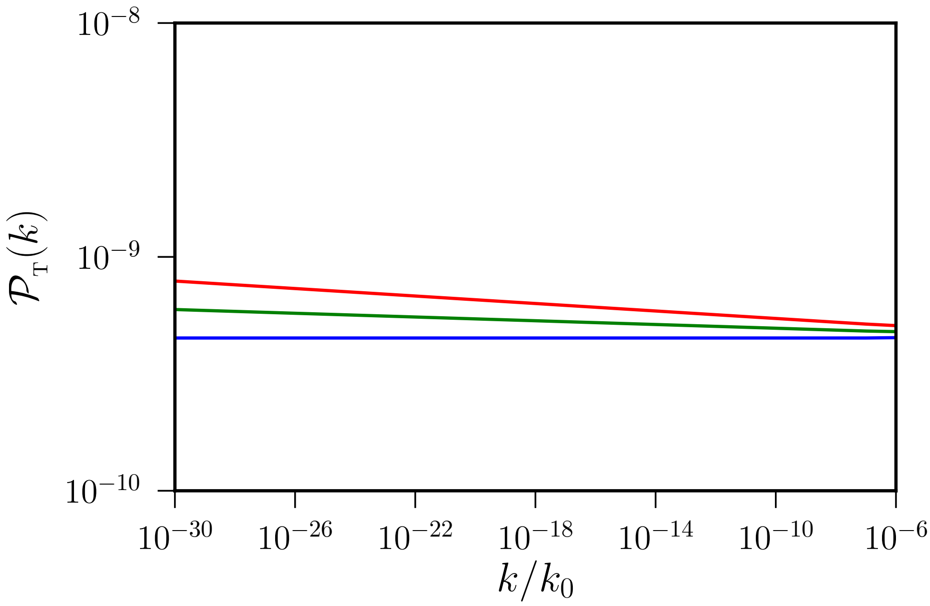

Figure 5.5: The tensor power spectra in bouncing models corresponding to $p = 1$ (in blue), $p = 1.001$ (in green) and $p = 1.002$ (in red) have been plotted as a function of k/k_0. We have set $k_0/(a_0\, M_{_{\rm Pl}}) = 10^{-5}$, $\alpha = 10^5$ and $\beta = 10^2$ as before. Note that the spectrum exhibits a red tilt for $p > 1$.

where, as earlier, $\tilde{g}(x)$ is given by Eq. (5.53), while the quantities $C_k^{(\gamma)}$ and $D_k^{(\gamma)}$ are given by

$$\begin{aligned} C_k^{(\gamma)} &= \frac{i}{2\, a_0\, \alpha^n}\, \sqrt{\frac{\pi}{k_0}}\, \frac{{\rm e}^{-i\, p\, \pi}}{\sin{(n\, \pi)}} \\ &\quad \times \left[J_{-n}(\alpha\, z_k\, k/k_0) - {\rm e}^{i\, n\, \pi} J_n(\alpha\, z_k\, k/k_0)\right] + D_k^{(\gamma)}\, \tilde{g}(\alpha), \qquad (5.58a) \\ D_k^{(\gamma)} &= -\frac{i}{2\, a_0\, \alpha^n}\, \left(\frac{z_k\, k}{k_0}\right)\, \sqrt{\frac{\pi}{k_0}}\, \frac{{\rm e}^{-i\, p\, \pi}}{\sin{(n\, \pi)}}\, \left(1+\alpha^2\right)^{2\, p} \\ &\quad \times \left[J_{-(n+1)}(\alpha\, z_k\, k/k_0) + {\rm e}^{i\, n\, \pi}\, J_{n+1}(\alpha\, z_k\, k/k_0)\right]. \qquad (5.58b) \end{aligned}$$

The resulting spectrum evaluated after the bounce at $\eta = \beta/k_0$ is given by

$$\mathcal{P}_{_{\rm T}}^{(\gamma)}(k) = \frac{8}{M_{_{\rm Pl}}^2}\, \frac{k^3}{2\, \pi^2}\, \vert C_k^{(\gamma)} + D_k^{(\gamma)}\, \tilde{g}(\beta)\vert^2. \qquad (5.59)$$

As in the case of the matter bounce, in Fig. 5.6, we have plotted the logarithm of the ratio of the CSL modified tensor power spectrum to the unmodified power spectrum, *i.e.*the quantity $\log{[\mathcal{P}_{_{\rm T}}^{(\gamma)}(k)/\mathcal{P}_{_{\rm T}}(k)]}$, for a two different values of p and different values of γ/k_0^2. It is clear from the figure that the behavior of the power spectrum and the corresponding conclusions are the same as we had arrived at in the case of the matter bounce.

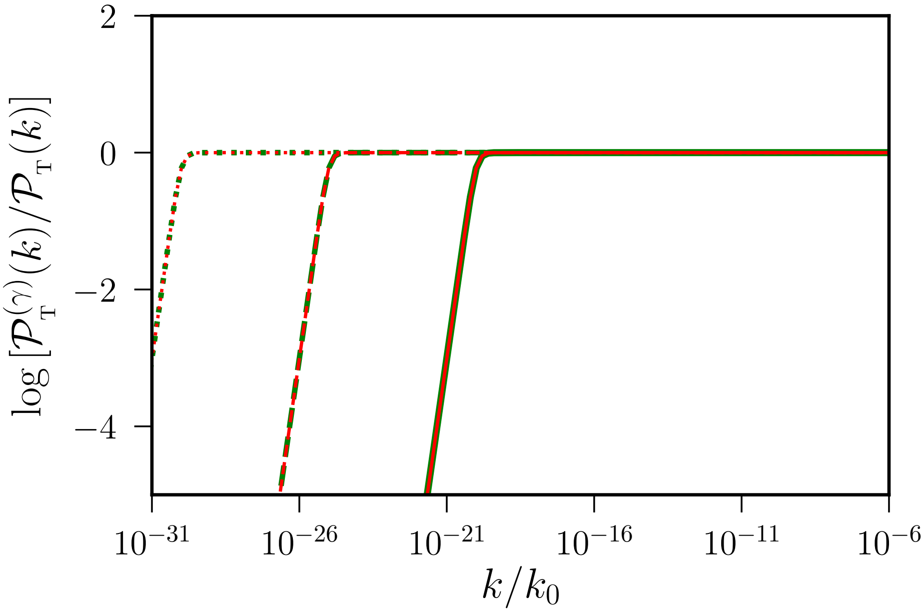

Figure 5.6: The behavior of $\log\,[\mathcal{P}_{_{\rm T}}^{(\gamma)}(k)/\mathcal{P}_{_{\rm T}}(k)]$ has been plotted as a function of k/k_0 for a bounce with scale factor described by the indices $p = 1.001$ (in green) and for $p = 1.002$ (in red). We have worked with the same values of $k_0/(a_0\, M_{_{\rm Pl}})$, α and β as in the earlier figures. The solid, dashed and dotted curves correspond to γ/k_0^2 of 10^{-40}, 10^{-50} and 10^{-60}, respectively. This figure clearly shows that the CSL mechanism leads to a suppression of power at large scales regardless of the value of p.

5.7 Discussion

Generation of perturbations from quantum fluctuations in the early universe and their evolution leading to anisotropies in the CMB and inhomogeneities in the LSS provides a wonderful avenue to understand physics at the interface of quantum mechanics and gravitation. One such fundamental issue that has to be addressed is the mechanism by which the quantum perturbations reduce to be described in terms of classical stochastic variables. In this work [100], we have investigated the quantum-to-classical transition of primordial quantum perturbations in the context of bouncing universes. Following the footsteps of earlier efforts in this direction [41], we have approached this issue from two perspectives.

In the first approach, we have investigated the extent of squeezing of the quantum state associated with a tensor mode as it evolves through a bounce. As in the context of inflation, the extent of squeezing grows as the modes leave the Hubble radius. However, in contrast to inflation where it can grow indefinitely (depending on the duration of inflation), we had found that the squeezing parameter reaches a maximum at the bounce and begins to decrease thereafter. We had found that this behavior is also reflected in the Wigner function.

Secondly, we had treated this issue as a quantum measurement problem set in the cosmological context, *i.e.* we had investigated the effects of the collapse of the original quantum state of the perturbations. An approach which have been proposed to achieve such a collapse is the CSL model. Using the model, we had examined if the tensor power spectra are modified due to the collapse in a class of bouncing universes. We had found that CSL mechanism leads to a suppression of the tensor power spectra at large scales, in a manner exactly similar to what occurs in the inflationary context.

It would be interesting to extend these analyses to the case of scalar perturbations in bouncing universes [85]. We are currently investigating such issues.

Chapter 6

Conclusions

In this chapter, after presenting a summary of the results arrived at in this thesis, we shall provide a brief outlook.

6.1 Summary

As we have repeatedly emphasized during the course of this thesis, since a complete quantum theory of quantum gravity still remains to be constructed, it is pragmatic to examine various phenomena in the domain of semi-classical gravity. Cosmology is the useful testbed in which the results of the investigations carried out in semi-classical gravity can be applied. Hence, in this thesis, we have studied various issues in semi-classical aspects of gravity and cosmology.

In Chap. 2, we had examined the semi-classical effects of the presence of a minimal length. As we had argued, one seems to require only a very few conceptual inputs from semi-classical gravity to gain an understanding about spacetime at small scales. The existence of a minimal length is one such input, since it is expected to be a fundamental feature of quantum gravity [18]. Bitensors can provide a geometric description of spacetime naturally to incorporate such a lower bound in spacetime intervals. Using a bitensor to describe the metric of spacetime (which we had referred to as the qmetric), while accounting for the existence of a minimal length, we had arrived at an expression for the Ricci biscalar [57]. The modified Ricci biscalar presents a natural basis for the description of gravitational dynamics by a nonlocal action. Such a term can be particularly relevant for the study of spacetime singularities, where one cannot use covariant Taylor expansions. We had found that the mathematical results we had obtained supports the so-called emergent gravity paradigm wherein the gravitational dynamics is described in terms of thermodynamics of horizons [58].

In the absence of a viable quantum theory of gravity, over the last two to three decades, there has been a substantial amount of effort in the literature to explore possible imprints of quantum gravity in low energy phenomena [23]. The polymer quantization approach is inspired by loop quantum gravity and the approach attempts to account for Planck scale modifications to propagators in given classical spacetimes [27, 28]. In Chap. 3, using the polymer quantization approach, we had examined a variant of the Unruh effect in flat spacetime. We had analyzed the response of a rotating Unruh-DeWitt detector which is coupled to a polymer quantized scalar field [70]. For the parameter ranges we have investigated, we had found that, while polymer quantization indeed modified the response of the detector, the changes do not prove to be substantial.

While it well known that small particles exhibit Brownian motion in a thermal bath, the question of whether such particles will diffuse in the quantum vacuum is an issue that remains to be resolved satisfactorily. With the aim of addressing this problem, in Chap. 4, we had studied the motion of a mirror that is immersed in a thermal bath. Working with a quantized scalar field in $(1+1)$-spacetime dimensions, we had calculated the average force as well as the fluctuations on a point mirror that is interacting with the scalar field. After establishing the fluctuation-dissipation theorem for the mirror, we had used the theorem to examine the nature of diffusion of the mirror at a finite temperature as well as in the quantum vacuum [78]. Importantly, in contrast to the prior efforts in this context [35], we have been able to arrive at a complete expression for the mean-squared displacement of the mirror that is valid at all times. While we recover the standard results at a finite temperature, interestingly, we had found that the mirror diffuses logarithmically at zero temperature, a result which confirms similar conclusions that have been arrived at earlier.

One of the issues that remains to be satisfactorily addressed in cosmology is the problem of the quantum-to-classical transition of primordial cosmological perturbations. In Chap. 5, we had examined such a transition of the tensor modes in the context of bouncing scenarios, which can provide an alternative mechanism to inflation for the generation of the primordial perturbations. We had shown that, as one approaches the bounce, the tensor modes corresponding to scales of cosmological interest get squeezed to roughly the same extent as they typically do during inflation. Moreover, we had examined the problem from the perspective of measurement in quantum mechanics using the CSL model. We had found that, depending on the choice of the parameter that leads to the spontaneous localization, the CSL mechanism can lead to a sharp drop in the tensor power spectrum on suitably large scales, reflecting similar results that arise in the context of inflation [100].

6.2 Outlook

In the light of investigations carried out in this thesis, it would be interesting to study some of the following issues in the near future.

In this thesis, upon taking into account the effects of the minimal length, we had described a given spacetime in terms of a biscalar, which we had referred to as the qmetric. As the Ricci scalar describes the dynamics of the gravitational field in general theory of relativity, we had also calculated Ricci bi-scalar corresponding to the qmetric. We had found that the Ricci bi-scalar had a non-local form, which does not reduce to the conventional Ricci scalar in the limit when the minimal length is set to zero. We had highlighted the fact that this property points to non-trivial dynamics induced by the presence of the minimal length. Needless to say, it will be interesting to examine the effects of the minimal length on Lagrangians that describe more non-trivial theories of gravity. In particular, it would be interesting to examine the signatures of the minimal length in Lagrangians such as the one that arises in the Gauss-Bonnet theory in higher dimensions. Such an analysis would be helpful in understanding whether the non-trivial imprints of the existence of a minimal length is a special feature of Einsteinian gravity, or it arises in higher curvature theories of gravity as well.

The relation between the unmodified, local, spacetime metric and the qmetric, which was a bi-tensor is commonly known as a disformal relation, and is a generalization of the more conventional conformal relation between two different metrics [102]. The so-called Lanczos-Lovelock gravity is a generalization of the general theory of relativity to arbitrary spacetime dimensions [101]. It will be interesting to examine the geometrical aspects of the disformally modified Lanczos-Lovelock theory of gravity, with the specific aim of calculating the effects of minimal length on the Lanczos-Lovelock Lagrangian.

One of the issues that this thesis had investigated was concerning the quantum-to-classical transition of primordial cosmological perturbations in the context of bouncing scenario. The tools we used to address this issue, *viz.* the Wigner function and the CSL mechanism, indicate towards such a transition. While the results obtained are suggestive, it ought to be admitted that they are not conclusive. It would be useful to utilize different quantifiers (such as, for instance, the extent of decoherence or quantum discord), to examine and address this issue in a more satisfying manner [103].

Appendix A

Appendices

A.1 Green's function condition: Fixing A

In maximally symmetric spacetimes, the expression for the non-local d'Alembartian operator (*viz.* Eq.(2.27)) simplifies to be

$$\widetilde{\Box} = \alpha\,\Box + 2\,\alpha\,\sigma^2\,\left[\ln\left(\alpha A^{D_1}\right)\right]'\,\frac{\partial}{\partial\sigma^2}, \tag{A.1}$$

where the local d'Alembartian operator $\Box$ is given by

$$\Box = \frac{\partial^2}{\partial\sigma^2} + \left(\frac{\partial}{\partial\sigma}\ln\Delta^{-1} + \frac{D_1}{\sigma}\right)\frac{\partial}{\partial\sigma}. \tag{A.2}$$

The Green's function condition then becomes

$$\widetilde{\Box}\,\widetilde{G}(\sigma^2) = \alpha\,\Box\,G(t^2) + 2\,\alpha\,\sigma^2\,\left[\ln\left(\alpha A^{D_1}\right)\right]'\,\frac{\partial G(t^2)}{\partial\sigma^2} = 0, \tag{A.3}$$

where $t^2 = S_{\ell_0}(\sigma^2)$.

For convenience, the local d'Alembartian operator $\Box$ can be rewritten as

$$\Box = \frac{1}{\alpha}\,\Box_t - 2\,\sigma^2\left\{\ln\left[\left(\frac{1}{S'_{\ell_0}}\frac{\Delta}{\Delta_S}\right)^2\left(\frac{S_{\ell_0}}{\sigma^2}\right)^D\right]\right\}'\frac{\partial}{\partial\sigma^2}, \tag{A.4}$$

where $\Box_t$ is given by

$$\Box_t = \frac{\partial^2}{\partial t^2} + \left(\frac{\partial}{\partial t}\ln\Delta_S^{-1} + \frac{D_1}{t}\right)\frac{\partial}{\partial t}. \tag{A.5}$$

Upon making use of these expressions in Eq. (A.3), we obtain that

$$\widetilde{\Box}\,\widetilde{G}(\sigma^2) = \Box_t G(t^2) - 2\,D_1\,\alpha\,\sigma^2\left\{\ln\left[\frac{1}{A}\,\frac{S_{\ell_0}}{\sigma^2}\,\left(\frac{\Delta}{\Delta_S}\right)^{2/D_1}\right]\right\}'\frac{\partial}{\partial\sigma^2}. \tag{A.6}$$

Demanding $\widetilde{\Box}\,\widetilde{G}(\sigma^2) = 0$, with $\Box_t G(t^2) = 0$, one arrives at

$$A = \frac{S_{\ell_0}}{\sigma^2}\left(\frac{\Delta}{\Delta_S}\right)^{2/D_1}. \tag{A.7}$$

A.2 Derivation of Eq. (2.39)

The complete derivation of Eq. (2.39) is lengthy, but there are several key structural aspects of the result which are worth highlighting, since these are responsible not only for the final simple form of $\widetilde{\mathbf{Ric}}(p, p_0)$, but also for

- Finiteness of the coincidence limit, $\left[\widetilde{\mathbf{Ric}}\right](p_0)$,
- Cancellation of any derivatives of $\mathcal{S}_{\ell_0}(x)$ higher than the first.

The first of these is purely a consequence of the correct identification of the dependence of the qmetric on VVD, and repeatedly using the identities $I1, I2$ for the same.

The second fact is more non-trivial, and there is no simple reason to have expected it! In fact, since q_{ab} depends on α, and α depends on $\mathcal{S}'_{\ell_0}$, one expects $\widetilde{\mathbf{Ric}}(p, p_0)$ to involve terms such as $\mathcal{S}'''_{\ell_0}$, which it does not. Although we do not have a completely geometric understanding of why this *must* happen, we highlight below *how* the cancellations happen which point to the following two reasons for these subtle cancellations:

- The fact that the coupling between q_{ab} and g_{ab} is *disformal* rather than *conformal*.
- The fact that the $\mathcal{S}''_{\ell_0}$ contribution of the conformal part is cancelled by a contribution coming from the disformal one.

To demonstrate these, we start from Eq. (2.37), and note that the only possibility of occurrence of second derivatives of $\mathcal{S}_{\ell_0}$ is from $\mathcal{J}_c$, which we write as

$$\mathcal{J}_c = \underbrace{\epsilon\,\left[2\,D_1\,\Omega^{-1}\,\Box\Omega + D_1\,D_4\,\Omega^{-2}\,(\nabla\Omega)^2\right]}_{\mathcal{J}_{c1}} + \underbrace{(K + D_1\,\nabla_{\boldsymbol{q}}\ln\Omega)\times\nabla_{\boldsymbol{q}}\ln\alpha\,\Omega^2}_{\mathcal{J}_{c2}}. \tag{A.8}$$

The cancellation of higher order derivatives happen between the terms $\mathcal{J}_{c1}$, which is the contribution of purely conformal transformation, and $\mathcal{J}_{c2}$, contributed by the disformal part. Simplifying the above expression, we get

$$\begin{aligned}\mathcal{J}_{c1} \quad &= \quad -\frac{1}{\sqrt{\alpha}}\,\frac{D_1}{\sqrt{\epsilon\,S}}\,\nabla_q\ln\alpha + 2\,\epsilon\,\frac{\sqrt{\epsilon\,S}}{\sqrt{\alpha}}\nabla_q\ln\alpha\,(\ln\Delta_s)^\bullet \\ &\quad\; + \text{terms that do not depend on } \mathcal{S}''_{\ell_0}\end{aligned} \tag{A.9}$$

and

$$\begin{aligned}\mathcal{J}_{c2} &= \frac{1}{\sqrt{\alpha}}\,\frac{D_1}{\sqrt{\epsilon\,S}}\,\nabla_q \ln\alpha - 2\,\epsilon\,\frac{\sqrt{\epsilon\,S}}{\sqrt{\alpha}}\,\nabla_q \ln\alpha\,(\ln\Delta_s)^{\bullet}\\ &\quad + \text{terms that do not depend on } \mathcal{S}''_{\ell_0}. \qquad \text{(A.10)}\end{aligned}$$

If the metrics q_{ab} and g_{ab} are conformally coupled, $\alpha = \Omega^{-2}$ and hence $\mathcal{J}_{c2} = 0$. In such a case, the higher derivatives of $\mathcal{S}_{\ell_0}$ would not cancel; the cancellation is solely a consequence of the disformal coupling between the metrics.

A.3 Non-relativistic limit of the noise kernels

In this appendix, we shall provide a few essential steps concerning the evaluation of the correlation function describing the fluctuating component of the radiation reaction force on the moving mirror we had discussed in Chap. 4.

Note that we are interested in the correlation function when the mirror is moving non-relativistically, *i.e.* when $|\dot{z}| \ll 1$. In such a limit, the noise-kernels (4.22) reduce to

$$\begin{aligned}\langle\hat{\mathcal{T}}^{ab}_{\rm R}(t,z)\,\hat{\mathcal{T}}^{cd}_{\rm R}(t',z')\rangle &\simeq \frac{\pi^2}{8\,\beta^4}\biggl[(-1)^{a+b+c+d} + (-1)^{a+b}\,(1+4\,\dot{z}')\\ &\quad + (-1)^{c+d}\,(1+4\,\dot{z}) + (1+4\,\dot{z})\,(1+4\,\dot{z}')\biggr]\\ &\quad \times \text{cosech}^4\left[\pi\,(\Delta t+\Delta z)/\beta\right], \qquad \text{(A.11a)}\\ \langle\hat{\mathcal{T}}^{ab}_{\rm L}(t,z)\,\hat{\mathcal{T}}^{cd}_{\rm L}(t',z')\rangle &\simeq \frac{\pi^2}{8\,\beta^4}\biggl[1 + (-1)^{a+b}\,(1-4\,\dot{z})\\ &\quad + (-1)^{c+d}\,(1-4\,\dot{z}') + (-1)^{a+b+c+d}\,(1-4\,\dot{z})\,(1-4\,\dot{z}')\biggr]\\ &\quad \times \text{cosech}^4\left[\pi\,(\Delta t-\Delta z)/\beta\right]. \qquad \text{(A.11b)}\end{aligned}$$

Upon substituting these results in the expression (4.19), we get

$$\begin{aligned}\langle\hat{\mathcal{R}}(t)\,\hat{\mathcal{R}}(t')\rangle &\simeq \frac{\pi^2}{2\,\beta^4}\biggl\{\text{cosech}^4\left[\pi\,(\Delta t-\Delta z)/\beta\right] + \text{cosech}^4\left[\pi\,(\Delta t+\Delta z)/\beta\right]\biggr\}\\ &\quad - \frac{\pi^2}{\beta^4}\,(\dot{z}+\dot{z}')\,\biggl\{\text{cosech}^4\left[\pi\,(\Delta t-\Delta z)/\beta\right] - \text{cosech}^4\left[\pi\,(\Delta t+\Delta z)/\beta\right]\biggr\}. \qquad \text{(A.12)}\end{aligned}$$

Using the series representation of $\mathrm{cosech}^4 z$ [cf. Eq. (4.31); also see App. A.4], we can write

$$\begin{aligned}\mathrm{cosech}^4\left[\pi\,\left(\Delta t\pm\Delta z\right)/\beta\right] &= \mathrm{cosech}^4\left(\pi\,\Delta t/\beta\right)\\ &\pm\frac{\Delta z}{\Delta t}\left\{\frac{4}{3\,\pi^2}\,\left(\frac{\beta}{\Delta t}\right)^2\sum_{n=-\infty}^{\infty}\frac{1}{\left[1+(i\,n\,\beta/\Delta t)\right]^3}\right.\\ &\left.-\frac{4}{\pi^4}\,\left(\frac{\beta}{\Delta t}\right)^4\sum_{n=-\infty}^{\infty}\frac{1}{\left[1+(i\,n\,\beta/\Delta t)\right]^5}\right\}\end{aligned}\tag{A.13}$$

and, if we now make use of Eq. (A.13) in (A.12), we finally arrive at

$$\langle\hat{\mathcal{R}}(t)\,\hat{\mathcal{R}}(t')\rangle=\frac{\pi^2}{\beta^4}\,\mathrm{cosech}^4\left(\pi\,\Delta t/\beta\right),\tag{A.14}$$

which is the result we have quoted.

A.4 Series representation of the correlation function

In this appendix, we shall outline the method to arrive at the series representation (4.31) for the function $C_{\mathcal{R}}(t)$.

We shall make use of the polygamma function $\psi_n(z)$ to arrive at the series representation for $\mathrm{cosech}^4(z)$. The polygamma function is defined as [77]

$$\psi_n(z)=\frac{\mathrm{d}^{n+1}}{\mathrm{d}z^{n+1}}\ln\Gamma(z),\tag{A.15}$$

where $\Gamma(z)$ is the gamma function. The function $\psi_n(z)$ can be represented as an integral as follows:

$$\psi_n(z)=(-1)^{n+1}\int_0^\infty\mathrm{d}t\,\frac{\mathrm{e}^{-z\,t}\,t^n}{1-\mathrm{e}^{-t}}.\tag{A.16}$$

Using this expression, we can write

$$\psi_1(i\,z)+\psi_1(-i\,z)=2\int_0^\infty\mathrm{d}t\,\frac{t\cos(z\,t)}{1-\mathrm{e}^{-t}}\tag{A.17}$$

and, upon expressing $\cos(z\,t)$ and $(1-\mathrm{e}^{-t})^{-1}$ as a power series, we obtain that

$$\psi_1(i\,z)+\psi_1(-i\,z)=2\sum_{m=0}^{\infty}\frac{(-1)^m\,z^{2\,m}}{(2\,m)!}\sum_{n=0}^{\infty}\int_0^\infty\mathrm{d}t\,\mathrm{e}^{-n\,t}\,t^{2\,m+1}.\tag{A.18}$$

Evaluating the integral, one obtains

$$\psi_1(iz)+\psi_1(-iz)=2\sum_{n=0}^{\infty}\frac{1}{n^2}\sum_{m=0}^{\infty}\left[(-1)^m\left(\frac{z}{n}\right)^{2\,m}+2\,(-1)^m\,m\,\left(\frac{z}{n}\right)^{2\,m}\right],\tag{A.19}$$

and carrying the sum over m leads to

$$\psi_1(i\,z) + \psi_1(-i\,z) = -\sum_{n=0}^{\infty}\left[\frac{1}{(z+i\,n)^2} + \frac{1}{(z-i\,n)^2}\right]. \tag{A.20}$$

This series can easily be summed to arrive at [77]

$$\sum_{n=0}^{\infty}\left[\frac{1}{(z+i\,n)^2} + \frac{1}{(z-i\,n)^2}\right] = \frac{1}{z^2} + \pi^2 \mathrm{cosech}^2(\pi\,z), \tag{A.21}$$

so that we have

$$\psi_1(i\,z) + \psi_1(-i\,z) = -\frac{1}{z^2} - \pi^2\,\mathrm{cosech}^2(\pi z). \tag{A.22}$$

From the definition of polygamma function it is clear that $\psi_3(z) = \mathrm{d}^2\psi_1(z)/\mathrm{d}z^2$. Upon substituting the result (A.22) in this identity, we obtain that

$$\psi_3(i\,z) + \psi_3(-i\,z) = \frac{6}{z^4} + 4\,\pi^4\,\mathrm{cosech}^2(\pi\,z) + 6\,\pi^4\,\mathrm{cosech}^4(\pi\,z). \tag{A.23}$$

From the integral representation of $\psi_n(z)$, we have

$$\psi_3(i\,z)+\psi_3(-i\,z) = 2\int_0^{\infty}\mathrm{d}t\,\frac{t^3\cos(z\,t)}{1-\mathrm{e}^{-t}} = 2\sum_{m=0}^{\infty}(-1)^m\,\frac{z^{2\,m}}{(2\,m)!}\sum_{n=0}^{\infty}\int_0^{\infty}\mathrm{d}t\,\mathrm{e}^{-n\,t}\,t^{2\,m+3}, \tag{A.24}$$

where, as we had done earlier, we have expressed $\cos(z\,t)$ and $(1-\mathrm{e}^{-t})^{-1}$ as a power series. Evaluating the integral and carrying out the sum over m leads to

$$\psi_3(i\,z) + \psi_3(-i\,z) = 6\sum_{n=0}^{\infty}\left[\frac{1}{(z+i\,n)^4} + \frac{1}{(z-i\,n)^4}\right]. \tag{A.25}$$

Comparing Eqs. (A.23) and (A.25) we arrive at the following series representation of $\mathrm{cosech}^4(\pi z)$:

$$\begin{aligned}\mathrm{cosech}^4(\pi\,z) \;\;=\;\; & -\frac{2}{3\,\pi^2}\left[\frac{1}{z^2} + \sum_{n=1}^{\infty}\frac{1}{(z+i\,n)^2} + \sum_{n=1}^{\infty}\frac{1}{(z-i\,n)^2}\right] \\ & + \frac{1}{\pi^4}\left[\frac{1}{z^4} + \sum_{n=1}^{\infty}\frac{1}{(z+i\,n)^4} + \sum_{n=1}^{\infty}\frac{1}{(z-i\,n)^4}\right],\end{aligned} \tag{A.26}$$

which is the result we have made use of in the text.

A.5 Evaluating the integrals $I_1(\alpha, t)$ and $I_2(\alpha, t)$

In this appendix, we shall outline the evaluation of the integrals $I_1(\alpha, t)$ and $I_2(\alpha, t)$ as described by Eqs. (4.49).

If we substitute $y' = \coth\left[\pi\,(t' + i\epsilon)/\beta\right]$ in the expression for $I_1(\alpha, t)$, it reduces to

$$I_1(\alpha, t) = -\frac{\beta}{\pi}\int_{-1}^{y} \mathrm{d}y'\,\left(\frac{y'+1}{y'-1}\right)^{p-1}\,\left[\frac{1}{y'-1} + \frac{1}{(y'-1)^2}\right], \tag{A.27}$$

where $p = \alpha\,\beta/(2\,\pi)$. If we now further set $u' = (y'+1)/(y'-1)$, we obtain that

$$I_1(\alpha, t) = -\frac{\beta}{\pi}\,\mathrm{e}^{\alpha\,t}\int_0^1 \mathrm{d}x\,x^{p-1}\,\left[\frac{1}{1 - \mathrm{e}^{2\,\pi\,t/\beta}\,(1 + i\,\epsilon)\,x} - \frac{1}{2}\right]. \tag{A.28}$$

We can make use of the following integral representation of the hypergeometric function to evaluate the above integral [104]

$${}_2F_1[a, b; c; z] = \frac{\Gamma(c)}{\Gamma(b)\Gamma(c-b)}\int_0^1 \mathrm{d}x\,x^{b-1}\,(1-x)^{c-b-1}\,(1 - z\,x)^{-a}, \tag{A.29}$$

for $\mathrm{Re.}\,c > \mathrm{Re.}\,b > 0$ and $|\arg(1-z)| < \pi$. We find that $I_1(\alpha, t)$ can be written as

$$I_1(\alpha, t) = \frac{\mathrm{e}^{\alpha\,t}}{\alpha}\left\{1 - 2\,{}_2F_1\left[1, p; p+1; \mathrm{e}^{2\,\pi\,t/\beta}\,(1 + i\,\epsilon)\right]\right\}. \tag{A.30}$$

Similarly, we can evaluate $I_2(\alpha, t)$ to arrive at

$$I_2(\alpha, t) = -\frac{\mathrm{e}^{-\alpha\,t}}{\alpha}\left\{1 - 2\,{}_2F_1\left[1, p; p+1; \mathrm{e}^{-2\,\pi\,t/\beta}\,(1 + i\,\epsilon)\right]\right\}. \tag{A.31}$$

Since the mean-squared displacement $\sigma^2(t)$ must be a real quantity, we write the integral $I_1(\alpha, t)$ as follows:

$$I_1(\alpha, t) = \frac{\mathrm{e}^{\alpha\,t}}{\alpha}\left\{1 - {}_2F_1\left[1, p; p+1; \mathrm{e}^{2\,\pi\,t/\beta}\,(1 + i\,\epsilon)\right] - {}_2F_1\left[1, p; p+1; \mathrm{e}^{2\,\pi\,t/\beta}\,(1 - i\,\epsilon)\right]\right\}. \tag{A.32}$$

Upon writing the quantity $I_2(\alpha, t)$ in a similar fashion and substituting the resultant expressions in Eq. (4.50), we obtain that

$$\sigma_z^2(t) = \frac{12}{\alpha_1\,\alpha_2}\left\{\gamma_{\mathrm{E}} + \ln\left[2\sinh(\pi\,t/\beta)\right]\right\} + \frac{12}{\alpha_1\,(\alpha_1 + \alpha_2)}\,F(p_1, t) + \frac{12}{\alpha_2\,(\alpha_1 + \alpha_2)}\,F(p_2, t), \tag{A.33}$$

where the function $F(p,t)$ is defined as

$$\begin{aligned} F(p,t) \;\;&\equiv\;\; \frac{1}{4\,p}\left\{{}_2F_1\left[1,p;p+1;\mathrm{e}^{2\,\pi\,t/\beta}\,(1+i\,\epsilon)\right]+{}_2F_1\left[1,p;p+1;\mathrm{e}^{2\,\pi\,t/\beta}\,(1-i\,\epsilon)\right]\right\} \\ &\quad+\frac{1}{2\,p}\,{}_2F_1\left[1,p;p+1;\mathrm{e}^{-2\,\pi\,t/\beta}\right]+\psi_0(p), \end{aligned} \tag{A.34}$$

with $\psi_n(z)$ being the polygamma function [77]. In order to write $F(p,t)$ more compactly we make use of the identity [69]

$$\begin{aligned} {}_2F_1\left[a,b;c;z\right] \;\;&=\;\; \frac{\Gamma(c)\,\Gamma(b-a)}{\Gamma(b)\Gamma(c-a)}\,(-z)^{-a}\,{}_2F_1\left[a,1-c+a;1-b+a;z^{-1}\right] \\ &\quad+\frac{\Gamma(c)\,\Gamma(a-b)}{\Gamma(a)\Gamma(c-b)}\,(-z)^{-b}\,{}_2F_1\left[b,1-c+b;1-a+b;z^{-1}\right], \end{aligned} \tag{A.35}$$

where $(a,b,c)\notin\mathbb{Z}$ or $(a-b)\notin\mathbb{Z}$ and $|\arg(-z)|<\pi$. We find that $F(p,t)$ can be written as

$$\begin{aligned} F(p,t) \;\;&=\;\; \frac{\pi}{2}\cot(\pi p)\,\mathrm{e}^{-2\,\pi\,p\,t/\beta}+\frac{\mathrm{e}^{-2\,\pi\,t/\beta}}{2\,(1-p)}\,{}_2F_1\left[1,1-p;2-p;\mathrm{e}^{-2\,\pi\,t/\beta}\right] \\ &\quad+\frac{1}{2\,p}\,{}_2F_1\left[1,p;p+1;\mathrm{e}^{-2\,\pi\,t/\beta}\right]+\psi_0(p), \end{aligned} \tag{A.36}$$

which is the result we have made use of in the text. We should clarify that since p_1 and p_2 are, in general, not integers [cf. Eqs. (4.53)], Eq. (A.33) is valid for all finite values of the mass m of the mirror and the inverse temperature β. We have quoted the result (A.33) with $F(p,t)$ given by Eq. (A.34) in the text.

A.6 Divergence in the mean-squared displacement in the limit of zero temperature

In this appendix, we shall discuss a subtle point concerning the zero temperature limit of the finite temperature result (A.33) for the mean-squared displacement of the mirror.

We find that a logarithmic divergence arises if we blindly take the zero temperature limit (*i.e.* $\beta\to\infty$) of the final result (A.33) for the mean-squared displacement of the mirror at a finite temperature. In the previous appendix, we had expressed the integrals integrals $I_1(\alpha,t)$ and $I_2(\alpha,t)$ in terms of the hypergeometric function using the definition (A.29). Note that the representation (A.29) is valid only for $\mathrm{Re.}\,c>\mathrm{Re.}\,b>0$ and $|\arg(1-z)|<\pi$. Hence, for the expression (A.34) describing $F(p,t)$ in terms of the hypergeometric functions to be valid, p_1 and p_2 should be positive definite for all values of β

and m. One can easily show that, while p_1 remains positive, p_2 tends to zero in the limit of $\beta \to \infty$. Since [cf. Eq. (A.29)]

$$\frac{1}{p_2}\,{}_2F_1\left[1, p_2; p_2+1; z\right] = \int_0^1 \mathrm{d}x\, x^{p_2-1}(1-z\,x)^{-1}, \tag{A.37}$$

we can write

$$\frac{1}{p_2}\,{}_2F_1\left[1, p_2; p_2+1; z\right] = \frac{z}{p_2+1}\,{}_2F_1\left[1, p_2+1; p_2+2; z\right] + \mathcal{I}(p_2), \tag{A.38}$$

where

$$\mathcal{I}(p_2) = \begin{cases} 1/p_2 & \text{when} \quad p_2 > 0, \\ -\ln\,\varepsilon & \text{when} \quad p_2 = 0, \end{cases} \tag{A.39}$$

with $\varepsilon \to 0$. On substituting Eq. (A.38) in Eq. (A.33) and making use of the following identity [69]:

$$\psi_m(z) = \psi_m(z+1) + \frac{(-1)^{m+1}\,m!}{z^{m+1}}, \tag{A.40}$$

we obtain that

$$\begin{aligned} \sigma_z^2(t) \;&=\; \frac{12}{\alpha_1\,\alpha_2}\left\{\gamma_{\mathrm{E}} + \ln\left[2\sinh(\pi\,t/\beta)\right]\right\} + \frac{12}{\alpha_1\,(\alpha_1+\alpha_2)}\,F(p_1, t) \\ &\quad + \frac{12}{\alpha_2\,(\alpha_1+\alpha_2)}\,\left[F(p_2+1, t) + \mathcal{J}(p_2)\right], \end{aligned} \tag{A.41}$$

where $\mathcal{J}(p_2)$ is given by

$$\mathcal{J}(p_2) = \begin{cases} 0 & \text{when} \quad \beta > 0, \\ -\ln\,\varepsilon & \text{when} \quad \beta \to \infty. \end{cases} \tag{A.42}$$

In other words, the expression (A.33) for the mean-squared displacement of the mirror at a finite temperature would diverge logarithmically if we naively consider the zero temperature limit.

Bibliography

[1] D. H. Perkins, *Introduction to High Energy Physics*, Fourth Edition (Cambridge University Press, Cambridge, England, 2000); C. P. Burgess and G. D. Moore, *The Standard Model: A Primer* (Cambridge University Press, Cambridge, England, 2007); D. Griffiths, *Introduction to Elementary Particles*, Second Edition (Wiley-VCH, New York, 2008).

[2] C. Itzykson and J.-B. Zuber, *Quantum Field Theory* (McGraw Hill, New York, 1980); S. Weinberg, *The Quantum Theory of Fields: Volume 1, Foundations*, First Edition (Cambridge University Press, Cambridge, England, 2005); S. Weinberg, *The Quantum Theory of Fields: Volume 2, Modern Applications*, Second Edition (Cambridge University Press, Cambridge, England, 2013); S. Weinberg, *The Quantum Theory of Fields: Volume 3, Supersymmetry*, Third Edition (Cambridge University Press, Cambridge, England, 2013).

[3] S. Weinberg, *Gravitation and Cosmology: Principles and Applications of the General Theory of Relativity* (John Wiley and Sons, New York, 1972); S. W. Hawking, G. F. R. Ellis, *The large scale structure of spacetime* (Cambridge University Press, Cambridge, England, 1973); R. M. Wald, *General Relativity* (University of Chicago Press, Chicago, 1984).

[4] B. P. Abbott *et al.* (LIGO Scientific Collaboration and Virgo Collaboration), Phys. Rev. Lett. **116**, 061102 (2016) [arXiv:1602.03837 [gr-qc]]; B. P. Abbott *et al.* (LIGO Scientific Collaboration and Virgo Collaboration), Phys. Rev. Lett. **116**, 241103 (2016) [arXiv:1606.04855 [gr-qc]]; B. P. Abbott *et al.* (LIGO Scientific and Virgo Collaboration), Phys. Rev. Lett. **118**, 221101 (2017) [arXiv:1706.01812 [gr-qc]]; B. P. Abbott et al. (LIGO Scientific and Virgo Collaboration), Phys. Rev. Lett. **119**, 141101 (2017) [arXiv:1709.09660 [gr-qc]].

[5] R. J. Adler, Am. J. Phys. **78**, 925 (2010) [arXiv:1001.1205 [gr-qc]].

[6] C. Rovelli, *Quantum Gravity* (Cambridge University Press, Cambridge, England, 2004); T. Thiemann, *Modern Canonical Quantum General Relativity* (Cambridge

University Press, Cambridge, England, 2007); C. Kiefer, *Quantum Gravity*, Second Edition (Oxford University Press, New York, 2007).

[7] S. Carlip, Rept. Prog. Phys. **64**, 885 (2001) [arXiv:0108040 [gr-qc]]; R. P. Woodard, Rep. Prog. Phys. **72**, 126002 (2009) [arXiv:0907.4238 [gr-qc]]; A. Ashtekar, M. Reuter and C. Rovelli, *From General Relativity to Quantum Gravity*, in *General Relativity and Gravitation: A Centennial Perspective*, Eds. A. Ashtekar, B. K. Berger, J. Isenberg and M. MacCallum (Cambridge University Press, Cambridge, England, 2015) [arXiv:1408.4336 [gr-qc]].

[8] L. I. Schiff, *Quantum Mechanics*, First edition (McGraw Hill, New York, 1949).

[9] N. D. Birrell and P. C. W. Davies, *Quantum Field Theory in Curved Space* (Cambridge University Press, Cambridge, England, 1982); S. A. Fulling, *Aspects of Quantum Field Theory in Curved Spacetime* (Cambridge University Press, Cambridge, England, 1989); R. M. Wald, *Quantum Field Theory in Curved Spacetime and Black Hole Thermodynamics* (University of Chicago Press, Chicago, 1994); B. S. DeWitt, *The Global Approach to Quantum Field Theory*, Volumes 1 and 2 (Clarendon Press, Oxford, 2003); V. Mukhanov and S. Winitzki, *Introduction to Quantum Effects in Gravity* (Cambridge University Press, Cambridge, England, 2007); L. Parker and D. Toms, *Quantum Field Theory in Curved Spacetime* (Cambridge University Press, Cambridge, England, 2009).

[10] B. S. DeWitt, Phys. Rep. **19**, 295 (1975); L. H. Ford, *Quantum Field Theory in Curved Spacetime* in *Proceedings of the Ninth Jorge Andre Swieca Summer School: Particles and Fields*, Eds. J. C. A. Barata, A. P. C. Malbouisson and S. F. Novaes (World Scientific, Singapore, 1998) [arXiv:9707062 [gr-qc]].

[11] S. W. Hawking, Nature **248**, 30 (1974); S. W. Hawking, Commun. Math. Phys. **43**, 199 (1975).

[12] J. Martin, Lect. Notes Phys. **738**, (2008) [arXiv:0704.3540 [hep-th]].

[13] S. A. Fulling, Phys. Rev. D **7**, 2850 (1973).

[14] W. G. Unruh, Phys. Rev. D **14**, 870 (1976).

[15] B. S. DeWitt, *Quantum gravity: The new synthesis*, in *General Relativity: An Einstein Centenary Survey*, Eds. S. W. Hawking and W. Israel (Cambridge University Press, Cambridge, England, 1979).

[16] L. C .B. Crispino, A. Higuchi and G. E. A. Matsas, Rev. Mod. Phys. **80**, 787 (2008) [arXiv:0710.5373 [gr-qc]].

[17] L. Sriramkumar and T. Padmanabhan, Int. J. Mod. Phys. D **11**, 1 (2002) [arXiv:9903054 [gr-qc]]; L. Sriramkumar, Fundam. Theor. Phys. **187**, 451 (2017) [arXiv:1612.08579 [gr-qc]].

[18] L. Garay, Int. J. Mod. Phys. A **10**, 145 (1995) [arXiv:9403008 [gr-qc]]; S. Hossenfelder, Living Rev. Relativity **16**, 2 (2013) [arXiv:1203.6191 [gr-qc]].

[19] D. M. Eardley and S. B. Giddings, Phys. Rev. D **66**, 044011 (2002) [arXiv:0201034 [gr-qc]]; S. D. H. Hsu, Phys. Lett. B **555**, 92 (2003) [arXiv:0203154 [hep-ph]].

[20] P. C. W. Davies, *Particles do not exist*, in *Quantum Theory of Gravity*, Ed. S. M. Christensen (Hilger, Bristol, 1984).

[21] S. Takagi, Prog. Theor. Phys. Suppl. **88**, 1 (1986).

[22] J. R. Letaw, Phys. Rev. D **23**, 1709 (1981); J. R. Letaw and J. D. Pfautsch, Phys. Rev. D **24**, 1491 (1981).

[23] G. Amelino-Camelia, Lect. Notes Phys. **669**, 59 (2005) [arXiv:0412136 [gr-qc]]; D. Mattingly, Living Rev. Rel. **8**, 5 (2005) [arXiv:0502097 [gr-qc]]; S. Hossenfelder and L. Smolin, Phys. Canada **66**, 99 (2010) [arXiv:0911.2761v1 [physics.pop-ph]]; G. Amelino-Camelia, Living Rev. Rel. **16**, 5 (2013) [arXiv:0806.0339 [gr-qc]].

[24] T. Jacobson, Prog. Theor. Phys. Suppl. **136**, 1 (1999) [arXiv:0001085 [hep-th]].

[25] R. H. Brandenberger and J. Martin, Int. J. Mod. Phys. A **17**, 3663 (2002) [arXiv:0202142 [hep-th]].

[26] K. Srinivasan, L. Sriramkumar and T. Padmanabhan, Phys. Rev. D **58**, 044009 (1998) [arXiv:9710104 [gr-qc]].

[27] G. M. Hossain, V. Husain and S. S. Seahra, Phys. Rev. D **82**, 124032 (2010) [arXiv:1007.5500 [gr-qc]].

[28] A. Ashtekar, J. Lewandowski and H. Sahlmann, Class. Quant. Grav. **20**, L11 (2003) [arXiv:0211012 [hep-th]]; A. Ashtekar, S. Fairhurst and J. L. Willis, Class. Quant. Grav. **20**, 1031 (2003) [arXiv:0207106 [gr-qc]].

[29] G. T. Moore, J. Math. Phys. **9**, 2679 (1970).

[30] S. A. Fulling and P. C. W. Davies, Proc. R. Soc. Lond. A **348**, 393 (1976).

[31] P. C. W. Davies and S. A. Fulling, Proc. R. Soc. A **356**, 237 (1977).

[32] M. T. Jaekel and S. Reynaud, Rep. Prog. Phys. **60**, 863 (1997) [arXiv:9706035 [quant-ph]]; V. V. Dodonov, Adv. Chem. Phys. **119**, 309 (2001) [arXiv:0106081 [quant-ph]].

[33] F. Reif, *Fundamentals of Statistical and Thermal Physics* (McGraw Hill, New York, 1965).

[34] H. B. Callen and T. A. Welton, Phys. Rev. **83**, 34 (1951); R. Kubo, J. Phys. Soc. Jap. **12**, 570 (1957); R. Kubo, Rep. Prog. Phys. **29**, 255 (1966).

[35] S. Sinha and R. D. Sorkin, Phys. Rev. **45**, 14 (1992); M. T. Jaekel and S. Reynaud, J. Phys. I (France), **3**, 339 (1993) [arXiv:9801072 [quant-ph]]; M. T. Jaekel and S. Reynaud, Phys. Lett. A **172**, 319 (1993) [arXiv:0101081 [quant-ph]].

[36] S. Dodelson, *Modern Cosmology*, (Academic Press, San Diego, 2003); V. F. Mukhanov, *Physical Foundations of Cosmology,* (Cambridge University Press, Cambridge, England, 2005); S. Weinberg, *Cosmology*, (Oxford University Press, Oxford, 2008).

[37] J. Martin, Lect. Notes Phys. **669**, 199 (2005) [arXiv:0406011 [hep-th]]; L. Sriramkumar, Curr. Sci. **97**, 868 (2009) [arXiv:0904.4584 [astro-ph.CO]]. L. Sriramkumar, *On the generation and evolution of perturbations during inflation and reheating*, in *Vignettes in Gravitation and Cosmology*, Eds. L. Sriramkumar and T. R. Seshadri (World Scientific, Singapore, 2012); A. Linde, *Inflationary Cosmology After Planck*, in *Proceedings of Post-Planck Cosmology: Lecture Notes of the Les Houches Summer School, Volume 100, July 2013*, Eds. C. Deffayet, P. Peter, B. Wandelt, M. Zaldarriaga and L. F. Cugliandolo (Oxford University Press, Oxford, 2015) [arXiv:1402.0526 [hep-th]]; J. Martin, Astrophys. Space Sci. Proc. **45**, 41 (2016) [arXiv:1502.05733 [astro-ph.CO]].

[38] M. Novello and S. P. Bergliaffa, Phys. Rept. **463**, 127 (2008) [arXiv:0802.1634 [astro-ph]]; R. H. Brandenberger, [arXiv:1206.4196 [astro-ph.CO]]; D. Battefeld and P. Peter, Phys. Rept. **571**, 1 (2015) [arXiv:1406.2790 [astro-ph.CO]]; R. Brandenberger and P. Peter, Found. Phys. **47**, 797 (2017) [arXiv:1603.05834 [hep-th]].

[39] A. M. Levy, Phys. Rev. D **95**, 023522 (2017) [arXiv:1611.08972 [gr-qc]].

[40] D. Polarski, A. A. Starobinsky, Class. Quant. Grav. **13**, 377 (1996) [arXiv:9504030 [gr-qc]]; J. Lesgourgues, D. Polarski, and A.A. Starobinsky, Nucl. Phys. B **497**, 479 (1997) [arXiv:9611019 [gr-qc]];C. Kiefer, D. Polarski and A. A. Starobinsky, Int. J. Mod. Phys. D **7**, 455 (1998) [arXiv:9802003 [gr-qc]]; C. Kiefer, Nucl. Phys. B Proc. Suppl. **88**, 255 (2000) [arXiv:0006252 [astro-ph]]; J. Weenink and T. Prokopec, arXiv:1108.3994 [gr-qc]. L. Sriramkumar and T. Padmanabhan, Phys. Rev. D **71**, 103512 (2005) [arXiv:gr-qc/0408034].

[41] J. Martin, V. Vennin and P. Peter, Phys. Rev. D **86** 103524 (2012) [arXiv:1207.2086 [hep-th]].

[42] For a small sample of relevant work which argue for the breakdown of locality, see: L. Garay, Phys. Rev. Lett. **80**, 2508 (1998) [arXiv:9801024 [gr-qc]]; S. Doplicher, K. Fredenhagen and J. Roberts, Comm. Math. Phy. **172**, 187 (1995) [arXiv:0303037

[hep-th]]; R. Sorkin, [arXiv:0703099 [gr-qc]]; S. Giddings, Phys. Rev. D **74**, 106006 (2006) [arXiv:0604072 [hep-th]].

[43] T. Padmanabhan: Ann. Phys. (N.Y.) **165**, 38 (1985); Phys. Rev. Lett. **78**, 1854 (1997) [arXiv:9608182 [hep-th]].

[44] D. Kothawala, Phys. Rev. D **88**, 104029 (2013) [arXiv:1307.5618 [gr-qc]].

[45] J. L. Synge, *Relativity: The General Theory* (North-Holland, Amsterdam, 1960).

[46] D. Kothawala and T. Padmanabhan, Phys. Rev. D **90**, 12406 (2014) [arXiv:1405.4967 [gr-qc]]; Phys. Lett. B **748**, 67 (2015) [arXiv:1408.3963 [gr-qc]].

[47] B. S. DeWitt and R. W. Brehme, Ann. Phys. **9**, 220 (1960).

[48] D. Kothawala, Gen. Rel. Grav. **46**, 1836 (2014) [arXiv:1406.2672 [gr-qc]].

[49] S. Christensen, Phys. Rev. D **14**, 2490 (1976).

[50] M. Visser, Phys. Rev. D **47**, 2395 (1993) [arXiv:hep-th/9303020 [hep-th]]; M. C. Gutzwiller, *Chaos in Classical and Quantum Mechanics*, Interdisciplinary Applied Mathematics 1 (Springer-Verlag, Berlin, 1990).

[51] I. G. Avramidi, *Covariant methods for the calculation of the effective action in quantum field theory and investigation of higher-derivative quantum gravity* (Ph.D. thesis, Moscow State University, 1986) [arXiv:9510140 [hep-th]].

[52] E. Poisson, A. Pound and I. Vega, Liv. Rev. Rel. **14**, 7 (2011) [arXiv:1102.0529 [gr-qc]].

[53] T. Jacobson, Phys. Rev. Lett. **75**, 1260 (1995) [arXiv:9504004 [gr-qc]].

[54] E. Poisson, *A Relativist's Toolkit* (Cambridge University Press, Cambridge, England, 2004).

[55] K. Parattu, S. Chakraborty, B. Majhi and T. Padmanabhan, Gen. Rel. Grav. **48**, 94 (2016) [arXiv:1501.01053 [gr-qc]].

[56] B. S. DeWitt, Phys. Rev. Lett. **47**, 1647 (1981); E. Alvarez, Phys. Lett. B **210**, 73 (1988); E. Alvarez, J. Cespedes, E. Verdaguer, Phys. Lett. B **289**, 51 (1992); Phys. Rev. D **45**, 2033 (1992), Phys. Lett. B **304**, 225 (1993) [arXiv:9303065 [hep-th]].

[57] D. J. Stargen and D. Kothawala, Phys. Rev. D **92**, 024046 (2015) [arXiv:1503.03793 [gr-qc]].

[58] T. Padmanabhan, Gen. Rel. Grav. **40**, 2031 (2008); T. Padmanabhan and A. Paranjape, Phys. Rev. D **75**, 064004 (2007) [arXiv:0701003 [gr-qc]].

[59] A. Kempf, Found. Phys. **44**, 472 (2013) [arXiv:1302.3680 [gr-qc]].

[60] A. Kempf, Banach Center Publications **40**, 379 (1997) [arXiv:9603115 [hep-th]].

[61] G. M. Hossain and G. Sardar, [arXiv:1705.01431 [gr-qc]].

[62] A. Garcia-Chung and J. D. Vergara, Int. J. Mod. Phys. A **31**, 1650166 (2016) [arXiv:1606.07406 [hep-th]].

[63] G. M. Hossain and G. Sardar, Class. Quant. Grav. **33**, 245016 (2016) [arXiv:1411.1935 [gr-qc]]; G. M. Hossain and G. Sardar, Phys. Rev. D **92**, 024018 (2015) [arXiv:1504.07856 [gr-qc]].

[64] N. Kajuri, Class. Quant. Grav. **33**, 055007 (2016) [arXiv:1508.00659 [gr-qc]].

[65] V. Husain and J. Louko, Phys. Rev. Lett. **116**, 061301 (2016) [arXiv:1508.05338 [gr-qc]].

[66] J. S. Bell and J. M. Leinaas, Nucl. Phys. B **284**, 488 (1987); W. G. Unruh, Phys. Rept. **307**, 163 (1998) [arXiv:9804158 [hep-th]]; J. I. Korsbakken and J. M. Leinaas, Phys. Rev. D **70**, 084016 (2004) [arXiv:0406080 [hep-th]].

[67] P. C. W. Davies, T. Dray and C. A. Manogue, Phys. Rev. D **53**, 4382 (1996) [arXiv:9601034 [gr-qc]].

[68] S. Gutti, S. Kulkarni and L. Sriramkumar, Phys. Rev. D **83**, 064011 (2011) [arXiv:1005.1807 [gr-qc]].

[69] M. Abramowitz and I. A. Stegun, *Handbook of Mathematical Functions* (Dover, New York, 1972).

[70] D. J. Stargen, N. Kajuri and L. Sriramkumar, Phys. Rev. D **96**, 066002 (2017) [arXiv:1706.05834 [gr-qc]].

[71] L. Sriramkumar and T. Padmanabhan, Class. Quant. Grav. **13**, 2061 (1996) [arXiv:9408037 [gr-qc]].

[72] M. T. Jaekel and S. Reynaud, Quant. Opt. **4**, 39 (1992) [arXiv:0101068 [quant-ph]].

[73] G. Gour and L. Sriramkumar, Found. Phys. **29**, 1917 (1999) [arXiv:9808032 [quant-ph]]; D. T. Alves, C. Farina and P. A. M. Neto, J. Phys. A **36**, 11333 (2003) [arXiv:0308157 [hep-th]]; C. H. Wu and D. S. Lee, Phys. Rev. D **71**, 125005 (2005) [arXiv:0501127 [quant-ph]]; Q. Wang and W. G. Unruh, Phys. Rev. D **89**, 085009 (2014) [arXiv:1312.4591 [gr-qc]]; Q. Wang and W. G. Unruh, Phys. Rev. D **92**, 063520 (2015) [arXiv:1506.05531 [gr-qc]].

[74] D. T. Alves, E. R. Granhen and M. G. Lima, Phys. Rev. D. **77**, 125001 (2008) [arXiv:0803.2638 [hep-th]].

[75] L. H. Ford and A. Vilenkin, Phys. Rev. D **25**, 2569 (1982).

[76] N. G. Phillips, B. L. Hu, Phys. Rev. D **63**, 104001 (2001) [arXiv:0010019 [gr-qc]]; N. G. Phillips, B. L. Hu, Phys. Rev. D **67**, 104002 (2003) [arXiv:0209056 [gr-qc]]; T. Cho and B. L. Hu, Class. Quantum Grav. **32**, 055006 (2015).

[77] I. S. Gradshteyn and I. M. Ryzhik, *Table of Integrals, Series and Products*, Seventh Edition (Academic Press, San Diego, 2007).

[78] D. J. Stargen, D. Kothawala and L. Sriramkumar, Phys. Rev. D **94**, 025040 (2016) [arXiv:1602.02526 [hep-th]].

[79] P. A. R. Ade *et al.*, Astron. Astrophys. **594**, A13 (2016) [arXiv:1502.01589 [astro-ph.CO]].

[80] P. A. R. Ade *et al.*, Astron. Astrophys. **594**, A20 (2016) [arXiv:1502.02114 [astro-ph.CO]].

[81] H. Kodama and M. Sasaki, Prog. Theor. Phys. Suppl. **78**, 1 (1984); V. F. Mukhanov, H. A. Feldman and R. H. Brandenberger, Phys. Rep. **215**, 203 (1992); J. E. Lidsey, A. Liddle, E. W. Kolb, E. J. Copeland, T. Barreiro and M. Abney, Rev. Mod. Phys. **69**, 373 (1997) [arXiv:9508078 [astro-ph]]; A. Riotto, arXiv:0210162 [hep-ph]; W. H. Kinney, arXiv:0301448 [astro-ph]; J. Martin, Lect. Notes Phys. **669**, 199 (2005) [arXiv:0406011 [hep-th]]; J. Martin, Braz. J. Phys. **34**, 1307 (2004) [arXiv:0312492 [astro-ph]]; B. Bassett, S. Tsujikawa and D. Wands, Rev. Mod. Phys. **78**, 537 (2006) [arXiv:0507632 [astro-ph]]; W. H. Kinney, arXiv:0902.1529 [astro-ph.CO]; L. Sriramkumar, Curr. Sci. **97**, 868 (2009) [arXiv:0904.4584 [astro-ph.CO]]; D. Baumann, arXiv:0907.5424 [hep-th]; L. Sriramkumar, in *Vignettes in Gravitation and Cosmology*, Eds. L. Sriramkumar and T. R. Seshadri (World Scientific, Singapore, 2012).

[82] R. Brandenberger, Phys. Tod. **61**, 44 (2008); P. Steinhardt, Sci. Am. **304**, 36 (2011); A. Ijjas, P. J. Steinhardt and A. Loeb, Sci. Am. **316**, 32 (2017).

[83] A. Ashtekar and P. Singh, Class. Quantum Grav. **28**, 21 (2011) [arXiv:1108.0893 [gr-qc]]; I. Agullo and A. Corichi, in *Springer Handbook of Spacetime*, Eds. A. Ashtekar and V. Petkov (Springer, Berlin, Heidelberg, 2014) [arXiv:1302.3833 [gr-qc]].

[84] F. Finelli and R. Brandenberger, Phys. Rev. D **65**, 103522 (2002) [arXiv:0112249 [hep-th]]; P. Peter and N. Pinto-Neto, Phys. Rev. D **66**, 063509 (2002) [arXiv:0203013 [hep-th]]; P. Creminelli and L. Senatore, JCAP **11**, 010 (2007) [arXiv:0702165 [hep-th]]; A. M. Levy, A. Ijjas and P. J. Steinhardt, Phys. Rev. D **92**, 063524 (2015) [arXiv:1506.01011 [astro-ph.CO]].

[85] R. N. Raveendran, D. Chowdhury and L. Sriramkumar, arXiv:1703.10061 [gr-qc].

[86] A. Albrecht, P. Ferreira, M. Joyce and T. Prokopec, Phys. Rev. D **50**, 4807 (1994); L. Grishchuk and Y. Sidorov, Phys. Rev. D **42**, 3413 (1990); L. Grishchuk, H. Haus and K. Bergman, Phys. Rev. D **46**, 1440 (1992).

[87] G. Leon, G. R. Bengochea and S. J. Landau, Eur. Phys. J. C **76**, 407 (2016) [arXiv:1605.03632 [gr-qc]].

[88] A. Perez, H. Sahlmann, and D. Sudarsky, Class. Quantum Grav. **23**, 2317 (2006) [arXiv:gr-qc/0508100 [gr-qc]]; A. De Unanue and D. Sudarsky, Phys. Rev. D **78**, 043510 (2008) [arXiv:0801.4702 [gr-qc]]; A. Diez-Tejedor, G. Leon, and D. Sudarsky, Gen. Rel. Grav. **44**, 2965 (2012) [arXiv:1106.1176 [gr-qc]].

[89] G. C. Ghirardi, A. Rimini and T. Weber, Phys. Rev. D **34**, 470 (1986); P. M. Pearle, Phys. Rev. A **39**, 2277 (1989); G. C. Ghirardi, P. M. Pearle and A. Rimini, Phys. Rev. A **42**, 78 (1990);

[90] A. Bassi and G.C. Ghirardi, Phys. Rept. **379**, 257 (2003) [arXiv:0302164 [quant-ph]]; A. Bassi, K. Lochan, S. Satin, T.P. Singh and H. Ulbricht, Rev. Mod. Phys. **85**, 471 (2013) [arXiv:1204.4325 [quant-ph]].

[91] S. Das, K. Lochan, S. Sahu and T. P. Singh, Phys. Rev. D **88**, 085020 (2013) [arXiv:1304.5094 [astro-ph.CO]].

[92] A. A. Starobinsky, JETP Lett. **30**, 682 (1979) [Pisma Zh. Eksp. Teor. Fiz. **30**, 719 (1979)].

[93] D. Wands, Phys. Rev. D **60**, 023507 (1999) [arXiv:9809062 [gr-qc]].

[94] D. Chowdhury, V. Sreenath and L. Sriramkumar, JCAP **11**, 002 (2015) [arXiv:1506.06475 [astro-ph.CO]].

[95] T. Bunch and P. C. W. Davies, Proc. Roy. Soc. Lond. A **360**, 117 (1978).

[96] L. Sriramkumar, K. Atmjeet and R. K. Jain, JCAP **09**, 010 (2015) [arXiv:1504.06853 [astro-ph.CO]].

[97] Mathematica (Wolfram Research, Version 8.0. Champaign, U.S.A., 2010).

[98] A. Bassi, J. Phys. A: Math. Gen. **38**, 3173 (2005) [arXiv:0410222 [quant-ph]].

[99] D. Chowdhury, L. Sriramkumar and R. K. Jain, Phys. Rev. D **94**, 083512 (2016) [arXiv:1604.02143 [gr-qc]].

[100] D. J. Stargen, V. Sreenath and L. Sriramkumar, arXiv:1605.07311v2 [gr-qc].

[101] T. Padmanabhan and D. Kothawala, Phys. Rept. **531**, 115 (2013) [arXiv:1302.2151 [gr-qc]].

[102] J. Bekenstein, Phys. Rev. D **48**, 3641 (1993).

[103] J. Martin and V. Vennin, Phys. Rev. D **93**, 023505 (2016) [arXiv:1510.04038 [astro-ph.CO]].

[104] N. N. Lebedev, *Special Functions and Their Applications* (Prentice-Hall, New Jersey, 1965).

List of papers on which this thesis is based

Papers in refereed journals

1. **D. Jaffino Stargen** and D. Kothawala, *Small scale structure of spacetime: The van Vleck determinant and equigeodesic surfaces*, Phys. Rev. D **92**, 024046 (2015) [arXiv:1503.03793 [gr-qc]].
2. **D. Jaffino Stargen**, D. Kothawala and L. Sriramkumar, *Moving mirrors and the fluctuation-dissipation theorem*, Phys. Rev. D **94**, 025040 (2016) [arXiv:1602.02526 [hep-th]].
3. **D. Jaffino Stargen**, V. Sreenath and L. Sriramkumar, *Quantum-to-classical transition and imprints of wavefunction collapse in bouncing universes* arXiv:1605.07311v2 [gr-qc], to be submitted for publication.
4. **D. Jaffino Stargen**, N. Kajuri and L. Sriramkumar, *Response of a rotating detector coupled to a polymer quantized field*, Phys. Rev. D **96**, 066002 (2017) [arXiv:1706.05834 [gr-qc]].

Presentations in conferences

1. *Small scale structure of spacetime*, poster in *The XXVIII Meeting of the Indian Association of General Relativity and Gravitation*, Raman Research Institute, Bengaluru, March 18–20, 2015.
2. *Small scale structure of spacetime — van Vleck determinant and equigeodesic surfaces*, contributed talk in *The Eighth International Conference on Gravitation and Cosmology*, Indian Institute of Science Education and Research, Mohali, December 14–18, 2015.

CURRICULUM VITAE

• Personal details:

Name:	D. Jaffino Stargen
Date of birth:	March 2, 1988
Gender:	Male
Permanent address:	Ellamavilai, Manakkavilai, Manalikkarai P.O., Kanyakumari District, Tamilnadu 629164

• Academic history:

2009–Present	Ph.D. Physics Department of Physics, Indian Institute of Technology Madras, Chennai Date of registration: December 21, 2011
2009–2011	M.Sc. Physics Scott Christian College, Nagercoil, Kanyakumari district, Tamilnadu
2006–2009	B.Sc. Physics Scott Christian College, Nagercoil, Kanyakumari district, Tamilnadu

DOCTORAL COMMITTEE

Guide:	Dr. L. Sriramkumar Professor, Department of Physics, Indian Institute of Technology Madras, Chennai
Co-guide:	Dr. Dawood Kothawala Assistant Professor, Department of Physics, Indian Institute of Technology Madras, Chennai
Members:	Dr. Prasanta Kumar Tripathy Associate Professor, Department of Physics, Indian Institute of Technology Madras, Chennai
	Dr. Manoj Gopalakrishnan Associate Professor, Department of Physics, Indian Institute of Technology Madras, Chennai
	Dr. Shanti Bhattacharya Associate Professor, Department of Electrical Engineering, Indian Institute of Technology Madras, Chennai
	Dr. Ghanashyam Date Professor, The Institute of Mathematical Sciences, Chennai